5-2010

EFFICACY AND MECHANISM OF â-DEFENSIN2 FUSED ANTIGEN PROTEIN VACCINES

Hyun J. Park

EFFICACY AND MECHANISM OF β-DEFENSIN2 FUSED ANTIGEN PROTEIN VACCINES

by

Hyun Jun Park, B.S.I.

APPROVED:

_____
Supervisory Professor, Larry W. Kwak, M.D., Ph.D.

_____
Michel Gilliet, M.D.

_____
Bradley W McIntyre, Ph.D.

_____
Sattva S Neelapu, M.D.

_____
Willem Overwijk, Ph.D.

_____
James M Reuben, Ph.D.

_____
Qing Yi, M.D., Ph.D.

APPROVED:

_____
Dean, The University of Texas at Houston's
Graduate School of Biomedical Sciences,
George M. Stancel, Ph.D.

EFFICACY AND MECHANISM OF β-DEFENSIN2 FUSED ANTIGEN PROTEIN VACCINES

A

DISSERTATION

Presented to the Faculty of

The University of Texas
Health Science Center at Houston

and

The University of Texas
M. D. Anderson Cancer Center

Graduate School of Biomedical Sciences

in Partial Fulfillment
of the Requirements
for the Degree of

DOCTOR OF PHILOSOPHY

by

Hyun Jun Park, B.S.I.
Houston, Texas

May, 2010

Dedication

This dissertation is dedicated to my mother who inspires me to find accessible, economical, and effective strategies to prevent, detect, and cure cancer.

Acknowledgements

Advisor

Dr. Kwak, Larry

Mentors (Alphabetical Order)

Dr. Cha, Soung Chul / Dr. Gilliet, Michel / Dr. McIntyre, Bradley / Dr. Neelapu, Sattva / Dr. Overwijk, Willem / Dr. Qin, Hong / Dr. Reuben, James / Dr. Yi, Qing

Research (Alphabetical Order)

Dr. Chu, Fuliang / Dr. Chung, Yeonseok / Cohen, Evan / Chuang, Carol / Dr. Dai, Zhimin / Delgado, David / Dr. Foglietta, Myriam / Dr. Gao, Hui / Dr. Hong Sungyoul / Dr. Hwu, Patrick / Dr. Kannan, Shibichakravarthy / Nattamai, Durgha / Dr. Rawal, Seema / Dr. Schluns, Kimberly / Dr. Sharma, Rakesh / Tonthat, Nam / Dr. Wei, Jinsong / Dr. Weng, Jinsheng / Dr. Wu, Weiguo

Other (Alphabetical Order)

Kim, Heetae / Liboy, Wilma / Ong, Juliana / Paick, Daniel / Turner, Sharon / Woo, Alison

Facilities

Baylor College of Medicine Baculovirus/Monoclonal Antibody Facility

M. D. Anderson - Center for Cancer Immunology Research

M. D. Anderson - The Flow Cytometry and Cellular Imaging Core Facility – South

M. D. Anderson - Veterinary Medicine and Surgery – South Campus Animal Resources

UTHSC at Houston and M. D. Anderson Cancer Center – GSBS

UTHSC at Houston and M. D. Anderson Cancer Center – Immunology Program

Abstract

Vaccines which use the strategy of fusing adjuvant murine β-defensin2 (mBD2) to an antigen in order to elicit stronger anti-antigen immune responses are referred to as murine β-defensin2 (mBD2) vaccines. Previous studies have validated the potential of mBD2 vaccines, thus in this study we focus on increasing vaccine efficacy as well as mechanism elucidation. Initially, we demonstrate superior IFN-γ release levels by antigen specific effector T cells when antigen is crosspresented by dendritic cells (DC) which absorbed mBD2 vaccine (mBD2 fused antigen protein) over antigen alone. We move unto an *in vivo* model and note significant increases in the expansion of antigen specific class I T cells but not class II T cells when receiving mBD2 vaccine over antigen alone. Further, knowing mBD2's link with CC chemokine receptor 6 (CCR6) and Toll-like receptor 4 (TLR4) we note that this enhanced class I T cell expansion is CCR6 independent but TLR4 dependent. With anti-tumor responses desired, we demonstrate in tumor protection experiments with mice, compelling tumor protection when combining adoptive T cell therapy and mBD2 vaccine immunization. We further note that mBD2 vaccines are not limited by the antigen and characterize a viable strategy for enhancing tumor antigen immunogenicity.

Table of Contents

List of Illustrations

Chapter 3. mBD2 Vaccine Production

Chapter 4. mBD2 Vaccine Efficacy

Chapter 5. mBD2 Vaccine Mechanism

Appendix. Chapter 5

List of Tables

Chapter 3. mBD2 Vaccine Production

Chapter 4. mBD2 Vaccine Efficacy

Chapter 5. mBD2 Vaccine Mechanism

Appendix. Chapter 4

Appendix. Chapter 5

Abbreviations

- APC – Antigen Presenting Cell
- BM-DC – Bone Marrow derived Dendritic Cell
- CCR6 – CC Chemokine Receptor 6
- CCR6KO – CCR6 KnockOut
- CLR – C-type Lectin Receptors
- CPG – C Phosphate G
- DC – Dendritic Cell
- gp100 – glycoprotein 100
- gp100F – glycoprotein 100 Full length
- gp100T – glycoprotein 100 Truncated of hydrophobic regions
- His-tag – hexa Histidine tag
- IDO – Indoleamine 2,3-DiOxygenase
- mBD2 – murine β-defensin2
- MCP-3 – Monocyte Chemoattractant Protein-3
- MIP-3α – Macrophage Inflammatory Protein-3α
- MPL – MonoPhosphoryl-Lipid A
- NLRS – NOD-Like ReceptorS
- OVA – OVAlbumin
- PBS – Phosphate Buffered Saline
- PFU – Plaque Forming Units
- PRR – Pattern Recognition Receptors

- RANTES – Regulated upon Activation, Normal T cell Expressed and Secreted
- RLH – RIG-Like Helicases
- SDS PAGE – Sodium Dodecyl Sulfate PolyAcrylamide Gel Electrophoresis
- SF9 - Spodoptera Frugiperda 9
- Thy-1 - Thymocyte differentiation antigen 1
- TLR – Toll-Like Receptor
- TLR4 – Toll-Like Receptor 4
- TLR4KO – TLR4 KnockOut
- TLR9 – Toll-Like Receptor 9
- Tregs – CD4+ regulatory T cells
- VEGF – Vascular Endothelial Growth Factor
- VSV – Vesicular Stomatitis Virus

Chapter 1. Introduction

Section 1. Background

Cancer Vaccines. The ultimate goal of a cancer vaccine is very simple, prevent or cure cancer effectively without causing collateral damage (1). Thus far, our current cancer vaccines have not been successful therapeutic agents for cancer patients (2). Additionally, mechanisms of immunological tolerance to cancer make the generation of immune response to cancer difficult (2). Therefore, new and safe strategies which can break immune tolerance against tumor antigens are needed in order to improve the efficacy of current cancer vaccines.

Chemokine Vaccines. Adjuvants, agents which help break immunological tolerance and enhance immune response, are a crucial component of cancer vaccines (1, 3). In order to enhance the capability of the adjuvant to generate antigen specific immunity, many laboratories have implemented strategies whereby adjuvants are fused to targeted antigen (4). With this concept in mind, what is internally known as a chemokine vaccine was formed. We refer to vaccines which use the strategy of enhancing the immunogenicity of self antigens via the fusion of an antigen with a chemokine or chemokine receptor ligand as a chemokine vaccine. Thus far, chemokine vaccines have been shown to elicit tumor antigen specific immunity (5-12).

mBD2 Vaccine. During chemokine vaccine testing and screening, murine β-defensin2 (mBD2) has consistently come out to be the antigen specific immune response enhancer of choice when used in the context of a chemokine vaccine (6, 8, 11, 12). mBD2, although not a chemokine, was initially tested for its ability to interact and bind to CC chemokine receptor 6 (CCR6) (6). mBD2 has been shown to play a role in both innate and adaptive immunity via Toll-like receptor 4 (TLR4) (8). However, the exact mechanism and function of mBD2 is still at its infancy. In this study, we refer to a vaccine which uses mBD2 as the chemokine receptor ligand of choice for a chemokine vaccine as an mBD2 vaccine.

Section 2. Purpose

Long term Objective. Our long-term objective is to develop new strategies to improve the efficacy of cancer vaccines. We aim to develop vaccines with the capacity to build up desirable cellular cytotoxic effects on tumor cells. We foresee knowledge obtained from these studies to be important in the development of new vaccination strategies for use in the clinic.

Main Objective. In this study we aimed to generate, test anti-antigen efficacy, and find the mechanism of the protein version of the mBD2 vaccine.

Section 3. The Problem

Summary. The mBD2 vaccine, as a DNA vaccine, has been shown to induce protective and therapeutic anti-tumor immune responses (6, 8, 11, 12). However, a stronger anti-tumor response is desired. In addition, elucidation of the mechanism of the DNA vaccine is difficult. It is theorized that the DNA vaccine eventually induces the production of its equivalent protein in order to generate its effect (13). Also, the mBD2 protein vaccine had not been thoroughly tested and the availability of mBD2 vaccine protein helped in the elucidation of mechanism of mBD2 vaccines. In addition, the mBD2 vaccine protein was used in the context of adoptive T cell therapy to enhance T cell response. This study is divided into three sections, divided by the three main questions that drove this study. The chapters are: mBD2 protein vaccine production, mBD2 vaccine anti-tumor efficacy, and mBD2 protein vaccine antigen specific immune mechanism.

mBD2 Vaccine Production Questions.

1.) How to generate mBD2 protein vaccine?

2.) How to purify mBD2 protein vaccine?

3.) How to store and maintain bioactivity of mBD2 protein vaccine?

mBD2 Vaccine Anti-tumor Efficacy Questions.

1.) Does mBD2 protein vaccine have protective anti-tumor effect?

2.) Do Toll-like receptor (TLR) agonist adjuvants enhance mBD2 protein vaccines?

3.) Does the mBD2 protein vaccine have a strong anti-tumor response when in conjunction with adoptive T cell therapy?

mBD2 Vaccine Antigen Specific Immune Mechanism Questions.

1.) Does the addition of mBD2 to antigen enhance immunogenicity of antigen?

2.) Is the mBD2 protein vaccine dependent on CCR6 and/or TLR4 for the antigen specific immune response?

3.) Is the mBD2 protein vaccine dependent on dendritic cells (DC) for antigen crosspresentation?

4.) Does the addition of mBD2 to antigen enhance antigen specific CD8+ and/or CD4+ T cell proliferation?

Section 4. Specific Aims and Research Hypothesis

Specific Aim 1. To construct and generate mBD2 chemokine vaccines.

Specific Aim 2. To assess the *in vivo* protective anti-tumor responses provided by vaccine built in Aim 1.

Specific Aim 3. To find the mechanism via which the vaccine built in Aim 1 produces responses assessed in Aim 2.

Central Hypothesis. Vaccination of mBD2 fused antigen protein generates protective antigen specific T cell immunity. The vaccine targets dendritic cells (DC) which absorbs the aforementioned protein, processes it, and crosspresents the antigen specific epitope unto antigen specific effector T cells and elicits an antigen specific T cell response.

Section 5. Significance of Study

Significance. The immunogenicity of most self antigens, such as those formulated for cancer vaccines, are poor. New and safe vaccination strategies which break immune tolerance against self-antigens are needed in order to improve the efficacy of current cancer vaccines. This study addresses this issue.

Section 6. Definition of Terms

Terms. The terms below were frequently used in this study and are concisely defined in the way it was meant to be understood.

- Adjuvant – Agent added to vaccine to enhance immunogenicity.
- Antigen – The target whereby an offensive immune response is desired. Also, an antigen is a component of vaccines (the sample of target) which is vaccinated to show the immune system the adversary target.
- Cancer vaccine – A vaccine that induces an immune response against cancer.
- Chemokine/Chemokine receptor ligand – Protein which attracts and binds to chemokine receptors.
- Chemokine vaccine – A vaccine that uses a chemokine or a chemokine receptor ligand and fuses it to the vaccine's antigen in order to improve antigen immunogenicity and also serve as vaccine adjuvant.
- Crosspresentation – The process by which antigen presenting cells such as dendritic cells absorb vaccine protein including antigen, process it, and present the processed antigen to antigen specific effector T cells.
- DNA vaccine – Vaccines made of deoxyribonucleic acid also referred to as genetic vaccines.
- Fusion – The joining of antigen and adjuvant component.
- Hydrophobicity/Hydrophobic – Regions of recombinant protein which make the purification of protein difficult.

- Immunogenicity – The state which describes how easily a target specific immune response can be generated.
- mBD2 (β-defensin2) – The adjuvant component tested in this study and fused to antigen to produce mBD2 vaccine.
- mBD2 vaccine – The vaccine tested in this study to produce enhanced anti-antigen immune response and uses mBD2 fusion.
- OT-I – Class I OVA specific T cells.
- OT-II – Class II OVA specific T cells.
- pmel-1 – Class I gp100 specific T cells.
- Protein vaccine - Vaccines made of amino acids also referred here as recombinant protein vaccine protein.
- Purification – The process of removing non-specific protein and eluting only the desired protein.
- Survival – The time mice are able to survive or maintain a status whereby tumor volume is lower than 400 mm^2 after receiving a tumor challenge.
- Tumor Challenge – The injection of mouse tumor cell line unto mice in order to simulate the development of tumor.
- Tumor Protection – The type of survival model whereby mice receive vaccine first and then tumor post vaccine.
- Vaccine – Agent given to subject to induce a target specific immune response which is either protective or therapeutic.

Section 7. Organization of Study

Organization. The study is organized into three main components.

Chapter 3 - mBD2 Vaccine Production which follows Specific Aim 1.

Chapter 4 - mBD2 Vaccine Efficacy which follows Specific Aim 2.

Chapter 5 - mBD2 Vaccine Mechanism which follows Specific Aim 3.

Chapters 1, 2, and 6 are introductory or concluding remarks.

Chapter 2. Review of Literature

Section 1. Cancer Vaccines Mini Review

Cancer Vaccines. The term cancer vaccine is a term that is very difficult to define. First, the term vaccine is a term of much debate as what exactly makes a vaccine is difficult to define. Thus, what products or interventions are cancer vaccines and which are not is still not clearly standardized. But, a vaccine is defined more for what it does than what it is; more simply a vaccine is any agent which is used to stimulate the immune system to mostly prevent a certain disease from overtaking a person. Thus, when one sees the term cancer vaccine, one might assume a cancer vaccine to be an intervention used to prevent cancer. But cancer vaccines are often used and designed to treat established cancer. In this text, cancer vaccines are defined to be any agent or intervention used to stimulate the immune system to prevent or treat cancer. Various authors have also defined cancer vaccines previously (1, 14-16)

Cancer Vaccine Problems. The problem with cancer vaccines is that thus far objective response rates are low (16). In fact, a reliable cancer vaccine with robust efficacy does not exist so far especially on well established solid tumors (17, 18). There is a wide variety of reasons for the poor performance of cancer vaccines to include but not limited to poor vaccine components, the development of an incorrect immune response, and the tumor microenvironment. Obviously, much effort exists to overcome this poor performance.

Cancer Vaccine Components. Most current cancer vaccines being tested have three main components: a tumor antigen, a carrier, and an adjuvant (14). The tumor antigen can be a tumor specific or tumor-associated and are often self-antigens. The carriers can be components such as liposomes which can serve as a delivery system (19). A plethora of adjuvants for vaccines exist and are often used with cancer vaccines as well (20). The platform of the vaccine also influences the immune response generated (13). Platforms of vaccines include but are not limited to DNA, recombinant protein, DC (21), and virus based (22) cancer vaccines. The number of permutations generated by only three variables is close to infinite, but it will be essential to tweak all the variables to generate the perfect cancer vaccine cocktail.

Improving Cancer Vaccines. Thus being aware of the problems behind a cancer vaccine's efficacy, much effort has been focused on choosing the right antigens, carriers, and adjuvants to promote the correct adaptive immune response through proper crosspresentation while breaking self-tolerance. Questions to answer include: What is the right antigen?, What is a proper immune response against cancer?, and How do you break self-tolerance? The questions are endless but many tumor-specific such as idiotype (23) and tumor-associated antigens such as survivin (24) have been tested. Generally, a T cell response is desired to eliminate cancer (25-27). Additionally, the tumor microenvironment and the body's own self-tolerance mechanism is generally to blame for tumor-tolerance by the immune system, and breaking tumor-tolerance has been very complicated and there is a lot of mystery surrounding it (28).

Cancer Vaccines and Immune Response. Cancer vaccines generally focus on generating an adaptive immune response against cancer. But, it is becoming evident that a proper adaptive immune response also depends on the proper initiation of the innate immune response via pattern recognition receptors such as Toll-like receptors (TLR) (29, 30). Thus, much research has focused on targeting pattern recognition receptors (PRR), via adjuvants in the case of vaccines (20, 31). Many preclinical observations allude to the enhancement of the efficacy of the antigens when combined with a TLR-agonist adjuvant (31-33). Toll-like receptors have received the most attention, but non-TLR receptors such as NOD-like receptors (NLRS), RIG-like helicases (RLH), C-type lectin receptors (CLRs), and other innate immune response receptors have the potential of being important targets as well (20). Additionally, the activation of innate receptors has been shown to downregulate inhibitory effects of immune regulatory cells as is in the case between TLR-8 and Treg cells (34). Moreover, new PRRs and their ligands are being identified and their inter/intra-play with other PRRs is being further elucidated. Thus, proper initiation of the innate immune response could induce the correct danger signals, overcome immune suppressive effects, and create a focused anti-tumor immune response.

Cancer Vaccines and Crosspresentation. The importance of crosspresentation of the antigen in the initiation of anti-tumor antigen immune response is undeniable. But exactly what type of crosspresentation is the most effective is a question that is still unanswered. Thus many receptors on antigen presenting cells including Fc (35), chemokine (5), and mannose receptors (36) have been targeted and have shown to elicit

antigen specific immunity. Recently, autophagy has also been a mechanism of crosspresentation where much focus is being placed (37). For the improvement of vaccine efficacy, the basis behind how the antigen is presented must be understood. For future vaccines, correct uptake and presentation of the antigen will also depend on the targeting of the correct antigen-uptake receptors.

Cancer Vaccines and Tumor Microenvironment. Finally, one must not forget that cancers are a malignancy of self-origin, and because tumors are of self-origin, generating effective anti-tumor immune response requires mounting an autoimmune attack, which involves breaking self-tolerance (38). It is also important to remember that the patient's immune surveillance mechanism has failed, thus the reason why a malignant cancer has progressed. How exactly the tumor has evaded immune surveillance is a matter of much controversy, and all the players protecting the tumor have yet to be elucidated (39).

Recently, much focus has been placed on CD4+ regulatory T cells (Tregs), cells which actively engage in the maintenance of immunological tolerance (40). Tregs are of interest in cancer as some cancers recruit Tregs into the tumor via use of chemokine CCL22 (41). Enhancement of anti-tumor immunity has been shown in murine models (42), renal cancer (43), melanoma (44), and ovarian cancer (45) when Tregs were depleted via use of denileukin diftitox (Ontak). Of course, other regulatory cell populations such as CD8+ T regs (46, 47), NKT cells (48), myeloid-derived suppressor cells (49), B7-H4+ myeloid cells (50), and gamma-delta T cells (51) might also play a role in the protection of the tumor. Thus, new vaccine formulations will have to override tumor protecting cells as well.

In addition to the regulatory cells which surround the tumor, it is also becoming evident that the tumor itself actively uses immune-evasion tactics to protect itself. First, tumors actively fights back via release of molecular immune suppression factors (38) such as IL-10 (52), transforming growth factor-beta TGF-β (38, 53), vascular endothelial growth factor (VEGF) (54) and indoleamine 2,3-dioxygenase (IDO) (55). Tumors can also downregulate their MHC class I molecules (56, 57). Also, tumors through constitutive stat-3 activation can induce chronic inflammation which could inhibit the release and sensing of danger signals in order to evade anti-tumor immune responses (57). Thus, to further improve the cancer vaccines, the vaccinologist will have to focus on breaking the immune barrier by which the tumor is shielded.

Cancer Vaccines with Fusion. Overcoming cancer immune tolerance in order to induce anti-tumor immune response is difficult. An anti-tumor immune response is desired in cancer, but the vaccination of tumor associated antigen by itself produces poor tumor-antigen specific immune response (2, 5). The idea of a fusion vaccine, whereby antigen is fused to an agent which induces antigen specific immune response, came about to overcome this obvious barrier (4). Vaccines which use the strategy of enhancing the immunogenicity of antigens via the fusion of antigen with a chemokine or chemokine receptor ligand is referred here as a chemokine vaccine. Over ten years of experience with chemokine vaccines have shown murine β-defensin2 (mBD2) to be one of the most promising chemokine vaccine fusion agents (6, 8, 11, 12). Vaccines which use mBD2 fusion to antigen are referred here as mBD2 vaccines.

Section 2. Historical Background – The Development of the Chemokine Vaccine

Introduction. The chemokine vaccine was invented and patented by Dr. Larry Kwak and Dr. Arya Biragyn. The development of the chemokine vaccine over the last decade (1999 to 2009) can be seen in eight seminal papers which I refer to as the Biragyn series after Dr. Arya Biragyn who is the author in all eight papers. The eight papers are listed below and the full reference can be seen on the reference portion of this thesis.

Biragyn Series #1 published in Nature Biotechnology, March 1999 (5).

Biragyn Series #2 published in the Journal of Immunology, December 2001 (6).

Biragyn Series #3 published in Blood, August 2002 (7).

Biragyn Series #4 published in Science, November 2002 (8).

Biragyn Series #5 published in the Journal of Leukocyte Biology, July 2004 (9).

Biragyn Series #6 published in Blood, October 2004 (10).

Biragyn Series #7 published in Blood, June 2006 (11).

Biragyn Series #8 published in the Journal of Immunology, July 2007 (12).

Biragyn #1. The first paper introduces the concept of the chemokine vaccine. In this issue, interferon inducible protein 10 (IP10) and monocyte chemotactic protein 3 (MCP3) were fused to lymphoma antigen, lymphoma Ig variable region (sFv). Biragyn #1 tests both protein and DNA vaccines while the rest of the series focuses on DNA vaccines for *in vivo* mouse vaccine protective immunity testing. The importance of the fusion is also demonstrated as vaccination of chemokine and antigen separately did not

elicit as potent of an immune response as their fused counterparts. The mechanism of the chemokine vaccine is not explored in depth in this issue. However, it is in this issue where T-cell immunity is demonstrated to be required for the vaccine to work.

Biragyn #2. The following paper introduces mBD2 and macrophage-inflammatory protein (MIP-3α) as the chemokine receptor ligands with the capacity to enhance antigen specific immune response. It is in this paper where mBD2 is shown to chemoattract bone marrow-derived CC chemokine receptor 6 (CCR6) positive immature dendritic cells (DCs) and also CCR6 expressing HEK293 cells. Mature DC and HEK293 without CCR6 expression were not chemoattracted to mBD2 protein thus showing mBD2 and CCR6 interaction. Protection was also demonstrated on mouse lymphoma challenge models when mBD2 and MIP-3α chemokine vaccines were used.

Biragyn #3. This paper moves away from cancer antigens and targets glycoprotein 120 (gp120) a human immunodeficiency virus-1 (HIV-1) antigen. mBD2, monocyte chemoattractant protein 3 (MCP-3/CCL7) and macrophage-derived chemokine (MDC/CCL22) are also tested. Vaccination with constructs with mBD2 produced antigen specific cytotoxic T cell lymphocyte activity and high titers of virus-neutralizing antibodies against gp120.

Biragyn #4. This important paper solely focuses on mBD2. The most important discovery in this paper is mBD2's ability to act on immature DC's Toll-like receptor 4 (TLR4) thus showing mBD2 as an endogenous ligand for TLR4. mBD2 induced up

regulation of costimulatory molecules and DC maturation on immature DC. Also, again demonstrated ability of mBD2 to render nonimmunogenic self tumor antigen immunogenic and elicit anti-tumor therapeutic immunity which requires interferon-γ activity.

Biragyn #5. This paper tries to move away from endogenous chemokines thus introduces two viral chemokines agonists, herpes simplex virus 8 derived macrophage inflammatory protein I (vMIP-I) and antagonist MC138. *In vivo* DNA vaccine tumor protection studies in mice provide evidence of enhanced antigen specific response by the viral chemokine fusions. The antigen tested in this paper is lymphoma antigen lymphoma idiotype.

Biragyn #6 and #7. Both papers are synergistic issues. Biragyn #6 focuses on the involvement of CD4+ T-cell class II pathway while Biragyn #7 focuses on class I CD8+ T-cell immunity. Both papers present the concept of chemokine receptor mediated endocytosis, intracellular trafficking/processing, and crosspresentation of antigen by antigen presenting cell (APC) to T cell. Biragyn #7 also tests additional antigens aside from lymphoma antigen lymphoma idiotype including melanoma antigen, glycoprotein 100 (gp100) and tumor associated embryonic antigen, oncofetal Ag-immature laminin receptor 37-kDa protein (OFA-iLRP).

Biragyn #8. Finally, the authors focus on targeting chemokine receptor CCR6 by using MIP-3α and mBD2. They are capable of demonstrating robust CD8+ T cell anti-tumor antigen specific immune response. The antigen tested is OFA-iLRP.

Section 3. Previous Literature – All about murine β-defensin2

Introduction. The defensin family in general including β defensins have been linked with antimicrobial, antiviral, toxin-neutralizing, and immunomodulatory properties (58).

mBD2. Mouse or murine β-defensin2 (mBD2) also referred to as β-defensin-2, defb2, mDF2β, mBD-2, and officially defensin beta 2 is a small β-sheet peptide linked with antimicrobial properties (8, 59). This defensin is not to be confused with human β-defensin2 whose murine homolog is murine β-defensin3 (60). mBD2 has been shown to play a role in both innate and adaptive immunity through the recruitment of dendritic cells (DC) via CCR6 (6) and activation of DC via TLR4 (8). mBD2's identification was first reported by Morrison et al. in 1999 (61) and shown to share 60% gene identity between mBD2 and murine β-defensin1.

mBD2 focused Papers. The role and mechanism of mBD2 is still unclear as not many papers focus exclusively on mBD2. In the few papers which do focus on mBD2, most papers focus on what induces mBD2 expression and not what it does. Below is a list of papers which focus mostly on mBD2. This is not an exhaustive unabridged list of papers about mBD2 but it is the main ones I was able to gather to date (December 2009). They are shown here in chronological order of publication.

mBD2 Paper #1. The very first paper published by Morrisson et al. in FEBS Lettters January 1999 (61). This is the first paper identifying mBD2. mBD2 is described as

similar to other airway β defensins in sequence. mBD2 is shown as an airway defensin which can be upregulated by lipopolysaccharide (LPS).

mBD2 Paper #2. This paper published by Palazzo et al. in the Journal of Immunology in April 2007 (62) reveals stimulated release of mBD2 by intestinal epithelium when treated with LPS (TLR4 agonist) or flagellin (TLR5 agonist) but not CpG-ODN (TLR9 agonist or CPG).

mBD2 Paper #3. This paper published by Selleri et al. in the British Journal of Dermatology in June 2007 (63) reveals induction of mBD2 by TLR2, TLR4, and TLR5 but not TLR9 agonists by murine hair follicle.

mBD2 Paper #4. Yet another induction paper published by Gariboldi in the Journal of Immunology August 2008 (64), this paper presents low molecular weight hyaluronic acid to induce keratinocytes to express mBD2 via TLR2 and TLR4 signaling.

mBD2 Paper #5. And one more induction paper published by Hussain et al. in the American Journal of Physiology - Lung Cellular and Molecular Physiology in September 2008 (65) shows mBD2 expression by murine pleural mesothelial cells via TLR2 by TLR2 agonist staphylococcal peptidoglycan.

mBD2 Paper #6. In a paper which could be an mBD2 focused extension on the Biragyn series, the authors reveal TLR4-dependent activation of DC by mBD2 (66). This paper was published in the Journal of Leukocyte Biology in April 2008 and is a continuation of

Biragyn #4 (8). The paper reveals that mBD2 can promote TLR-4/MyD88 mediated and Nf-κB dependent death of DC and macrophages via TNFR2. This suggests mBD2 could play a role in the modulation of immune cells and APCs possibly via a mechanism which eliminates activated APCs.

mBD2 Papers #7 and #8. These are two mBD2 papers published by Wu et al. both in the Journal of Immunology 2009 (59, 67). mBD2 paper #8 demonstrates the requirement of mBD2 to prevent Pseudomonas aeurginosa infection in the cornea thus showing anti Gram-negative bacterial properties. mBD2 paper #9 demonstrates mBD2 teaming with mBD3 to eliminate Pseudomonas aeruginosa infection in the cornea more effectively.

Section 4. Previous Literature - murine β-defensin2 and Cancer

Introduction. Due to their role in both innate and adaptive immunity β defensins have cancer therapeutic potential (8, 58). There are three papers to date that use mBD2 for anti-cancer therapy aside from those in the Biragyn series.

mBD2 in Cancer #1 and #2. These two papers are from the same team at Peking Union Medical College. mBD2 in cancer #1 was published in Cancer Research in January 2006 (68) and mBD2 in cancer #2 on Gene Therapy in May 2007 (69). In these papers, the authors use the L1210 murine leukemia model. They use a gene therapy system whereby they transfect an mBD2 expressing expression vector unto L1210 cells to confer its secretion. Accordingly, they produced a vaccine made of irradiated mBD2+ L1210 (L1210-MBD2) cells. The vaccine produced both protective and therapeutic effects. They also revealed the need of natural killer (NK) and CD8+ cells for the vaccine's anti-leukemia activity. Paper #2 shows mBD2 synergy with IL-18 for the anti-leukemia response by the vaccine.

mBD2 in Cancer #3. This paper was published by Wang et al. in Clinical Cancer Research in November 2007 (70). In mBD2 in cancer #3, the authors generated a vaccine using the fusion principle used in the Biragyn series. DNA vaccines consisting of mBD2 fused to murine vascular endothelial growth factor 2 (mFlk-1) antigen was tested, and the vaccine produced protective and therapeutic antitumor immunity. They reveal CD8+ T cell as well as B cell responses to play a role in the antitumor immunity.

Section 5. Contribution of the Study

Contribution in Summary. The study in this dissertation is a continuation of work previously established by the Biragyn series. More specifically, this study focuses on the protein version of the vaccines tested in the Biragyn series. Moreover, this study focuses on testing mBD2 vaccines. The antigen of choice for the vaccine is model antigen soluble chicken ovalbumin (OVA). Antigens human gp100 and murine survivin were also used and tested. To complement the vaccine, TLR agonists were combined as adjuvants with mBD2 vaccines to test synergy. Separately, the vaccine's interaction with crosspresentation, CCR6/TLR4 receptors, and CD8+/CD4+ T cell subsets were explored. Lastly, the protein mBD2 vaccine was tested for synergy with antigen specific adoptive T cell transfer.

As a result, this study adds to previous studies by further exploring mBD2 vaccines as proteins instead of extensively tested DNA, for the first time combining the vaccine with adoptive T cell therapy, exploring the vaccine's effect on vaccine antigen specific class I and class II T cells directly rather than indirectly, and further confirming roles of CCR6 and TLR4 in mBD2 fusion protein vaccine dependent crosspriming. The study revealed that mBD2 vaccines specifically induce CCR6-independent and TLR4-dependent CD8+ T cell directed immunity via an mBD2 fusion mediated crosspresentation enhancement, which challenges the chemokine receptor dependent theoretical model of the mBD2 vaccine. Finally, the study demonstrated the viability and synergy of the combination of mBD2 vaccine with adoptive T cell immunotherapy against tumor.

Chapter 3. mBD2 Vaccine Production

Section 1. Materials

Subsection 1A. Chemokines

β-defensin2. Mouse origin β-defensin2 is also officially known as Defb2 or defensin beta 2 (GeneID: 13215) referred here as simply mBD2. Gene cloning as previously described (6). Sequence is below.

ATGGAACTTGACCACTGCCACACCAATGGAGGGTACTGTGTCAGAGCCATTTGTCCTCC
TTCTGCCAGGCGTCCTGGGAGCTGTTTCCCAGAGAACAACCCCTGTTGCAAGTACATGA
AAGATCTT

MIP-3α. Mouse origin MIP-3α is also officially known as CCL20 chemokine (C-C motif) ligand 20 (GeneID: 20297). Gene cloning as previously described (6). Sequence is below.

ATGGCAAGCAACTACGACTGTTGCCTCTCGTACATACAGACGCCTCTTCCTTCCAGAGC
TATTGTGGGTTTCACAAGACAGATGGCCGATGAAGCTTGTGACATTAATGCTATCATCT
TTCACACGAAGAAAAGAAAATCTGTGTGCGCTGATCCAAAGCAGAACTGGGTGAAAAGG
GCTGTGAACCTCCTCAGCCTAAGAGTCAAGAAGATG

MCP-3. human origin MCP-3 is also officially known as CCL7 chemokine (C-C motif) ligand 7 (GeneID: 6354). Gene cloning as previously described (5). Sequence is below.

ATGGCGCAACCGGTAGGTATAAACACAAGCACAACCTGTTGCTATCGTTTCATAAATAA

AAAGATACCGAAGCAACGTCTGGAAAGCTATCGCCGTACCACTTCTAGCCACTGTCCGC

GTGAAGCTGTTATATTCAAAACGAAACTGGATAAGGAGATCTGCGCCGACCCTACACAG

AAATGGGTTCAGGACTTTATGAAGCACCTGGATAAAAAGACACAGACGCCGAAACTG

RANTES. Mouse origin RANTES is also known as CCL5 chemokine (C-C motif) ligand 5 (GeneID: 20304). Sequence is below. Cloning primers were also provided and was a kind gift by Dr. Hong Qin (M. D. Anderson Cancer Center, Houston, TX).

ATGTCACCATATGGCTCGGACACCACTCCCTGCTGCTTTGCCTACCTCTCCCTCGCGCT

GCCTCGTGCCCACGTCAAGGAGTATTTCTACACCAGCAGCAAGTGCTCCAATCTTGCAG

TCGTGTTTGTCACTCGAAGGAACCGCCAAGTGTGTGCCAACCCAGAGAAGAAGTGGGTT

CAAGAATACATCAACTATTTGGAGATGAGC

RANTES PCR Primers.

Forward - 5'- TTG GAT CCT CGA CAT GGC CTC ACC ATA TGG CTC GGA -3'

Reverse - 5'- TTG AAT CCG CTC ATC TCC AAA TAG TTG AT -3'

Chemokine Spacer. Sequence between the chemokine and antigen is necessary (5) Sequence is below.

GAATTCAACGACGCTCAGGCGCCGAAGAGTCTCGAG

Subsection 1B. Antigens

gp100. Human origin gp100 is also officially known as SILV silver homolog (GeneID: 6490). Sequence is below. The full length gp100 cDNA (Entrez gene ID: 6490) was a kind gift by Dr. Greg Lizee (M. D. Anderson Cancer Center, Houston, TX).

ATGGATCTGGTGCTAAAAAGATGCCTTCTTCATTTGGCTGTGATAGGTGCTTTGCTGGC

TGTGGGGGCTACAAAAGTACCCAGAAACCAGGACTGGCTTGGTGTCTCAAGGCAACTCA

GAACCAAAGCCTGGAACAGGCAGCTGTATCCAGAGTGGACAGAAGCCCAGAGACTTGAC

TGCTGGAGAGGTGGTCAAGTGTCCCTCAAGGTCAGTAATGATGGGCCTACACTGATTGG

TGCAAATGCCTCCTTCTCTATTGCCTTGAACTTCCCTGGAAGCCAAAAGGTATTGCCAG

ATGGGCAGGTTATCTGGGTCAACAATACCATCATCAATGGGAGCCAGGTGTGGGGAGGA

CAGCCAGTGTATCCCCAGGAAACTGACGATGCCTGCATCTTCCCTGATGGTGGACCTTG

CCCATCTGGCTCTTGGTCTCAGAAGAGAAGCTTTGTTTATGTCTGGAAGACCTGGGGCC

AATACTGGCAAGTTCTAGGGGGCCCAGTGTCTGGGCTGAGCATTGGGACAGGCAGGGCA

ATGCTGGGCACACACACCATGGAAGTGACTGTCTACCATCGCCGGGGATCCCGGAGCTA

TGTGCCTCTTGCTCATTCCAGCTCAGCCTTCACCATTACTGACCAGGTGCCTTTCTCCG

TGAGCGTGTCCCAGTTGCGGGCCTTGGATGGAGGGAACAAGCACTTCCTGAGAAATCAG

CCTCTGACCTTTGCCCTCCAGCTCCATGACCCCAGTGGCTATCTGGCTGAAGCTGACCT

CTCCTACACCTGGGACTTTGGAGACAGTAGTGGAACCCTGATCTCTCGGGCACTTGTGG

TCACTCATACTTACCTGGAGCCTGGCCCAGTCACTGCCCAGGTGGTCCTGCAGGCTGCC

ATTCCTCTCACCTCCTGTGGCTCCTCCCCAGTTCCAGGCACCACAGATGGGCACAGGCC

AACTGCAGAGGCCCCTAACACCACAGCTGGCCAAGTGCCTACTACAGAAGTTGTGGGTA

CTACACCTGGTCAGGCGCCAACTGCAGAGCCCTCTGGAACCACATCTGTGCAGGTGCCA

ACCACTGAAGTCATAAGCACTGCACCTGTGCAGATGCCAACTGCAGAGAGCACAGGTAT

GACACCTGAGAAGGTGCCAGTTTCAGAGGTCATGGGTACCACACTGGCAGAGATGTCAA

CTCCAGAGGCTACAGGTATGACACCTGCAGAGGTATCAATTGTGGTGCTTTCTGGAACC

ACAGCTGCACAGGTAACAACTACAGAGTGGGTGGAGACCACAGCTAGAGAGCTACCTAT

CCCTGAGCCTGAAGGTCCAGATGCCAGCTCAATCATGTCTACGGAAAGTATTACAGGTT

CCCTGGGCCCCCTGCTGGATGGTACAGCCACCTTAAGGCTGGTGAAGAGACAAGTCCCC

CTGGATTGTGTTCTGTATCGATATGGTTCCTTTTCCGTCACCCTGGACATTGTCCAGGG

TATTGAAAGTGCCGAGATCCTGCAGGCTGTGCCGTCCGGTGAGGGGGATGCATTTGAGC

TGACTGTGTCCTGCCAAGGCGGGCTGCCCAAGGAAGCCTGCATGGAGATCTCATCGCCA

GGGTGCCAGCCCCCTGCCCAGCGGCTGTGCCAGCCTGTGCTACCCAGCCCAGCCTGCCA

GCTGGTTCTGCACCAGATACTGAAGGGTGGCTCGGGGACATACTGCCTCAATGTGTCTC

TGGCTGATACCAACAGCCTGGCAGTGGTCAGCACCCAGCTTATCATGCCTGGTCAAGAA

GCAGGCCTTGGGCAGGTTCCGCTGATCGTGGGCATCTTGCTGGTGTTGATGGCTGTGGT

CCTTGCATCTCTGATATATAGGCGCAGACTTATGAAGCAAGACTTCTCCGTACCCCAGT

TGCCACATAGCAGCAGTCACTGGCTGCGTCTACCCCGCATCTTCTGCTCTTGTCCCATT

GGTGAGAATAGCCCCCTCCTCAGTGGGCAGCAGGTCTGAGTA

gp100 Truncated. gp100 (Residues 22-236) (gp100T) or gp100 with hydrophobic regions removed while retaining immunogenic epitopes was previously described (11). Sequence is below.

ATGGGGGCTACAAAAGTACCCAGAAACCAGGACTGGCTTGGTGTCTCAAGGCAACTCAG

AACCAAAGCCTGGAACAGGCAGCTGTATCCAGAGTGGACAGAAGCCCAGAGACTTGACT

GCTGGAGAGGTGGTCAAGTGTCCCTCAAGGTCAGTAATGATGGGCCTACACTGATTGGT

GCAAATGCCTCCTTCTCTATTGCCTTGAACTTCCCTGGAAGCCAAAAGGTATTGCCAGA

TGGGCAGGTTATCTGGGTCAACAATACCATCATCAATGGGAGCCAGGTGTGGGGAGGAC

AGCCAGTGTATCCCCAGGAAACTGACGATGCCTGCATCTTCCCTGATGGTGGACCTTGC

CCATCTGGCTCTTGGTCTCAGAAGAGAAGCTTTGTTTATGTCTGGAAGACCTGGGGCCA

ATACTGGCAAGTTCTAGGGGGCCCAGTGTCTGGGCTGAGCATTGGGACAGGCAGGGCAA

TGCTGGGCACACACACCATGGAAGTGACTGTCTACCATCGCCGGGGATCCCGGAGCTAT

GTGCCTCTTGCTCATTCCAGCTCAGCCTTCACCATTACTGACCAGGTGCCTTTCTCCGT

GAGCGTGTCCCAGTTGCGGGCCTTGGATGGAGGGAACAAGCACTTCCTGAGAAATCAG

Ovalbumin. Chicken origin ovalbumin is referenced by tag LOC396058 or NP_990483.1. The full length OVA cDNA (Refseq ID: NM_205152) was a kind gift by Dr. Xiao-Feng Qin (M. D. Anderson Cancer Center, Houston TX). Sequence is below.

ATGGGCTCCATCGGCGCAGCAAGCATGGAATTTTGTTTTGATGTATTCAAGGAGCTCAA

AGTCCACCATGCCAATGANAACATCTTCTACTGCCCCATTGCCATCATGTCAGCTCTAG

CCATGGTATACCTGGGTGCAAAAGACAGCACCAGGACACAAATAAATAAGGTTGTTCGC

TTTGATAAACTTCCAGGATTCGGAGACAGTATTGAAGCTCAGTGTGGCACATCTGTAAA

CGTTCACTCTTCACTTAGAGACATCCTCAACCAAATCACCAAACCAAATGATGTTTATT

CGTTCAGCCTTGCCAGTAGACTTTATGCTGAAGAGAGATACCCAATCCTGCCAGAATAC

TTGCAGTGTGTGAAGGAACTGTATAGAGGAGGCTTGGAACCTATCAACTTTCAAACAGC

TGCAGATCAAGCCAGAGAGCTCATCAATTCCTGGGTAGAAAGTCAGACAAATGGAATTA

TCAGAAATGTCCTTCAGCCAAGCTCCGTGGATTCTCAAACTGCAATGGTTCTGGTTAAT

GCCATTGTCTTCAAAGGACTGTGGGAGAAAGCATTTAAGGATGAAGACACACAAGCAAT

GCCTTTCAGAGTGACTGAGCAAGAAAGCAAACCTGTGCAGATGATGTACCAGATTGGTT

TATTTAGAGTGGCATCAATGGCTTCTGAGAAAATGAAGATCCTGGAGCTTCCATTTGCC

AGTGGGACAATGAGCATGTTGGTGCTGTTGCCTGATGAAGTCTCAGGCCTTGAGCAGCT

TGAGAGTATAATCAACTTTGAAAAACTGACTGAATGGACCAGTTCTAATGTTATGGAAG

AGAGGAAGATCAAAGTGTACTTACCTCGCATGAAGATGGAGGAAAAATACAACCTCACA

TCTGTCTTAATGGCTATGGGCATTACTGACGTGTTTAGCTCTTCAGCCAATCTGTCTGG

CATCTCCTCAGCAGAGAGCCTGAAGATATCTCAAGCTGTCCATGCAGCACATGCAGAAA

TCAATGAAGCAGGCAGAGAGGTGGTAGGGTCAGCAGAGGCTGGAGTGGATGCTGCAAGC

GTCTCTGAAGAATTTAGGGCTGACCATCCATTCCTCTTCTGTATCAAGCACATCGCAAC

CAACGCCGTTCTCTTCTTTGGCAGATGTGTTTCCCCTTAA

Survivin. Mouse origin survivin is also officially known as BIRC5 baculoviral IAP repeat-containing 5 (GeneID: 11799). Survivin gene cloning as previously described (71). Sequence is below.

ATGGGAGCTCCGGCGCTGCCCCAGATCTGGCAGCTGTACCTCAAGAACTACCGCATCGC

CACCTTCAAGAACTGGCCCTTCCTGGAGGACTGCGCCTGCACCCCAGAGCGAATGGCGG

AGGCTGGCTTCATCCACTGCCCTACCGAGAACGAGCCTGATTTGGCCCAGTGTTTTTTC

TGCTTTAAGGAATTGGAAGGCTGGGAACCCGATGACAACCCGATAGAGGAGCATAGAAA

GCACTCCCCTGGCTGCGCCTTCCTCACTGTCAAGAAGCAGATGGAAGAACTAACCGTCA

GTGAATTCTTGAAACTGGACAGACAGAGAGCCAAGAACAAAATTGCAAAGGAGACCAAC

AACAAGCAAAAAGAGTTTGAAGAGACTGCAAAGACTACCCGTCAGTCAATTGAGCAGCT

GGCTGCCTAA

Subsection 1C. Peptides

SIINFEKL. Ovalbumin from chicken (residues 257-264) peptide, anti-MHC Class I (H-2Kb), SIINFEKL (Cat No. H-4866, Bachem, Torrance, CA).

KVPRNQDWL. gp100 (residues 25-33) peptide, anti-MHC Class I (H-2Kb), KVPRNQDWL, was a kind gift by Dr. Willem Overwijk (M. D. Anderson Cancer Center, Houston TX).

mBD2-gp100$_{25\text{-}33}$. mBD2 fused to gp100$_{25\text{-}33}$ epitope (61mer) was custom generated (PiProteomics, Hunstville, AL).

Sequence as follows:

```
MELDHCHTNGGYCVRAICPPSARRPGSCFPENNPCCKYMKDLEFNDAQAPKSKVPRNQDWL
12345678901234567890123456789012345678901234567890123456789012345678901
00000000001111111112222222222333333333344444444455555555566
```

Cysteine residues

C[6] to C[35]

C[13] to C[28]

C[18] to C[36]

Section 2. Protocols

Subsection 2A. DNA Vaccine Production

DNA Vaccine Production. The pCMVE vector based DNA vaccine constructs containing mBD2, murine MIP-3α, murine RANTES, and human MCP-3 fused to full length human gp100 (1989 bp) were generated. The pCMVE vector is an expression DNA vaccine vector described previously (5, 6). The insert of the construct can be removed using restriction enzymes *XhoI* and *SmaI* and replaced with desired new insert. The insert can be amplified by PCR primers and inserted via restriction enzyme cutting and ligation into the pCMVE vector.

Figure 3-2A-1. Schema of all DNA Vaccines.

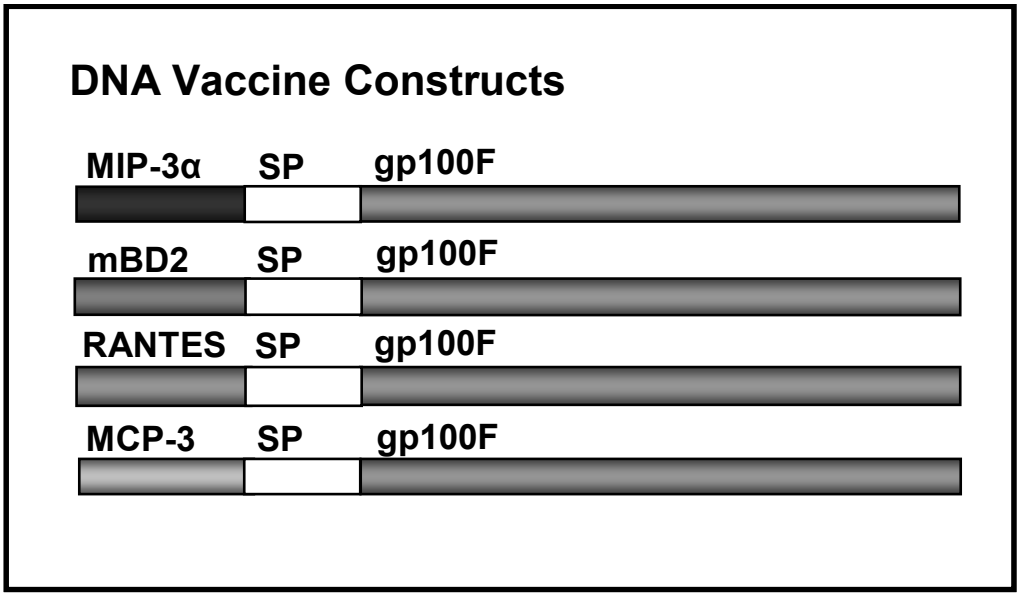

Figure 3-2A-1. The schema of DNA vaccines used on chemokine screen. Candidates mBD2, murine MIP-3α, murine RANTES, and human MCP-3 fused to spacer (SP) then full length melanoma antigen gp100 (gp100F) were tested.

Subsection 2B. Baculovirus Production

Subsection 2B(i). Insert Cloning

pENTR™ TOPO Gateway Intermediate Vector. Intermediate clones using the pENTR™/D vector (Cat No. K2400-20, Invitrogen, Carlsbad, CA) were generated. Incorporation of desired insert into intermediate vector was done as directed in *pENTR™ Directional TOPO® Cloning Kit Manual* (Invitrogen, Carlsbad, CA). The final constructs are as follow: MIP-3α-gp100F, mBD2-gp100F, gp100F, MIP-3α-gp100T, mBD2-gp100T, gp100T, MIP-3α-OVA, mBD2-OVA, OVA, mBD2-survivin, and survivin.

MIP-3α – pENTR™ Primers.

Forward - 5'- CAC CAT GGC AAG CAA CTA CGA CTG T -3'

Forward Extended - 5′ - CAC CAT GGC AAG CAA CTA CGA CTG TTG CCT CTC GTA CAT A -3′

mBD2 – pENTR™ Primers.

Forward - 5'- CAC CAT GGA ACT TGA CCA CTG CCA C -3'

Forward Extended - 5′- CAC CAT GGA ACT TGA CCA CTG CCA CAC CAA TGG AGG GTA C -3′

gp100 Full length – pENTR™ Primers. gp100 Full length is also referred as gp100F.

Forward - 5'- CAC CAT GGA TCT GGT GCT AAA AAG ATG CCT T -3'

Reverse with No Stop Codon - 5'- CTG CTG CCC ACT GAG GAG GGG GCT ATT CTC ACC AAT -3'

gp100 Truncated – pENTR™ Primers. gp100 Truncated is also referred as gp100T.

Forward - 5'- CAC CGA ATT CCT CGA GAT GGG GGC TAC AAA AGT ACC CAG AAA C -3'

Reverse with No Stop Codon - 5'- CTG ATT TCT CAG GAA GTG CTT GTT CCC TCC ATC CAA -3'

Ovalbumin – pENTR™ Primers.

Forward – 5′- CAC CAT GGG CTC CAT CGG CGC AGC AAG C -3′

Reverse with No Stop Codon - 5'- AGG GGA AAC ACA TCT GCC AAA GAA GAG AAC GGC GTT GGT -3'

Survivin – pENTR™ Primers.

Forward - 5'- CAC CAT GGG AGC TCC GGC GCT GCC CCA G -3'

Reverse with No Stop Codon - 5'- GGC AGC CAG CTG CTC AAT TGA CTG ACG GGT AGT CTT TGC -3'

Subsection 2B(ii). Baculovirus Recombination

Summary. The baculovirus specific to the pENTR™ constructs described above was generated as specified in *BaculoDirect™ Baculovirus Expression System Manual* - Version I 16 January 2009 (Cat No. 12562-013, Invitrogen, Carlsbad, CA).

Virus Generation Protocol.

1. Perform a LR recombination reaction with single pENTR™ intermediate vector clones described in section above and BaculoDirect™ Linear C-Term DNA (Cat No. 12562-019, Invitrogen, Carlsbad, CA) using LR Clonase II for BaculoDirect™ Kits (Cat No. 11791023 Invitrogen, Carlsbad, CA) using guidelines from pages 9-11 of the *BaculoDirect™ Baculovirus Expression System Manual.*
2. Transfect recombinant baculovirus generated in step 1 unto SF9 insect cells using steps described from pages 12-17 of the *BaculoDirect™ Baculovirus Expression System Manual* to obtain P1 virus.
3. Send P1 virus to Baylor College of Medicine's Baculovirus/Monoclonal Antibody Core Facility (Houston, TX) for further Baculovirus tittering and eventual expansion. Protocols for virus tittering and virus expansion are proprietary of the Baylor College of Medicine's Baculovirus/Monoclonal Antibody Core Facility (Houston, TX) which was headed by Kurt Christensen as of December 2009. But the tittering and expansion principles are similar to the ones described in the *BaculoDirect™ Baculovirus Expression System Manual* under the Plaque Assay and Preparing High-Titer Viral Stock sections.
4. Prior to the production of a high-titer viral stock, perform baculovirus isolation from single plaques in order to generate a viral stock from a single viral clone. Perform virus isolation from plaques after a plaque assay through Baylor College of Medicine's Baculovirus/Monoclonal Antibody Core Facility (Houston, TX). Pick ten clones at random for each baculovirus for each plaque assay to see if

desired insert has integrated in the baculovirus. Infect SF9 cells with baculovirus at M. O. I. of 2 for 48 hours, pellet, and send for screening.

5. Test the ten single clone pellets to see if they infected the insect cells to express the desired protein. In order to do this, lyse pellets with single detergent lysis buffer. Test the lysed protein supernatant for binding with desired primary antibodies via Western Blot. Use the following antibodies to test desired protein expression. All proteins were tested with anti-6x His-Tag antibody (His-probe (His17): sc-51946, Santa Cruz Biotechnology, Santa Cruz, CA). OVA proteins were tested with anti-OVA antibody (Cat No. sc58820, Santa Cruz Biotechnology, Santa Cruz, CA) or anti-OVA antibody (Cat No. AB1225, Chemicon, Temecula, CA). Survivin proteins were tested with anti-survivin antibody (Cat No. sc58820, Santa Cruz Biotechnology, Santa Cruz, CA). gp100 protein was tested with anti-gp100 antibody (Cat No. 36-0500, Zymed, San Francisco, CA).
6. After verification of pellets which are positive for desired product, expand the single clone baculovirus to produce a high titer viral stock through Baylor College of Medicine's Baculovirus/Monoclonal Antibody Core Facility (Houston, TX).

Inventory. The final baculovirus constructs inventory is as follow: MIP-3α-gp100F, mBD2-gp100F, gp100F, MIP-3α-gp100T, mBD2-gp100T, gp100T, MIP-3α-OVA, mBD2-OVA, OVA, mBD2-survivin, and survivin.

Table 3-2B(ii)-1. Table of Protein Predicted Sizes.

Protein	Weight (kDa)
mBD2-gp100F	76
mBD2-gp100T	29.9
mBD2-OVA	48.5
mBD2-survivin	22.3
MIP-3α-gp100F	79.7
MIP-3α-gp100T	33.3
MIP-3α-OVA	52.2
Gp100F	70.3
Gp100T	23.9
OVA	42.8
Surviving	16.3

Table 3-2B(ii)-1. Predicted sizes for inventory of recombinant proteins generated for vaccination. Predicted weight sizes assist in the validation of the expression of desired protein by protein specific baculovirus infected SF9 cells. Predicted sizes were determined using Compute pI/Mw (http://www.expasy.ch/tools/pi_tool.html).

Subsection 2C. Protein Vaccine Production

Subsection 2C(i). Protein Expression

Summary. Once again, Baylor College of Medicine's Baculovirus/Monoclonal Antibody Core Facility (Houston, TX) was in charge of producing high-throughput large-scale quantities of baculovirus infected SF9 insect cell protein. Small quantities were originally expressed in conventional spinner cultures, but large quantities, the amount used through most of the experiments, were expressed using 5L oxygenated bioreactors (Applikon 5L oxygenated bioreactors). Protocols for large-scale protein expression are proprietary of Baylor College of Medicine's Baculovirus/Monoclonal Antibody Core Facility (Houston, TX) which was headed by Kurt Christensen as of December 2009. But the core principles of protein expression are similar to the ones described in the *BaculoDirect™ Baculovirus Expression System Manual* (Invitrogen, Carlsbad, CA) under the Expressing Recombinant Protein heading. For large-scale protein production the cells used were SF9 insect cells infected with an M. O. I. of 2 and cell harvest after 48 hours post initial infection. The average number of SF9 cells is 10 billion cells. The baculoviruses used do not have a secretion leader hence the desired protein is expressed intracellularly. We asked the core facility to harvest the cells in aliquots of $500x10^6$ in 20 vials. The aliquots were to be centrifuged and washed twice with PBS and then pelleted in 50 mL polypropylene conical centrifuge tubes (Cat No. 352070, Becton Dickinson, Franklin Lakes, NJ). The pellets were then stored at negative 80°C till purification.

Subsection 2C(ii). Protein Purification

Summary. Purification of proteins were performed with the use of Ni-NTA affinity chromatography. Protein purification conditions for protein purification varied and were optimized according to protein. *The QIAexpressionist Handbook - A handbook for high-level expression and purification of 6xHis-tagged proteins* (June 2003 Edition) (QIAGEN, Valencia, CA), Protocol 16 (Purification of 6xHis-tagged proteins from baculovirus infected insect cells under native conditions) was used as purification guideline. The final optimized general protocol in detail was used with minor modifications throughout to purify all proteins. The final proteins are as follow: MIP-3α-gp100T, mBD2-gp100T, gp100T, MIP-3α-OVA, mBD2-OVA, OVA, mBD2-survivin, and survivin.

Figure 3-2C(ii)-1. Schema of all Vaccine Proteins

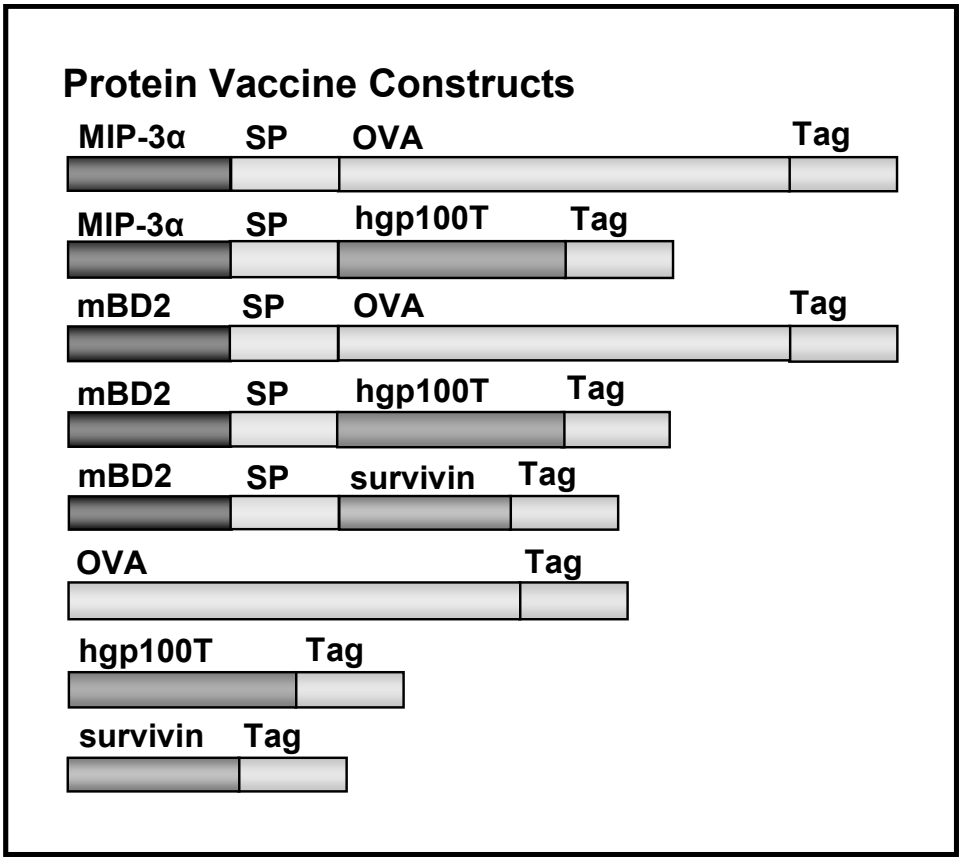

Figure 3-2C(ii)-1. The final recombinant proteins are as follow: MIP-3α-gp100T, mBD2-gp100T, gp100T, MIP-3α-OVA, mBD2-OVA, OVA, mBD2-survivin, and survivin. Fusion proteins with full length gp100 (gp100F) were purified but with very much difficulty and thus we focused on truncated gp100 (gp100T) protein instead.

Protocol for Protein Purification.

The protocol assumes the purification of one vial of $500x10^6$ pelleted and frozen insect cells provided by the Baylor College of Medicine's Baculovirus/Monoclonal Antibody Core Facility (Houston, TX) as described in Subsection 2C(i).

Buffers as described on *Qiaexpressionist* manual pg. 114 – summary reposted below.

Lysis Buffer: 50mM NaH2PO4, 300 mM NaCl, 10 mM imidazole, pH = 8.0

Wash Buffer: 50mM NaH2PO4, 300 mM NaCl, 20 mM imidazole, pH = 8.0

Elution Buffer: 50mM NaH2PO4, 300 mM NaCl, 250 mM imidazole, pH = 8.0

1. Resuspend vial in 10mL of Lysis Buffer with 2% Igepal CA-630 (Cat No. I8896-100ML, Sigma-Aldrich, St. Louis, MO) to lyse the cells. Vortex the vial until frozen pellet dissolves and becomes a homogeneous mixture with Lysis buffer.
2. Sonicate mixture for 15-30 seconds on Branson Sonifier 150 Sonicator (Branson, Danbury, CT) at Level 7 (100 watts of power).
3. Centrifuge the mixture in 50mL polypropylene conical tube described above at 10,000rpm (11,292g) on a Sorvall Legend RT (Thermo Scientific, Waltham, MA) at 4°C for 10 minutes.
4. Save supernatant and place supernatant on new 50mL polypropylene conical tube. Discard pellet with cellular debris. Repeat Step 3.
5. Save supernatant and discard pellet. Place supernatant in new 50mL polypropylene conical tube with 1mL of Ni-NTA Superflow slurry (Cat No. 30430, Qiagen, Valencia, CA). Mix gently by placing on rotary sharker 200 rpm at 4°C for 1 hour.

6. Load lysate with Ni-NTA unto Econo-Pac Chromatography Column (Cat No. 732-1010, Bio-Rad, Hercules, CA). Remove column cap and let flow through pass. Wash with 10mL of Wash buffer and let flow through pass. Discard flow through.
7. Place Econo-Column funnel (Cat No. 731-0003, Bio-Rad, Hercules, CA) onto column. Wash column with 90mL of Wash buffer. Let flow through pass.
8. The force of gravity might not be enough to pull flow-through down. In this case, break the column (by taking serological pipette and homogenizing Ni-NTA with lysate and wash buffer) to reinitiate flow and/or take lysate with Ni-NTA unto new column. Let flow through run until all the Wash buffer has flowed through. Discard flow through. Alternatively, the Bio-Rad Econo Pump (Model EP-1 Econo Pump 731-8140EDU, Bio-Rad, Hercules, CA) can be used. Making sure to stop pump before all the wash buffer runs out as this could cause loss of protein.
9. Once all the Wash buffer has flowed through. Immediately elute protein by placing 7mL of Elution Buffer. Collect all elution buffer flow through. After 3mL of flow has been collected, cap the Econo-Column Funnel with the Funnel cap connected via tube to a 30mL syringe. Once cap is placed place 30mL of additional air-pressure with syringe in order to elute the remaining elution buffer.
10. Save eluate and store at 4°C.
11. The eluate's buffer must be exchanged. Place eluate on Amicon Ultra-4 Centrifugal Filter Unit with Ultracel-3 membrane (Cat No. UFC800308, Millipore, Bilerica, MA). Centrifuge eluate at 3000 rpm (1016 g) for 10 minutes on a Sorvall Legend RT (Thermo Scientific, Waltham, MA) at 4°C. Add PBS to brim. Repeat

centrifugation and addition of PBS fifteen times, also making sure to resuspend protein to solvent.

12. Store all protein at 4°C protected from light.
13. Check protein for endotoxin levels by QCL-1000® Endpoint Chromogenic LAL (Limulus Amebocyte Lysate) Assay (Cat No. 50-647U, Lonza, Basel, Switzerland) as instructed by their protocol.
14. Remove endotoxin from protein using Detoxi-Gel Endotoxin Removing Columns (Cat No. 20344, Thermo Scientific, Waltham, MA) as instructed in their protocol.

Subsection 2C(iii). Protein Validation

Protein Validation by Electrophoresis on SDS PAGE. 5µg of protein along with sample buffer was loaded unto 8-16% Polyacrylamide Gels (Cat No. NG11-816, NuSep, Lawrenceville, GA) in Tris/Glycine/SDS running buffer (25 mM Tris, 192 mM glycine, 0.1% SDS, pH 8.3, Cat No. 161-0772, Bio-Rad, Hercules, CA). After protein electrophoresis, gel with separated protein was placed with Imperial™ Protein Stain (Cat No. 24615, Thermo Scientific, Waltham, MA) for one hour. Gel was then washed with deionized water until bands were visible. Purity of protein was determined by the relative amount of unspecific bands versus target protein.

Protein Validation by Mass Spectrometry Analysis of Proteins. After protein electrophoresis and coomasie staining, bands of correct size of desired protein were cut and sent to the Proteomics Facility at The University of Texas M. D. Anderson Cancer Center (Houston, TX) headed as of December 2009 by David H. Hawke, Ph.D.

Protein Validation via Western Blot. Protein was validated by western blot with corresponding antibodies. Following antibodies were used to test desired protein expression. All proteins were tested with anti-6x His-Tag antibody (His-probe (His17): sc-51946, Santa Cruz Biotechnology, Santa Cruz, CA). OVA proteins were tested with anti-OVA antibody (Cat No. sc58820, Santa Cruz Biotechnology, Santa Cruz, CA). Survivin proteins were tested with anti-survivin antibody (Cat No. sc58820, Santa Cruz Biotechnology, Santa Cruz, CA). gp100 proteins were tested with anti-gp100 antibody (Cat No. 36-0500, Zymed, San Francisco, CA). Appropriate Secondary antibodies were used. Optimization of antibodies was also necessary.

Section 3. Results

Subsection 3A. Protein Validation by Electropheresis on SDS PAGE

Summary. All proteins were validated on SDS PAGE to test for the availability of desired protein band as well as undesired bands. Purity was determined based on the amount of desired bands and undesired bands. All OVA series of proteins were relatively easy to purify. Survivin series of proteins were also easy to purify (Data not shown). On the other hand, gp100 series of proteins were extremely difficult to purify.

gp100T Validation by SDS PAGE with Coomasie Stain.

Date: March 22, 2008

Image 3-3A-1. gp100T SDS PAGE.

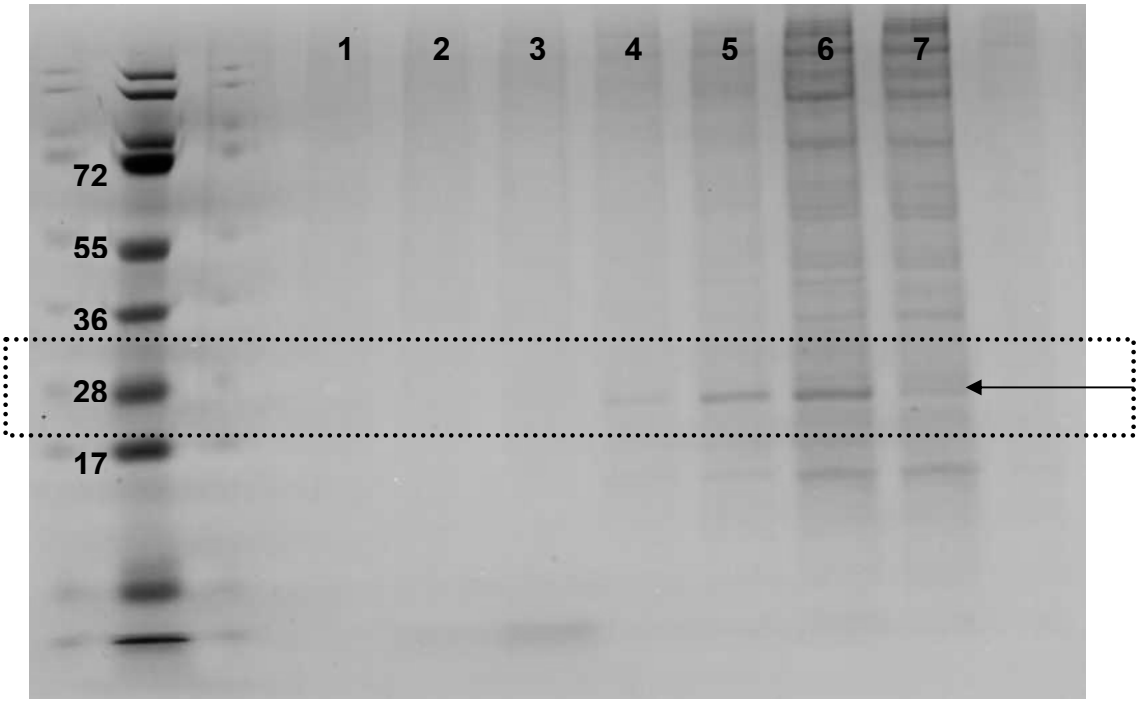

Image 3-3A-1. gp100T protein was purified and elution was collected in fractions of 500µl. gp100T has a predicted size of 23.9 kDa. Fraction 5 shows single dominant band near predicted size. Same band in a separate experiment was later cut and sent for mass spectrometry and shown to have gp100 aligning sequences. Fraction 6 shows gp100T along with impurities.

mBD2-gp100T Validation SDS PAGE with Coomasie Stain.

Date: March 24, 2008

Image 3-3A-2. mBD2-gp100T SDS PAGE.

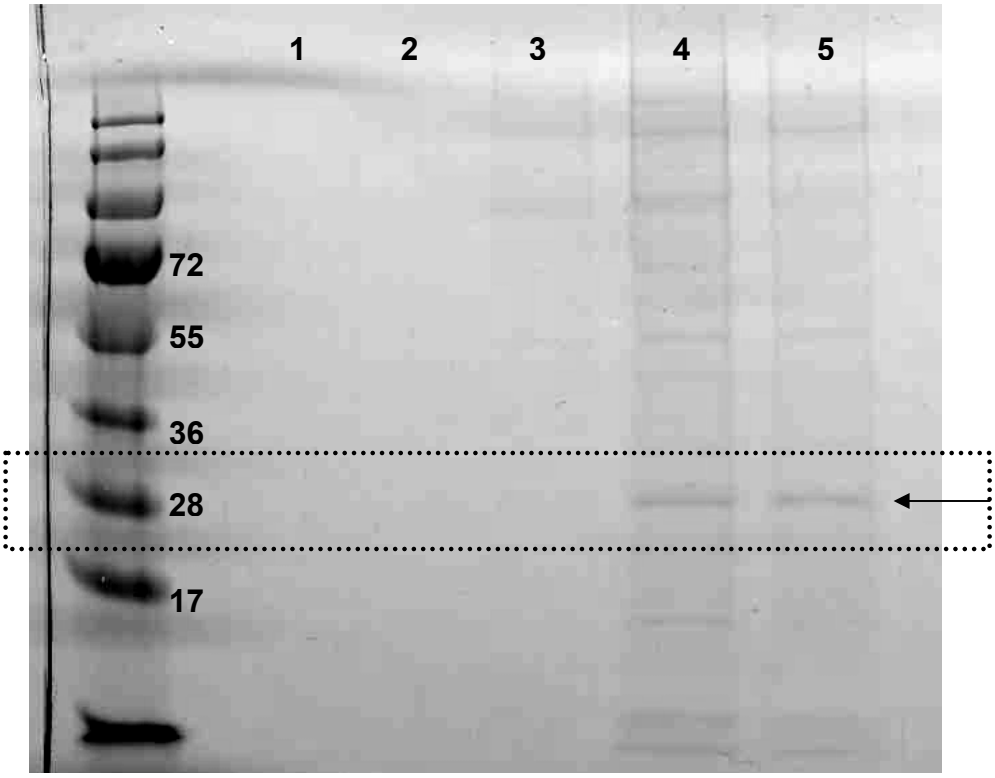

Image 3-3A-2. mBD2-gp100T protein was purified and elution was collected in fractions of 500µl. mBD2-gp100T has a predicted size of 29.9 kDa. Fraction 4 and 5 shows a dominant band near predicted size. Same band in a separate experiment was later cut and sent for mass spectrometry and shown to have gp100 aligning sequences.

mBD2-OVA Validation SDS PAGE with Coomasie Stain.

Date: March 18, 2008

Image 3-3A-3. mBD2-OVA SDS PAGE.

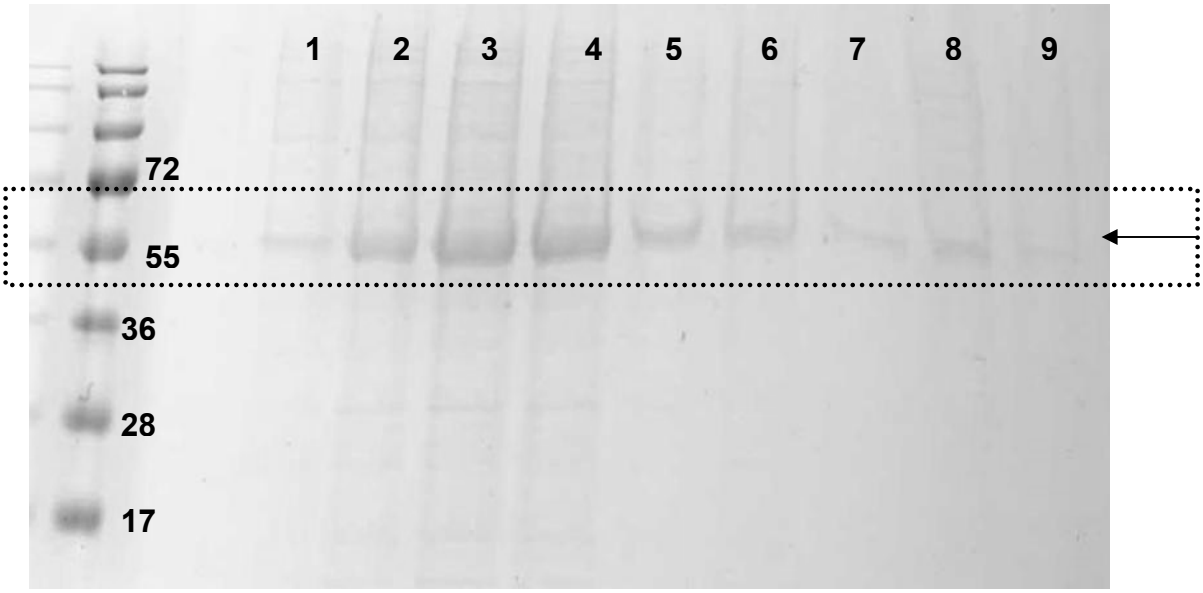

Image 3-3A-3. mBD2-OVA protein was purified and elution was collected in fractions of 500µl. mBD2-OVA has a predicted size of 48.5 kDa. On all fractions a very dominant band near predicted size appears, especially on fractions 2-4. Same band in a separate experiment was later cut and sent for mass spectrometry and shown to have OVA aligning sequences.

MIP-3α-OVA, OVA, and mBD2-OVA Validation SDS PAGE with Imperial Blue Stain

Date: October 2, 2009

Image 3-3A-4. MIP-3α-OVA, OVA, and mBD2-OVA SDS PAGE.

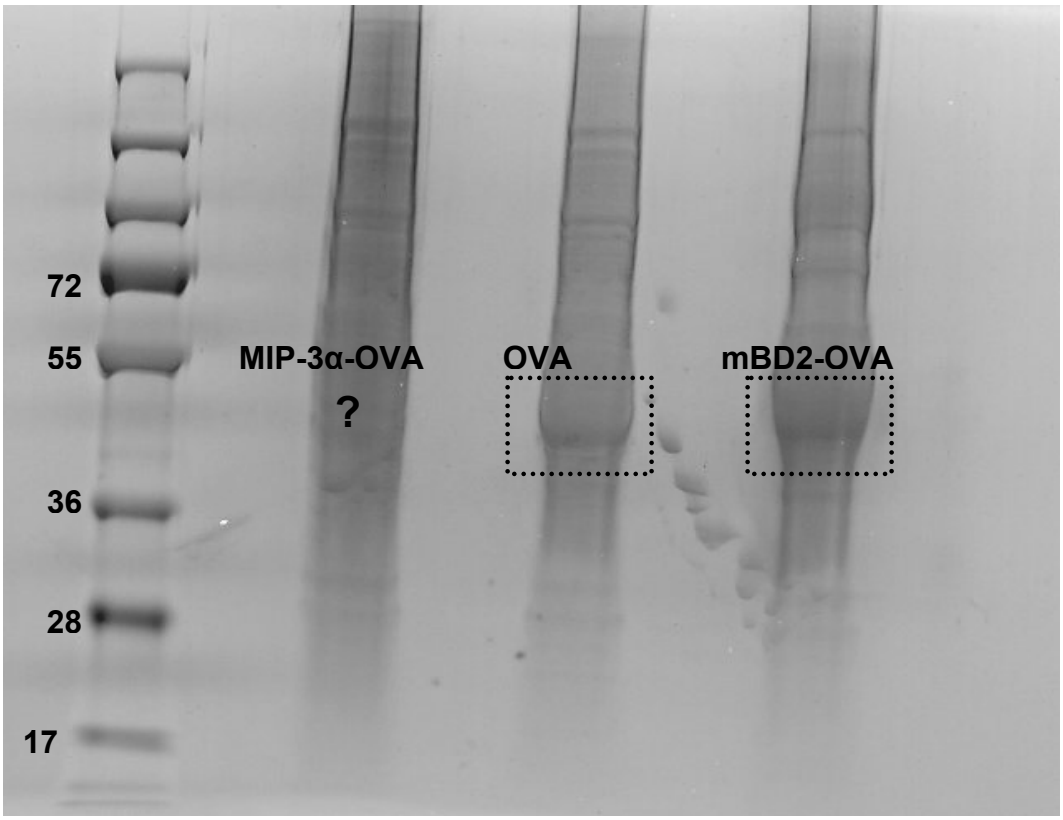

Image 3-3A-4. MIP-3α-OVA, OVA, and mBD2-OVA proteins were purified and concentrated. The image shows concentrated protein. Approximately 20μg of protein has been loaded unto each well. MIP-3α-OVA has a predicted size of 52.2 kDa, OVA has a predicted size of 42.8 kDa, mBD2-OVA has a predicted size of 48.5 kDa. Dominant bands on predicted sizes of respective protein is visible for OVA and mBD2-OVA.

Subsection 3B. Protein Validation by Mass Spectrometry Analysis of Proteins

Subsection 3B(i). Reference Sequences

mBD2 Protein Sequence.

MELDHCHTNGGYCVRAICPPSARRPGSCFPENNPCCKYMKDL

Spacer Protein Sequence.

EFNDAQAPKSLE

gp100T Protein Sequence.

MGATKVPRNQDWLGVSRQLRTKAWNRQLYPEWTEAQRLDCWRGGQVSLKVSNDGPTLIG

ANASFSIALNFPGSQKVLPDGQVIWVNNTIINGSQVWGGQPVYPQETDDACIFPDGGPC

PSGSWSQKRSFVYVWKTWGQYWQVLGGPVSGLSIGTGRAMLGTHTMEVTVYHRRGSRSY

VPLAHSSSAFTITDQVPFSVSVSQLRALDGGNKHFLRNQ

OVA Protein Sequence

MGSIGAASMEFCFDVFKELKVHHANXNIFYCPIAIMSALAMVYLGAKDSTRTQINKVVR

FDKLPGFGDSIEAQCGTSVNVHSSLRDILNQITKPNDVYSFSLASRLYAEERYPILPEY

LQCVKELYRGGLEPINFQTAADQARELINSWVESQTNGIIRNVLQPSSVDSQTAMVLVN

AIVFKGLWEKAFKDEDTQAMPFRVTEQESKPVQMMYQIGLFRVASMASEKMKILELPFA

SGTMSMLVLLPDEVSGLEQLESIINFEKLTEWTSSNVMEERKIKVYLPRMKMEEKYNLT

SVLMAMGITDVFSSSANLSGISSAESLKISQAVHAAHAEINEAGREVVGSAEAGVDAAS

VSEEFRADHPFLFCIKHIATNAVLFFGRCVSP

Subsection 3B(ii). Mass Spectrometry Analysis Results.

mBD2-gp100T Coverage by Mass Spectrometry.

MELDHCHTNGGYCVRAICPPSARRPGSCFPENNPCCKYMKDLEFNDAQAPKSLEMGATK

VPRNQDWLGVSRQLRTKAWNRQLYPEWTEAQRLDCWRGGQVSLKVSNDGPTLIGANASF

SIALNFPGSQKVLPDGQVIWVNNTIINGSQVWGGQPVYPQETDDACIFPDGGPCPSGSW

SQKRSFVYVWKTWGQYWQVLGGPVSGLSIGTGRAMLGTHTMEVTVYHRRGSRSYVPLAH

SSSAFTITDQVPFSVSVSQLRALDGGNKHFLRNQPAFLYKVVRMNQDLGKPIPNPLLGL

DSTRTGHHHHHH

Note:

MELDHCHTNGGYCVRAICPPSARRPGSCFPENNPCCKYMKDLEFNDAQAPKSL

E is mBD2 with spacer portion.

gp100T Coverage by Mass Spectrometry.

MELDHCHTNGGYCVRAICPPSARRPGSCFPENNPCCKYMKDLEFNDAQAPKSMGATKVP

RNQDWLGVSRQLRTKAWNRQLYPEWTEAQRLDCWRGGQVSLKVSNDGPTLIGANASFSI

ALNFPGSQKVLPDGQVIWVNNTIINGSQVWGGQPVYPQETDDACIFPDGGPCPSGSWSQ

KRSFVYVWKTWGQYWQVLGGPVSGLSIGTGRAMLGTHTMEVTVYHRRGSRSYVPLAHSS

SAFTITDQVPFSVSVSQLRALDGGNKHFLRNQ

gp100T Mascot Search Results.

User : Mascot Daemon182

Email :

Search title : Submitted from kwak-park by Mascot Daemon on LMT07-221

MS data file : F:\data\050608gtpL.RAW

Database : Sprot 55.1 (359942 sequences; 129199355 residues)

Taxonomy : Homo sapiens (human) (18957 sequences)

Timestamp : 7 May 2008 at 16:58:33 GMT

Enzyme : Trypsin

Variable modifications : Dioxidation (M),Gln->pyro-Glu (N-term Q),Oxidation (M),Sulfonate (C),Dioxidation (C),Trioxidation (C),Trp->Hydroxykynurenin (W),Trp->Kynurenin (W),Trp->Oxolactone (W)

Mass values : Average

Protein Mass : Unrestricted

Peptide Mass Tolerance : ± 2 Da

Fragment Mass Tolerance: ± 1 Da

Max Missed Cleavages : 2

Instrument type : ESI-TRAP

Number of queries : 948

Protein hits :

K2C1_HUMAN Keratin, type II cytoskeletal 1 - Homo sapiens (Human)

K1C9_HUMAN Keratin, type I cytoskeletal 9 - Homo sapiens (Human)

PME17_HUMAN Melanocyte protein Pmel 17 precursor - Homo sapiens (Human)

K1C10_HUMAN Keratin, type I cytoskeletal 10 - Homo sapiens (Human)

mBD2-OVA Coverage by Mass Spectrometry.

MELDHCHTNGGYCVRAICPPSARRPGSCFPENNPCCKYMKDLEFNDAQAPKSMGSIGAA

SMEFCFDVFKELKVHHANXNIFYCPIAIMSALAMVYLGAKDSTRTQINKVVRFDKLPGF

GDSIEAQCGTSVNVHSSLRDILNQITKPNDVYSFSLASRLYAEERYPILPEYLQCVKEL

YRGGLEPINFQTAADQARELINSWVESQTNGIIRNVLQPSSVDSQTAMVLVNAIVFKGL

WEKAFKDEDTQAMPFRVTEQESKPVQMMYQIGLFRVASMASEKMKILELPFASGTMSML

VLLPDEVSGLEQLESIINFEKLTEWTSSNVMEERKIKVYLPRMKMEEKYNLTSVLMAMG

ITDVFSSSANLSGISSAESLKISQAVHAAHAEINEAGREVVGSAEAGVDAASVSEEFRA

DHPFLFCIKHIATNAVLFFGRCVSP

mBD2-OVA Mascot Search Results.

User : Mascot Daemon LTQ

Email : dhawke@mdanderson.org

Search title : 050608chordata-sprot (C:\Program Files\Matrix Science\Mascot Daemon\chordata-sprot.par), submitted from Daemon on LTQ10156

MS data file : C:\Xcalibur\data\08Q2\050608bov.RAW

Database : Sprot 55.1 (359942 sequences; 129199355 residues)

Taxonomy : Chordata (vertebrates and relatives) (73901 sequences)

Timestamp : 6 May 2008 at 19:30:49 GMT

Enzyme : Trypsin

Variable modifications : Gln->pyro-Glu (N-term Q),Oxidation (M),Sulfonate (C)

Mass values : Average

Protein Mass : Unrestricted

Peptide Mass Tolerance : ± 2 Da

Fragment Mass Tolerance: ± 1 Da

Max Missed Cleavages : 2

Instrument type : ESI-TRAP

Number of queries : 1801

Protein hits :

ALBU_BOVIN Serum albumin precursor - Bos taurus (Bovine)

K1C10_HUMAN Keratin, type I cytoskeletal 10 - Homo sapiens (Human)

OVAL_CHICK Ovalbumin - Gallus gallus (Chicken)

K22E_HUMAN Keratin, type II cytoskeletal 2 epidermal - Homo sapiens (Human)

K2C1_HUMAN Keratin, type II cytoskeletal 1 - Homo sapiens (Human)

K1C9_HUMAN Keratin, type I cytoskeletal 9 - Homo sapiens (Human)

TRYP_PIG Trypsin precursor - Sus scrofa (Pig)

TBA1C_BOVIN Tubulin alpha-1C chain - Bos taurus (Bovine)

CASA1_BOVIN Alpha-S1-casein precursor - Bos taurus (Bovine)

K2C75_BOVIN Keratin, type II cytoskeletal 75 - Bos taurus (Bovine)

CASA2_BOVIN Alpha-S2-casein precursor [Contains: Casocidin-1 - Bos taurus (Bovine)

TBB1_GADMO Tubulin beta-1 chain - Gadus morhua (Atlantic cod)

CXCR3_BOVIN C-X-C chemokine receptor type 3 - Bos taurus (Bovine)

RBBP4_BOVIN Histone-binding protein RBBP4 - Bos taurus (Bovine)

UVS2_XENLA Embryonic protein UVS.2 precursor - Xenopus laevis (African clawed frog)

MED11_XENLA Mediator of RNA polymerase II transcription subunit 11 - Xenopus laevis (African clawed frog)

CASK_BOVIN Kappa-casein precursor [Contains: Casoxin-C; Casoxin-6; Casoxin-A; Casoxin-B; Casoplatelin] - Bos taurus (Bovine)

KV6A9_MOUSE Ig kappa chain V-VI region NQ6-8.3.1 - Mus musculus (Mouse)

SYIM_CIOIN Probable isoleucyl-tRNA synthetase, mitochondrial - Ciona intestinalis (Transparent sea squirt)

MYH11_CHICK Myosin-11 - Gallus gallus (Chicken)

Subsection 3B(iii). Protein Validation by Western Blot

Summary. All proteins were individually bound to nitrocellulose membrane then coincubated with target specific antibody to test presence of target. Target proteins included gp100 and OVA. Protein presence was also validated with 6x His-tag antibody as all recombinant proteins had a 6x His-tag. Presence of mBD2 was seen by the size shift when comparing the same protein with or without mBD2 fusion.

Western Blot Membrane of gp100T, mBD2-gp100T, and mBD2-OVA with His-tag Antibody

Date: August 11, 2008

Image 3-3C-1. Western Blot Membrane of gp100T, mBD2-gp100T, and mBD2-OVA

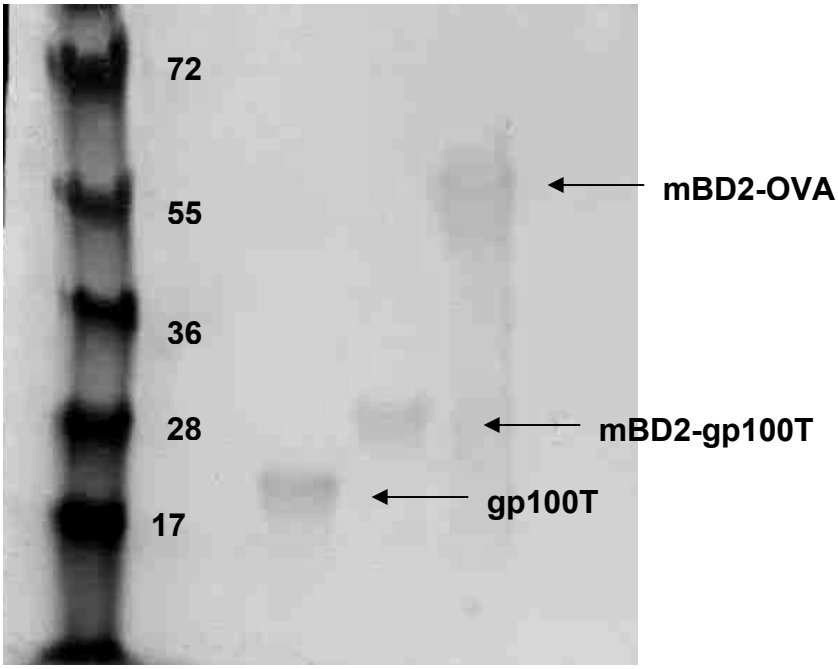

Image 3-3C-1. This image is of nitrocellulose membrane bound with gp100T, mBD2-gp100T, and mBD2-OVA protein which was incubated with anti 6x His-Tag antibody (1:5000 dilution) and later HRP conjugated anti-Mouse IgG secondary antibody (1:5000 dilution). This is not the film but the nitrocellulose membrane itself which after exposure with chemiluminescent substrate left visible brown stains on nitrocellulose. The stains correspond to the correct predicted sizes of the target proteins.

Western Blot of mBD2-gp100T, gp100T, and mBD2-OVA with His-tag Antibody

Date: October 6, 2008

Image 3-3C-2. Western Blot of mBD2-gp100T, gp100T, and mBD2-OVA

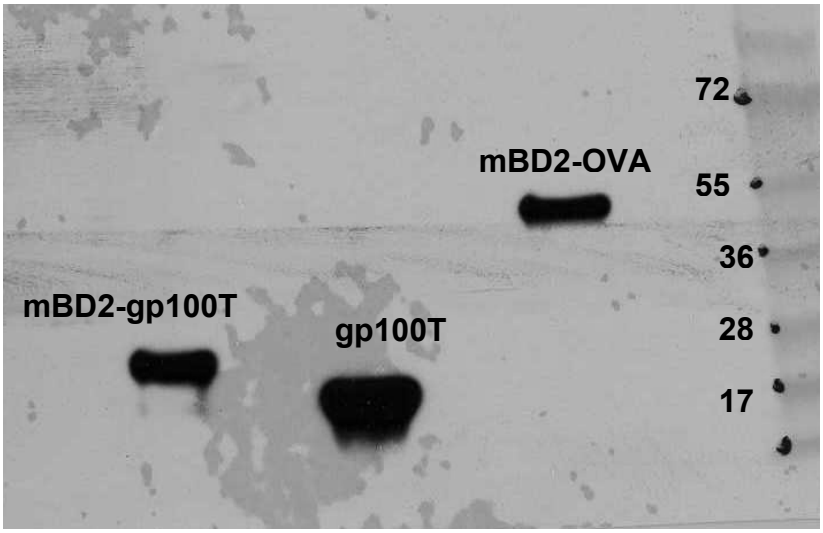

Image 3-3C-2. Predicted size for respective proteins are: mBD2-gp100T - 33.3 kDa, gp100T – 23.9 kDa, and mBD2-OVA – 48.5 kDa. Protein bound membrane was incubated with anti-6x His-Tag antibody (1:10000 dilution). Predicted sizes match the bands visible on corresponding size.

Western Blot of gp100, mBD2-gp100T, and gp100T with gp100 Antibody

Date: October 7, 2008

Image 3-3C-3. Western Blot of gp100F, mBD2-gp100T, and gp100T

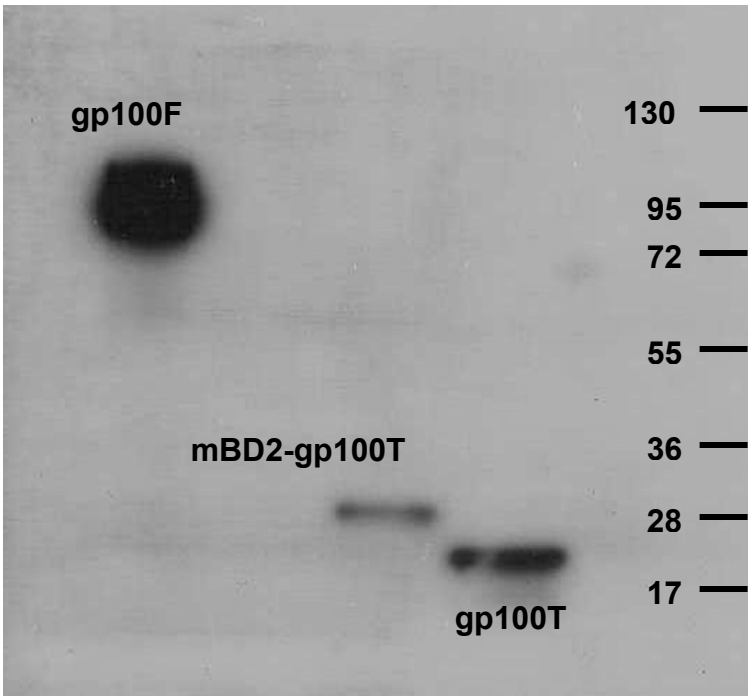

Image 3-3C-3. Predicted size for respective proteins are: gp100F – 70.3 kDa, mBD2-gp100T – 29.9 kDa, and gp100T – 23.9 kDa. Protein bound membrane was incubated with anti-gp100 antibody (1:5000 dilution) and secondary HRP conjugated anti-chicken IgG antibody (1:10000 dilution). Predicted sizes match the bands visible on corresponding size.

Western Blot of OVA (Commercial), MIP-3α-OVA, and mBD2-OVA with OVA Antibody

Date: February 12, 2008

Image 3-3C-4. Western Blot of OVA, MIP-3α-OVA, and mBD2-OVA

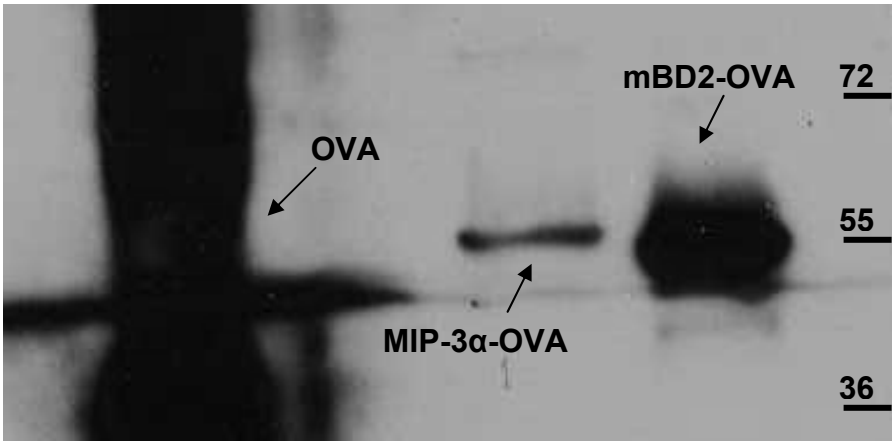

Image 3-3C-4. Predicted size for respective proteins are: OVA – 42.8 kDa, MIP-3α-OVA – 52.2 kDa, and mBD2-OVA – 48.5 kDa. Commercial OVA was used as positive control on left hand side. Protein bound membrane was incubated with anti-OVA antibody (1:2000 dilution) and secondary HRP conjugated anti-rabbit IgG antibody (1:4000 dilution). Predicted sizes match the bands visible on corresponding size.

Western Blot of mBD2-OVA and OVA with OVA Antibody

Date: June 29, 2009

Image 3-3C-5. Western Blot of mBD2-OVA and OVA

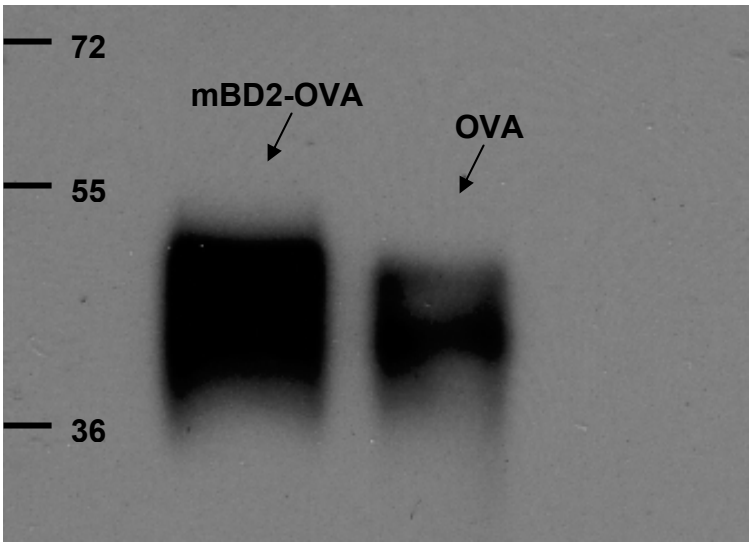

Image 3-3C-5. Predicted size for respective proteins are: mBD2-OVA – 48.5 kDa and OVA – 42.8 kDa. 1 µg of protein bound membrane was incubated with anti-OVA antibody (1:5000 dilution) and secondary HRP conjugated anti-rabbit IgG antibody (1:10000 dilution). Predicted sizes match the bands visible on corresponding size.

Section 4. Discussion

mBD2 Protein Vaccine Construction and Purification.

Thus far, the anti-antigen responses of DNA vaccines have been poor (72). Thus, we hypothesized that the protein counterpart of our DNA vaccines could potentially generate a stronger antigen specific immune response. Indeed, preclinical studies try to avoid recombinant protein vaccine studies because such vaccines come with higher costs and difficulties in production over DNA vaccines (13, 72). Also, protein vaccines are also known for their poor induction of CD8+ T cells (13, 72). We wanted to verify if an mBD2 vaccine could overcome this poor induction and generate a strong CD8+ T cell immune response. In addition, the availability of the protein could help in the elucidation of the mechanism of the chemokine vaccine.

Thus, we placed much effort in generating recombinant MIP-3α and mBD2 fused antigen protein. We decided to focus our efforts in using model antigens, where the antigens have been studied extensively. Thus, we chose ovalbumin (OVA) and gp100. Although, OVA is not a tumor antigen, the availability of transgenic T cell mice for both CD4 and CD8 epitopes made the antigen highly attractive. In addition, tumor models expressing OVA have been used in many studies (73). Thus, the recombinant proteins were generated as shown (Figure 3-2C(ii)-1).

We also decided to generate the protein in a baculovirus insect cell protein expression system over the previously tested bacterial system (5, 8). The bacterial system presented with the problem of high endotoxin contamination. Nevertheless, our proteins have been filtered through an endotoxin removing column and verified for endotoxin contamination.

Overall, optimizing the conditions for protein purification was exceedingly time-consuming. Purifying gp100 protein was especially difficult. After failed attempts of purifying full length gp100 protein, we moved to purifying a gp100 with the hydrophobic regions removed (gp100 Residues 22-236 or gp100T). Even with the truncation, obtaining a very pure fraction of gp100 or chemokine fused gp100 is difficult. MIP-3α in itself presented a problem. The addition of MIP-3α to gp100 made the already difficult purifying process almost impossible. We later decided to outsource production of synthetic MIP-3α fused to gp100 epitope $gp100_{25\text{-}33}$ with the correct folding and disulfide bonds. However, the company also had difficulty synthesizing this protein and after four failed attempts decided to quit the synthesis. However, no problems occurred in the synthesis of mBD2-$gp100_{25\text{-}33}$ with three cyclic disulfide bonds.

On the other hand, the purification of OVA protein has been easier and mBD2-OVA's purification was as easy as well. We again faced difficulty in purifying a MIP-3α protein, MIP-3α-OVA was once again difficult to purify. Difficulty in MIP-3α protein purification was a small reason for focusing on mBD2 for our studies.

Chapter 4. mBD2 Vaccine Efficacy

Section 1. Materials

Mice. C57BL/6 (H-2^b) mice were purchased from the National Cancer Institute (Baltimore, MD). All animals were housed at M. D. Anderson, South Campus Research Building Animal Facility (Houston, TX). Animal care was provided in accordance to M.D. Anderson's institutional animal care and use committee guidelines. Six to ten week old C57BL/6 mice were used for all vaccine efficacy assessment experiments. OT-I (C57BL/6-Tg(TcraTcrb)1100Mjb/J, Stock No. 003831, The Jackson Laboratory, Bar Harbor, ME) were purchased or generously provided by by Dr. Kimberly Schluns (74). pmel-1 mice were provided in cooperation by Dr. Willem Overwijk (75).

Tumors. Mouse melanoma tumors B16 (76) and OVA expressing mouse melanoma tumors B16-OVA (73) were provided as described.

Splenocyte media. RPMI Medium 1640 with GLUTAMAX™-I (Cat No. 61870-127, Invitrogen, Carlsbad, CA) with 10% Fetal Bovine Serum, Certified (Cat No. 16000-044)

Vaccines. The inventory of DNA vaccines: mBD2-gp100F, MIP-3α-gp100F, RANTES-gp100F, and MCP-3-gp100F (Figure 3-2A-1). The inventory of vaccine proteins: MIP-3α-gp100T, mBD2-gp100T, gp100T, MIP-3α-OVA, mBD2-OVA, OVA, mBD2-survivin, and survivin (Figure 3-2C(ii)-1).

Section 2. Protocols

Splenocyte Isolation. OT-I, OT-II, or pmel-1 mice were euthanized via CO_2 chamber. Spleens were removed and placed over a cell strainer which is over a 50mL conical tube and washed with 5mL of splenocyte media. Spleens were smashed with a 3CC syringe plunge over filter and further washed with 10mL of splenocyte media. Cells were spun down at 1500 rpm (485g) on a Sorvall Legend RT+ (Thermo Scientific, Waltham, MA) for 5 min at 4˚C. Wash and spinning was repeated twice more. Splenocytes were resuspended in 3mL RPMI Medium 1640 with GLUTAMAX™-I.

Adoptive Transfer. Each recipient C57BL/6 wildtype ($CD45.2^+$ background) mouse received freshly isolated splenocytes from donor mouse (OT-I, OT-II, or pmel-1) (1/30 of total donor spleen ~1-2x10^6 lymphocytes for OT-I/OT-II and 1/10 of total donor spleen ~3-6x10^6 lymphocytes for pmel-1) via intravenous adoptive transfer on the tail. 100µl of the 3mL splenocyte solution referred above was adoptively infused into each mouse.

DNA Vaccine Immunization. In prophylactic DNA vaccine studies, 50µg of the individual plasmid chemokine vaccine was injected 3 times intramuscularly at two week intervals on right flank of leg.

Protein Vaccine Immunization. With protein vaccine studies, 150µg of recombinant protein for OVA series proteins and 1500µg of recombinant protein for gp100T series

proteins was injected once subcutaneously on right flank of leg right after intravenous adoptive transfer of antigen specific T cells (OT-I or pmel-1). When adjuvants were combined, 50μg of MPL-A (TLR4 agonist, Invivogen, San Diego, CA) or 50μg of CpG ODN 1826 (TLR9 agonist (CPG), IDT Technologies, Coralville, IA) were mixed with recombinant protein and vaccinated using recombinant protein vaccination procedure.

Vesicular Stomatitis Virus Vaccine Immunization. With Vesicular Stomatitis Virus (VSV) immunization, 10^7 PFU of VSV (VSV-OVA or VSV-gp100) was injected once per mouse intraperitoneally after intravenous adoptive transfer of antigen specific T cells.

Tumor Challenge. Tumor Challenge with melanoma tumor cell lines B16 (76) or B16-OVA (73) was done via subcutaneous injection of $1x10^5$ tumor cells/mouse on right flank of leg. This challenge was done 2 weeks after final DNA vaccination or 1 week after adoptive T cell therapy and recombinant protein vaccination.

Tumor Measure and Recording. Tumors were measured with calipers and size (the products of the perpendicular diameters in mm^2) was recorded. Mice with tumor size greater than $400mm^2$ were sacrificed. Survival was recorded and used to determine statistical significant difference via Kaplan-Meier survival analysis with log-rank significance pairwise over strata comparison test. Tumor size and survival was recorded every other day. We performed a minimum of two tumor challenge experiments with the same vaccination schedule and more repetitions followed when the results varied widely.

Statistical Analysis. Statistical analysis to evaluate tumor growth rate differences between experimental and control groups was performed by ANOVA and Wilcoxon's rank-sum tests. Kruskal-Wallis test was used to compare tumor sizes between experimental and control groups. Analysis of survival was compared between experimental and control groups via log-rank significance test. All statistical analysis was done using SPSS statistical software (SPSS, Chicago, IL).

Section 3. Experimental Setup

DNA Vaccine Challenge. For tumor protection experiments, mice were grouped as follows. Group 1 served as the no vaccine control group and was vaccinated with Phosphate Buffered Saline (PBS) solution. Groups 2 to 5 were the experimental groups and received mBD2-gp100F, MCP3-gp100F, MIP-3α-gp100F, and RANTES-gp100F DNA vaccine respectively. Fourteen mice per group were vaccinated subcutaneously on the right thigh three times at 2 week intervals with 50 μg of group determined DNA vaccine aforementioned with the exception of group 1. Two weeks after final booster vaccination, $1x10^5$ B16 melanoma cells (H-2b, gp100+, National Cancer Institute, Frederick, MD) were injected subcutaneously on the right thigh (Tumor Challenge). The groups tested were: mBD2, MCP-3, MIP-3α, and RANTES

Figure 4-3-1. DNA Vaccine Challenge Schema

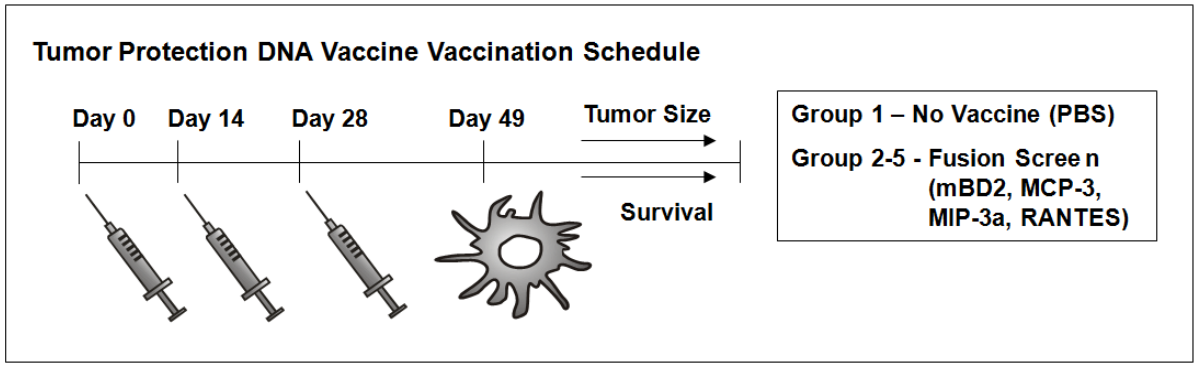

Figure 4-3-1. The vaccination schedule for the screening of mBD2, MCP3, MIP-3α, and RANTES DNA chemokine vaccines in mouse melanoma tumor challenge model.

OT-I Adoptive T cell Therapy and Protein Vaccine Challenge. For tumor protection experiments, mice were grouped as follows. Group 1 served as the no vaccine control group and was vaccinated with Phosphate Buffered Saline (PBS) solution. Group 2 served as an antigen control (to detect effect of antigen alone on protective response) and received OVA protein alone. Group 3 was the experimental group and received mBD2-OVA. Five mice per group underwent adoptive T cell therapy as well as subcutaneous vaccination on the right flank of leg once immediately after adoptive T cell therapy (OT-I) along with 150 μg of group determined protein vaccine aforementioned with the exception of group 1. One week after final booster vaccination, $1x10^5$ B16 melanoma cells (H-2b, gp100+, National Cancer Institute, Frederick, MD) were injected subcutaneously on the right thigh (Tumor Challenge). The groups tested were: mBD2-OVA, OVA, and PBS.

pmel-1 Adoptive T cell Therapy and Protein Vaccine Challenge. For tumor protection experiments, mice were grouped as follows. Group 1 served as the no vaccine control group and was vaccinated with Phosphate Buffered Saline (PBS) solution. Group 2 served as an antigen control (to detect effect of antigen alone on protective response) and received gp100T protein alone. Group 3 was the experimental group and received mBD2-gp100T. Five mice per group underwent adoptive T cell therapy along with subcutaneous vaccination on the right flank of leg once immediately after adoptive T cell therapy (pmel-1) with 1500 μg of group determined protein vaccine aforementioned with the exception of group 1. One week after final booster vaccination, $1x10^5$ B16 melanoma cells (H-2b, gp100+, National Cancer Institute, Frederick, MD) were injected

subcutaneously on the right thigh (Tumor Challenge). The groups tested were: mBD2-gp100T, gp100T, and PBS.

Figure 4-3-2. Adoptive T cell Therapy and Protein Vaccine Challenge Schema

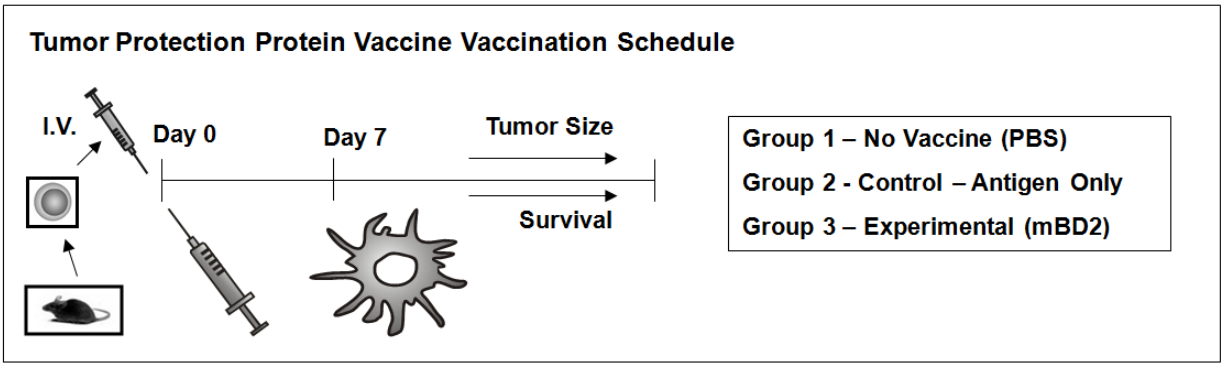

Figure 4-3-2. The vaccination schedule for combination adoptive T cell therapy and protein vaccine test. Experimental (mBD2) was compared against non-mBD2 enhanced antigen alone vaccine and no vaccine groups in mouse melanoma tumor challenge model.

Section 4. Results

Subsection 4A. Chemokine DNA Vaccine Challenge Screen

Summary of Experiment. One DNA vaccine based chemokine screen experiment was performed. A large screen with fourteen mice per group was performed using protocols described in Chapter 4's Section 2 DNA Vaccine Immunization and Section 3 DNA Vaccine Challenge. Chemokines to be screened were mBD2, MCP-3, MIP-3α, and RANTES. Enhanced performance was determined against PBS (No vaccine) control group.

Experiment Date: July 23, 2007 – See Appendix for Chapter 4 (Table A4-4A-1, Table A4-4A-2, Table A4-4A-3, Table A4-4A-4, and Table A4-4A-5) for survival details.

Table 4-4A-1. Chemokine DNA Vaccine Screen Statistical Analysis

Log-rank Pairwise Comparisons

Vaccine	MIP-3α-gp100		mBD2-gp100		MCP-3-gp100		RANTES-gp100		PBS	
	x^2	Sig.	x^2	Sig.	x^2	Sig.	x^2	Sig.	x^2	Sig.
MIP-3α-gp100			.617	.432	3.078	.079	5.506	.019	6.431	.011
mBD2-gp100	.617	.432			1.743	.187	4.676	.031	5.669	.017
MCP-3-gp100	3.078	.079	1.743	.187			.070	.792	.204	.651
RANTES-gp100	5.506	.019	4.676	.031	.070	.792			.030	.862
PBS	6.431	.011	5.669	.017	.204	.651	.030	.862		

Table 4-4A-1. Kaplan-Meier survival analysis with log-rank significance pairwise over strata comparison test. Event based on death and grouped by vaccine type received. The statistical analysis was done using SPSS (SPSS, Chicago, IL). MIP-3α and mBD2 groups have a statistical survival difference with $p < 0.011$ and $p < 0.017$ respectively against PBS group. MCP-3 and RANTES groups do not.

Figure 4-4A-1. mBD2-gp100F DNA Vaccine versus PBS

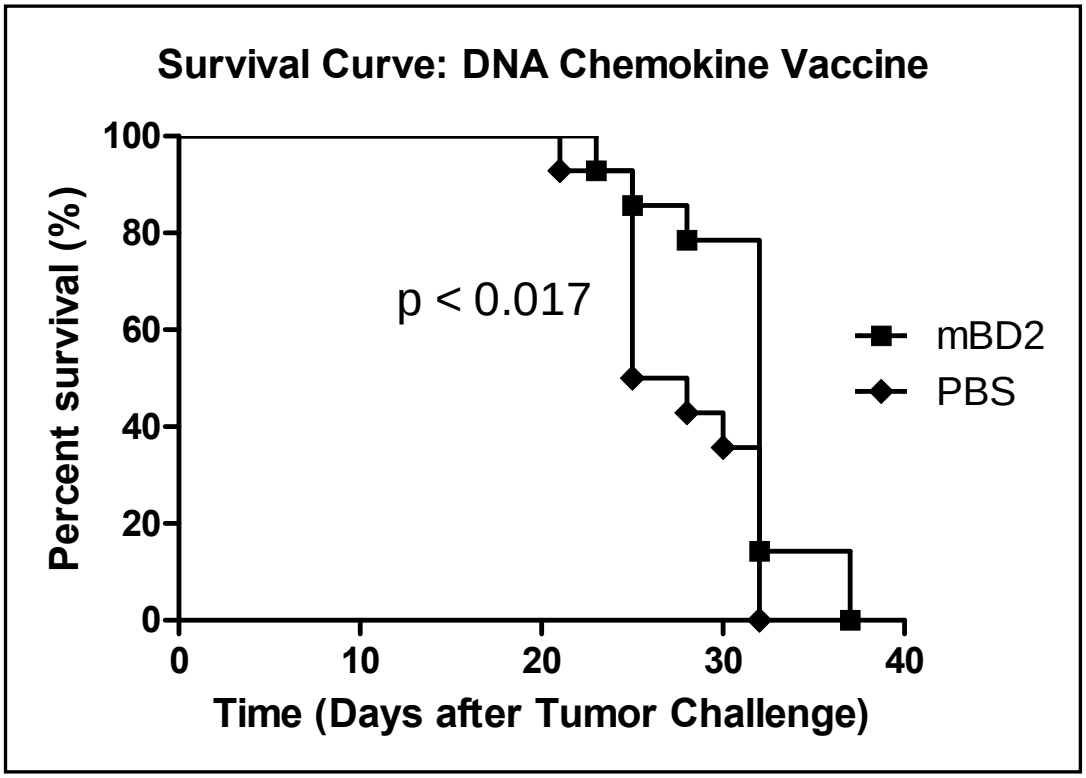

Figure 4-4A-1. Survival curve for mBD2-gp100F versus mock vaccine group which shows statistical difference. Fourteen C57BL/6 mice per group received three 50µg of individual plasmid mBD2 vaccinne or PBS mock vaccine intramuscularly at two week intervals. Two weeks after final vaccination, all mice were challenged with a lethal dose of $1x10^5$ B16 melanoma cells by intraperitoneal injection and were followed for survival. Survival differences between groups were analyzed by log-rank test.

Figure 4-4A-2. MIP-3α-gp100F DNA Vaccine versus PBS

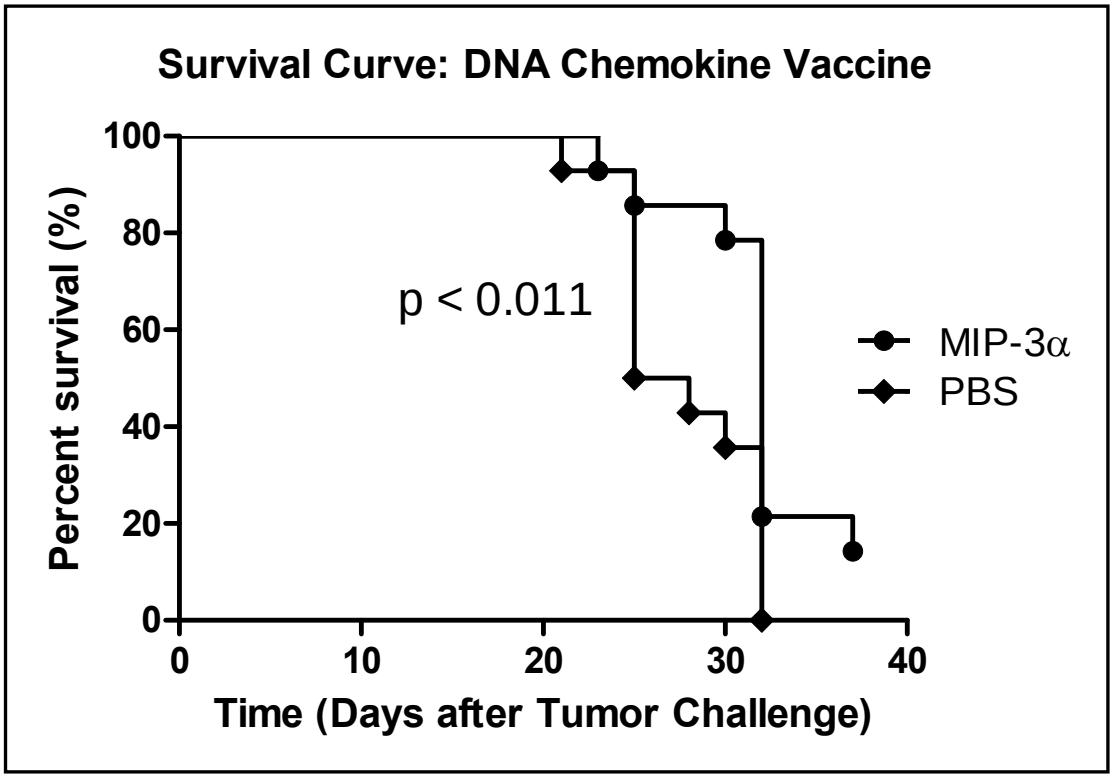

Figure 4-4A-2. Survival curve for MIP-3α-gp100F versus mock vaccine group which shows statistical difference. Fourteen C57BL/6 mice per group received three 50μg of individual plasmid chemokine vaccinne or PBS mock vaccine intramuscularly at two week intervals. Two weeks after final vaccination, all mice were challenged with a lethal dose of $1x10^5$ B16 melanoma cells by intraperitoneal injection and were followed for survival. Survival differences between groups were analyzed by log-rank test.

Figure 4-4A-3. MCP3 or RANTES gp100F DNA Vaccine versus PBS

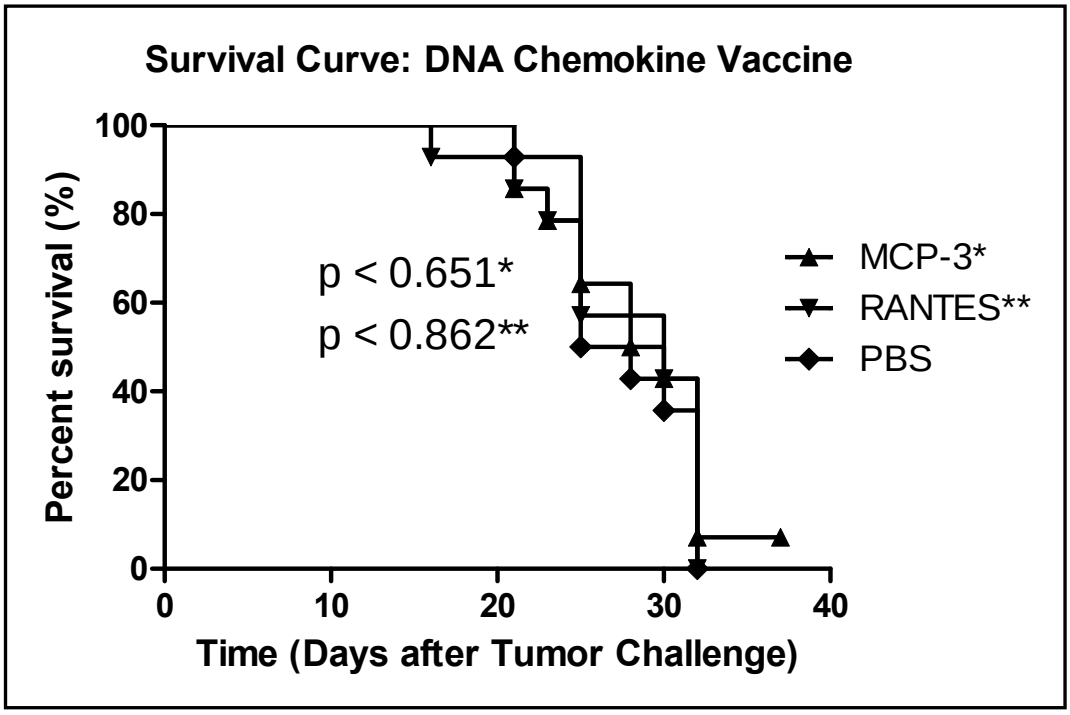

Figure 4-4A-3. Survival Curve for MCP-3-gp100F or RANTES-gp100F versus mock vaccine group which shows no statistical difference. Fourteen C57BL/6 mice per group received three 50µg of individual plasmid chemokine vaccinne or PBS mock vaccine intramuscularly at two week intervals. Two weeks after final vaccination, all mice were challenged with a lethal dose of $1x10^5$ B16 melanoma cells by intraperitoneal injection and were followed for survival. Survival differences between groups were analyzed by log-rank test.

Interpretation of Experiment. DNA vaccines that encode melanoma gp100 antigen fused with various chemokine receptor ligands including mBD2, MIP-3α, MCP-3 and RANTES were generated and compared head-to-head for protective anti-tumor immunity against murine B16 melanoma to determine the optimal ligand for fusion vaccines. Consistent with previous results (11, 12), mBD2 and MIP-3α fusion vaccines were the most potent in protecting mice from lethal dose tumor challenge. No protection was observed in mice vaccinated with MCP-3 or RANTES fused gp100 DNA vaccine. Given the additional advantage of mBD2 in activating TLR4 (8), mBD2 was considered the optimal candidate for further development of corresponding fusion protein vaccines.

Subsection 4B. OT-I Adoptive T cell Therapy and Protein Vaccine Challenge

Summary of Experiments. OT-I adoptive T cell and protein vaccine combination therapy was tested four separate times for tumor protection with groups of five mice per group. The same experiment was repeated using protocols described in Chapter 4's Section 2 Protein Vaccine Immunization and Section 3 OT-I Adoptive T cell Therapy and Protein Vaccine Challenge. These experiments included a vaccine dosage of 150 μg of protein vaccine along with 1/30 of OT-I mouse donor spleen intravenous infusion. mBD2 fused to OVA antigen was the main focus group with OVA (antigen alone) control and PBS (no vaccine) controls tested concurrently. Enhanced performance was determined if the mBD2-OVA group performed statistically better than both OVA and/or PBS groups.

Experiment #1 Date: August 27, 2009

Experiment #2 Date: September 15, 2009

Experiment #3 Date: October 28, 2009

Experiment #4 Date: November 18, 2009

See Appendix for Chapter 4 (Table A4-4B-1, Table A4-4B-2, and Table A4-4B-3) for survival details for all four experiments.

Table 4-4B-1. OT-I Adoptive T cell Therapy and Protein Vaccine Survival Statistical Analysis

Log-rank Pairwise Comparisons

Vaccine	mBD2-OVA		OVA		PBS	
	x^2	Sig.	x^2	Sig.	x^2	Sig.
mBD2-OVA			13.201	.000	39.644	.000
OVA	13.201	.000			14.886	.000
PBS	39.644	.000	14.886	.000		

Table 4-4B-1. Kaplan-Meier survival analysis with log-rank significance pairwise over strata comparison test. Event based on death and grouped by vaccine type received. The statistical analysis was done using SPSS (SPSS, Chicago, IL). Statistical survival difference p-values are as follow: mBD2-OVA versus OVA: 2.798572187848908E-4, mBD2-OVA versus PBS: 3.0480778759356397E-10, and OVA versus PBS - 1.1419146936646935E-4.

Figure 4-4B-1. OT-I Adoptive T cell Therapy and Protein Vaccine Survival Curve Graph

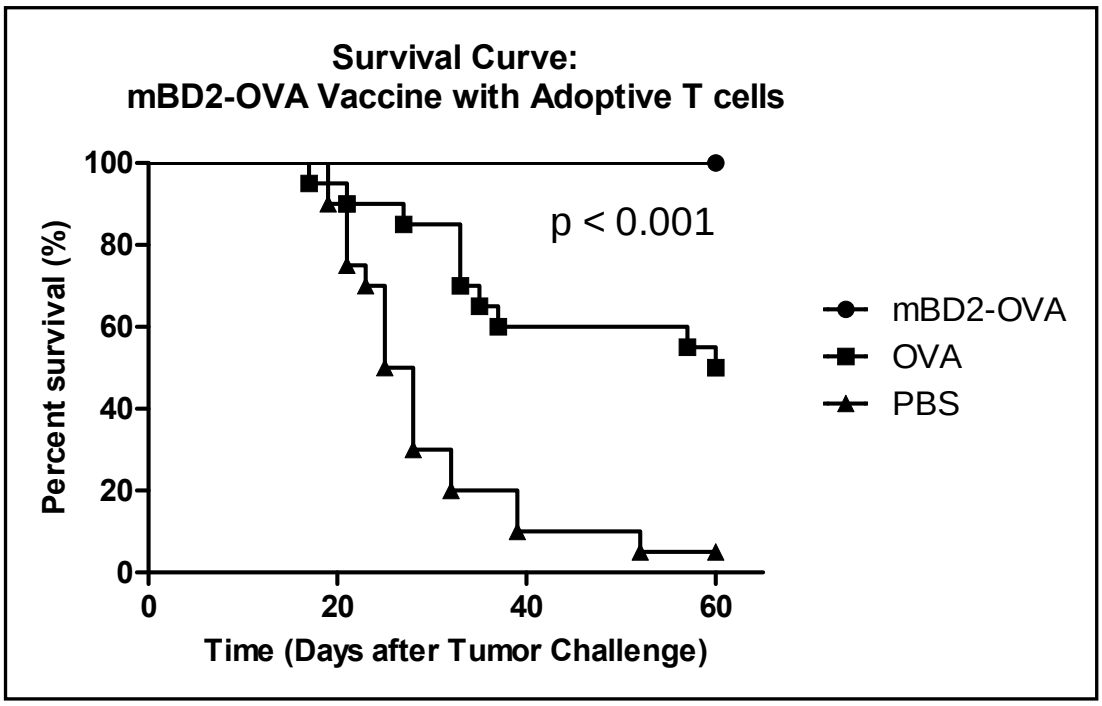

Figure 4-4B-1. Survival curve for mBD-OVA group versus mock vaccine (PBS) and antigen alone vaccine (OVA) group which shows statistical difference. C57BL/6 mice received freshly isolated splenocytes (~1-2x10^6 cells) intravenously from OT-I+ transgenic mice, followed by subcutaneous immunization with either mBD2-OVA recombinant fusion protein or OVA protein. One week after vaccination, all mice were challenged with a lethal dose of 1x10^5 B16-OVA melanoma cells by subcutaneous injection and were followed for survival for 60 days. Survival differences between groups were analyzed by log-rank test. Data represents pooled data from 4 independent experiments with a total of 20 mice per group.

Interpretation of Experiments. Mice first received adoptively transferred OT-I splenocytes, followed by vaccination with mBD2-OVA or OVA protein, and then challenge with a lethal dose of OVA-expressing B16 melanoma cells (B16-OVA) one week later. The OT-I and mBD2-OVA combination showed a potent effect on protecting mice from tumor challenge, achieving a long-term survival in all mice. This anti-tumor protection was significantly greater than that achieved by OT-I transfer and vaccination with unfused OVA protein.

Subsection 4C. pmel-1 Adoptive T cell Therapy and Protein Vaccine Challenge

Summary of Experiments. pmel-1 adoptive T cell and protein vaccine combination therapy was tested two separate times for tumor protection with groups of five mice per group in experiment #1 and ten mice per group on experiment #2 except in experiment #2 gp100T (antigen alone) group only had five mice per group as well. The same experiment was repeated using protocols described in Chapter 4's Section 2 Protein Vaccine Immunization and Section 3 pmel-1 Adoptive T cell Therapy and Protein Vaccine Challenge. These experiments included a vaccine dosage of 1500 μg of protein vaccine along with 1/10 of pmel-1 mouse donor spleen intravenous infusion. mBD2 fused to gp100T antigen was the main focus group with gp100T (antigen alone) control and PBS (no vaccine) controls tested concurrently. Enhanced performance was determined if the mBD2-gp100T group performed statistically better than both gp100T and/or PBS groups.

Experiment #1 Date: October 2, 2009

Experiment #2 Date: January 7, 2010

See Appendix for Chapter 4 (Table A4-4C-1, Table A4-4C-2, Table A4-4C-3) for survival details for both experiments.

Table 4-4C-1. pmel-1 Adoptive T cell Therapy and Protein Vaccine Challenge Statistical Analysis

Log-rank Pairwise Comparisons

Vaccine	mBD2-gp100T		gp100T		PBS	
	x^2	Sig.	x^2	Sig.	x^2	Sig.
mBD2-gp100T			12.642	.000	22.568	.000
gp100T	12.642	.000			2.256	.133
PBS	22.568	.000	2.256	.133		

Table 4-4C-1. Kaplan-Meier survival analysis with log-rank significance pairwise over strata comparison test. Event based on death and grouped by vaccine type received. The statistical analysis was done using SPSS (SPSS, Chicago, IL). Statistical survival difference p-values are as follow: mBD2-gp100T versus gp100T: 3.772539301443277E-4, mBD2-gp100T versus PBS: 2.028026244140242E-6, and gp100T versus PBS: 0.13307444085973746.

Figure 4-4C-1. pmel-1 Adoptive T cell Therapy and Protein Vaccine Survival Graph

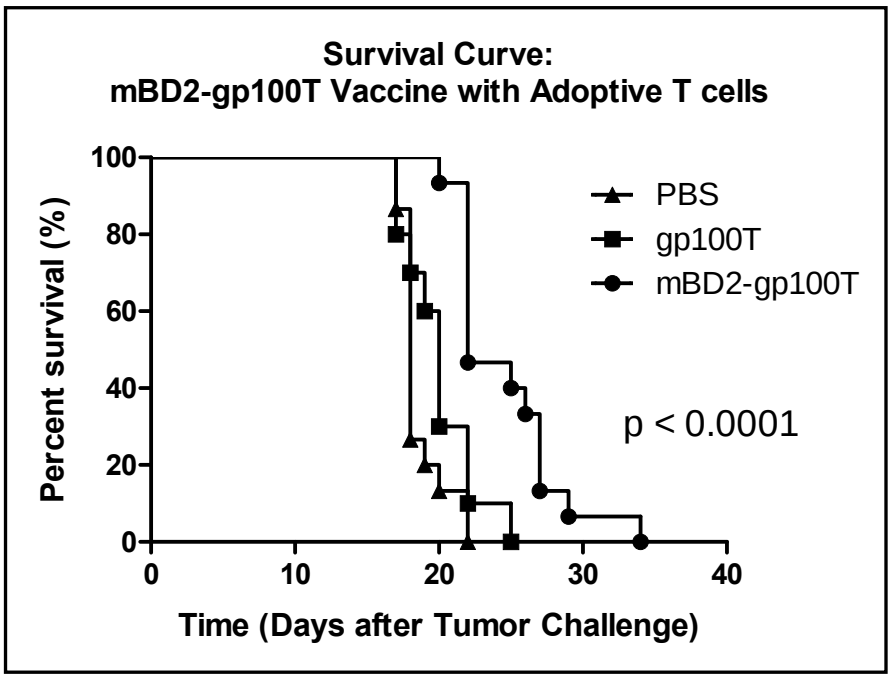

Figure 4-4C-1. Survival curve for mBD-gp100T group versus mock vaccine (PBS) and antigen alone vaccine (gp100T) group which shows statistical difference. mBD2-gp100T group has statistically different better survival. Ten to fifteen C57BL/6 mice per group received freshly isolated splenocytes (~3-6x10^6 cells) intravenously from pmel-1 transgenic mice followed by subcutaneous immunization with 1.5 mg mBD2-gp100T fusion or gp100T recombinant protein, or PBS. One week later, all mice were challenged with a lethal dose of 1x10^5 B16 melanoma cells by subcutaneous injection and were followed for survival. Survival differences between groups were analyzed by log-rank test.

Interpretation of Experiments. Compared with unfused gp100T, vaccination of mice with mBD2-gp100T fusion protein improved the protective effect of adoptively transferred pmel-1 T cells against lethal challenge with B16 melanoma.

Section 3. Discussion

mBD2 and MIP-3α fusion elicits Better Tumor Protection over other Chemokine fusions. The validity of chemokine vaccines have been proven previously (5-12). Knowing that chemokine vaccines worked, we were ready to optimize the conditions necessary to enhance the efficacy of these vaccines. First, the best chemokine or chemokine receptor ligand for the chemokine vaccines had not been determined. Thus, we determined to do an additional screen to answer this question. Based on previous experience we knew mBD2, MIP-3α, and MCP-3 were the strongest candidates (5) (12). We also wanted to target immature DC. Immature DC express CCR1, CCR2, CCR5, CCR6, CXCR1, CXCR2, CXCR3, CXCR4 (77, 78). We knew that MCP-3 (CCL7) binds CCR1, CCR2, and CCR3 (79). We also knew MIP-3α (CCL20) and mBD2 bind CCR6 (6, 8, 79). We wanted a target for CCR5 and sought RANTES (CCL5) which binds CCR1, CCR3, and CCR5 and is also a chemokine involved with dendritic cell trafficking (79). Finally, we also wanted a cancer vaccine on a very well established cancer vaccine model. We chose the gp100 melanoma antigen model because the epitope was very well established and a transgenic T cell mouse against epitope existed (pmel-1) (75). Thus, we generated DNA vaccines with aforementioned chemokines fused to gp100 antigen (Figure 3-2A-1).

Thus, we grouped mice into five groups with 14 mice per group. We used Phosphate Buffer Saline (PBS) as our mock immunization control group. We immunized each mouse three times over a 2-week interval with 50μg of intramuscular DNA vaccine corresponding to their group (mBD2, MCP-3, MIP-3α, RANTES, PBS). 2 weeks after

the final immunization, mice were challenged with subcutaneous injection of $1x10^5$ B16 tumor cells on their abdomen as recommended by protocol (76). Tumor growth was assessed every other day by caliper tumor measure. Mice with tumors larger than $400mm^2$ were euthanized. Significance of differences in survival were assessed based on Kaplan-Meier survival analysis with log-rank significance pairwise over strata comparison test. Statistical analysis showed MIP-3α and mBD2 to be statistically different over the PBS group at $p < 0.011$ and $p < 0.017$ respectively. Meanwhile, there was no statistical difference between MCP-3 or RANTES over PBS. Statistical difference between MIP-3α or mBD2 over RANTES was shown but not for MCP-3.

From this screen alone, we knew both MIP-3α and mBD2 were the best candidates. We remarked at the coincidence of both candidates being CCR6 ligands and this finding was also alluded to by others (12). Thus, we later explore the possible role of CCR6. With this data and previous data considered (5-12), we decided to further optimize chemokine vaccines with mBD2 in mind.

Complete Tumor Protection by Adoptive T cell Therapy and mBD2 Vaccine. It had been previously demonstrated that the mBD2 vaccine was capable of inducing protective anti-tumor responses in many cancer models (6, 11) (8, 12). We knew that although an anti-tumor response could be produced, this anti-tumor response was not strong enough to eliminate a large number of tumor cells. We also knew that a B16 tumor challenge was inherently very aggressive with guaranteed fatality after subcutaneous implantation of a tumorigenic dose and no treatment (76). Immunotherapies against tumors with vaccine alone have not been very successful (1, 2, 14, 80). However, an immunotherapy

regiment combining vaccine and adoptive T cell therapy (75, 81) has promise to be a successful. Thus, we wanted to see anti-tumor responses after adoptive T cell implantation and vaccination. More specifically, we wanted to see if an mBD2 vaccine would indeed enhance tumor protection.

Thus, we intravenously implanted OT-I T cells unto wildtype mice and vaccinated the mice with mBD2-OVA, OVA, or PBS. One week after vaccination we implanted $1x10^5$ B16 cells/mouse subcutaneously on their right leg. We recorded tumor size and survival every other day. We did this experiment in four separate tests of five mice per vaccine group. We found that over 95% of the mice under the PBS group developed tumors and all the mice which developed tumors had to be euthanized due to a large tumor burden ($> 400mm^2$) or died due to tumor burden. We also noted that the tumor protection response of mice receiving OT-I and OVA alone was strong with about 60% being tumor free after 60 days. The other 40% of mice showed delayed but ultimately fatal tumor growth. Nevertheless, we noted that not a single mouse developed tumor (100% tumor free) or died because of tumor in any of our tumor protection tests if the mice received OT-I and mBD2-OVA . Thus, the survival curve will show mBD2-OVA being the best treatment option followed by OVA then PBS (Figure 4-4B-1). Differences between mBD2-OVA and OVA were statistically significant (Table 4-4B-1).

Enhancement of Tumor Antigen Immunogenicity and Anti-tumor Antigen Response by the fusion of mBD2. Lastly, in two separate experiments we intravenously implanted pmel-1 T cells unto wildtype mice and vaccinated the mice with mBD2-

gp100T, gp100T, or PBS. One week after vaccination we implanted $1x10^5$ B16 cells/mouse subcutaneously on their right leg. After recording tumor size and survival, we noted statistically significantly different survival rates between mBD2-gp100T versus gp100T (Table 4-4C-1). We saw that there was no statistically significant difference in survival between PBS versus gp100T (Table. 4-4C-1). On a side note, we had developed mBD2-$gp100_{25-33}$ and this peptide showed statistically significant results on our first experiment but failed on the second experiment, but the data looks promising as some mice were completely tumor free in a model where tumor development is almost certain (Data not shown).

Chapter 5. mBD2 Vaccine Mechanism

Section 1. Materials

Subsection 1A. Mice

Mice. All animals were housed at M. D. Anderson, South Campus Research Building Animal Facility (Houston, TX). Animal care was provided in accordance to M. D. Anderson's institutional animal care and use committee guidelines.

Subsection 1A(i). Mice for *In vitro* Studies

C57BL/6. Wildtype C57BL/6 (H-2^b) mice were purchased from the National Cancer Institute (Baltimore, MD).

OT-I or OT-I+CD45.1+. OTI-I (C57BL/6-Tg(TcraTcrb)1100Mjb/J, Stock No. 003831) were purchased from the Jackson Laboratory (Bar Harbor, MN). OT-I+CD45.1+ mice were generously provided by Dr. Kimberly Schluns (74).

pmel-1 or pmel-1+Thy1.1+ . pmel-1 mice were provided in cooperation by Dr. Willem Overwijk (75).

CCR6KO. CCR6 knockout mice (B6.129P2-Ccr6tm1Dgen/J, Stock No. 005793) were purchased from the Jackson Laboratory (Bar Harbor, MN).

Subsection 1A(ii). Mice for *In vivo* studies

C57BL/6. See Chapter 5 Subsection 1A(i).

OT-I+CD45.1+. See Chapter 5 Subsection 1A(i).

OT-II+CD45.1+. OT-II+CD45.1+ mice were generously provided by Dr. Yeonseok Chung (82).

TLR4KO. TLR4 knockout mice (B6.B10ScN-Tlr4lps-del/JthJ, Stock No. 007227) were purchased from the Jackon Laboratory (Bar Harbor, MN).

CCR6KO. See Chapter 5 Subsection 1A(i).

Subsection 1B. Other Materials

Adjuvants. CpG ODN 1826 (CPG), CpG Type B for Mouse, was custom generated by IDT Inc (Coralville, IA). Sequence is as follows: 5'- T*C*C* A*T*G* A*CG* T*T*C* C*T*G* A*CG* T*T -3'. MPL, Monophosphoryl Lipid A from S. Minnesota (Cat No. tlrl-mpl, Invivogen, San Diego, CA), was also purchased.

Vesicular Stomatitis Viruses (VSV). VSV-gp100 and VSV-OVA viruses were provided by Dr. Kimberly Schluns (74).

Splenocyte or Cell Media. RPMI Medium 1640 with GLUTAMAX™-I (Cat No. 61870-127, Invitrogen, Carlsbad, CA) with 10% Fetal Bovine Serum, Certified (Cat No. 16000-044, Invitrogen, Carlsbad, CA). Alternatively, RPMI Medium 1640 with GLUTAMAX™-I with 10% Fetal Bovine Serum, Certified with 500µl (for every 500mL RPMI Medium 1640) of 2-mercaptoethanol (Cat No. 21985-023, Invitrogen, Carlsbad, CA), and 7mL (for every 500mL RPMI Medium 1640) of Penicillin-Streptomycin (Cat No. 15140-122, Invitrogen, Carlsbad, CA).

Vaccines. The inventory of vaccine proteins used for mechanistic studies was as follows: MIP-3α-gp100T, mBD2-gp100T, gp100T, MIP-3α-OVA, mBD2-OVA, OVA, and OVA (Commercial) (Figure 3-2C(ii)-1). See Chapter 3 for full details on the vaccine production and specifications.

Section 2. Protocols

Subsection 2A. *In vitro* Mechanistic Studies Protocols

BM-DC Generation and Protein Loading.

1. Prepare cell media - See Chapter 5 Section 1B, Splenocyte or Cell Media.
2. Euthanize mouse and dip mouse bodies in 70% ethanol.
3. Move to hood, starting from now, all steps have to be completed in hood.
4. Prepare two sets of surgical tools, a beaker to collect waste liquid. Cover the hood bench with a piece of tin foil.
5. Cut mouse skin from back to explore behind legs. Separate legs from body without breaking bones. Dip legs in a 50 ml tube filled with 70% ethanol till all legs are collected.
6. Use scissors to get rid of muscular tissues from bone without breaking bones.
7. Collect bones in a 50 ml tube filled with sterile cell media.
8. Wash bones 3 times with 70% ethanol followed by 3 times with Phosphate Buffered Saline (PBS).
9. Cut both ends of bones. Use 26-27G (thin) needle (attached to a 20cc syringe) to flush bone marrow out from both ends. Collect cells in Petri-dish. After rinsing, the color of bone should turn to white color.
10. Use 16G (thick) needle (attached to a 20cc syringe) to separate and transfer cells (passing through) to a 50 ml tube.

11. Spin cells down at 1500 rpm (485g) on a Sorvall Legend RT+ (Thermo Scientific, Waltham, MA) for 5 minutes at 4°C.
12. Resuspend cells in 3mL RBC lysis buffer (Cat No. 158904, Qiagen, Valencia, CA) per leg. Incubate cells in RBC lysis buffer for 8 min, and then add equal volume of splenocyte media. Spin cells down at 1500 rpm (485g) on a Sorvall Legend RT+ for 5 minutes at 4°C.
13. Resuspend cells in 10 ml cell media and filter cells with cell strainer.
14. Spin cells down at 1500 rpm (485g) on a Sorvall Legend RT+ for 5 minutes at 4°C. Resuspend cells with cell media and count cells.
15. Collect $6x10^6$ cells or more cells.
16. Prepare 24 mL of media for $6x10^6$ cells or 4mL per $1x10^6$cells. Put 8µl of GM-CSF cytokine which is at a concentration of (10ng/µl) (GM-CSF x2) per 4mL of media.
17. Spin down the cells and resuspend in 24 mL of media with GM-CSF for $6x10^6$ cells.
18. Put 4mL of media with cells into each well of 6 well plate. Final count is $1x10^6$ cells/well.
19. On Day 4, add GM-CSF to each well. (Put 4µl of cytokine which is at a concentration of 10ng/µl) (GM-CSF x1).
20. On Day 6, add desired protein at 50µg/mL media or 200µg of protein per well with antigen presenting cells (APC).
21. On Day 7 change media and optionally add maturation factor. You change media by placing tip on the wall and sucking out supernatant so APCs are left behind. Then add 4mL of new cell media to each well. If maturation factor is added, add

GM-CSF, IL-1β, and TNF-α by putting 4 µl of cytokine which are all at concentration of 10ng/µl) (GM-CSF, IL-1β, TNF-α x1).

22. On Day 8 collect dendritic cells (DC) for coincubation with antigen specific splenocytes.

Splenocyte Isolation, Stimulation, and Maintenance

1. Obtain spleens from OT-I or pmel-1 mice and place in PBS. Smash spleen with a 3CC syringe plunge over cell strainer which is over 50 mL tube. Make splenocyte media with Penicillin-Streptomycin - See Chapter 5 Section 1B Splenocyte or Cell Media.
2. Spin cells down at 1500 rpm (485g) on a Sorvall Legend RT+ (Thermo Scientific, Waltham, MA) for 5 minutes at 4°C.
3. After removing the supernatant, add 4 ml RBC lysis buffer (Cat No. 158904, Qiagen, Valencia, CA). Incubate cells with lysis buffer for 8 min at room temperature.
4. Add 3 times volume of splenocyte media. Filter cell through cell strainer and use a 50 ml tube to collect the flow through. Rinse tubes with 10 ml splenocyte media. Bring volume to 20 mL. Spin cells down at 1500 rpm (485g) on a Sorvall Legend RT+ for 5 minutes at 4°C.
5. Remove the supernatant and re-suspend cells with 48 ml splenocyte media
6. Place 1mL of media with cells into each well unto two 24 well plates (48 wells).
7. Add 300 IU of IL-2/mL of media per well of cells.

8. Add 1µg of pmel-1 specific or OT-I specific peptide/mL of media per well of cells.
9. Check cells every day and split, add new media, and add 300 IU of IL-2/mL as necessary (when media is yellow) until Day 8, DC coincubation step.

DC/Splenocyte Coincubation and Intracellular Staining

Note: Intracellular Staining of IFN-γ is based on protocol for BD Cytofix/Cytoperm Plus Fixation/Permiabilization Kit (with BD GolgiPlug protein transport inhibitor containing brefeldin A) (Cat. No. 555028, Becton Dickinson, Franklin Lakes, NJ)

1. Wash previously generated and protein loaded DC and previously activated and expanded splenocytes with RPMI (RPMI Medium 1640 with GLUTAMAX™-I (Cat No. 61870-127, Invitrogen, Carlsbad, CA)) and resuspend cells at $1x10^6$ cells/mL for DC and $5x10^6$ cells/mL for splenocytes in RPMI.
2. Add 2µl of brefeldin A (BD GolgiPlug (Cat No. 555029, Becton Dickinson, Franklin Lakes, NJ) (2x concentration) for every 1 ml of media with splenocytes.
3. Place and coincubate DC and splenocytes at 1:5 ratio or ($1x10^5$ to $5x10^5$ cells) respectively on 96 well V bottom plate (100µl of DC resuspension and 100µl of splenocyte resuspension for a total of 200µl of media with cells per well).
4. Incubate DC and splenocytes for 5.5 hours at 37°C in CO_2 chamber.
5. Wash cells twice with 200 µl staining buffer (Cat No. 554656, Becton Dickinson, Franklin Lakes, NJ) at the end of incubation by spinning cells down at 1500 rpm

(485g) on a Sorvall Legend RT+ for 5 minutes at 4°C, removing supernatant and re-adding staining buffer.

6. Remove the supernatant after final wash and fix/permeabilize cells. Tap the plate to loose cells and then add 100 µl of BD Fixation/Permeabilization (Cat No. 555028, Becton Dickinson, Franklin Lakes, NJ) solution in each well, thoroughly resuspend cells, and incubate on ice for 20 minutes in the dark.
7. Wash cells twice with 200 µl of 1x BD Perm/Wash buffer (Cat No. 555028, Becton Dickinson, Franklin Lakes, NJ) (dilute from 10x BD Perm/Wash concentrate with deionized distilled water). Remove the supernatant after final wash.
8. While washing, prepare intracellular and surface marker staining solution. In general, dilute antibodies 1:200 in 1x BD Perm/Wash buffer (# of wells x 50 µl = total volume). Antibodies used are as follow: FITC labeled CD3 (Cat No. 553062, Becton Dickinson, Franklin Lakes, NJ), Optional PE labeled gp100 (T20209 KVPRNQDWL, Beckman Coulter, Brea, CA) or OVA tetramer (T20076 SIINFEKL, Beckman Coulter, Brea, CA), PerCP labeled CD8 (Cat No. 553036, Becton Dickinson, Franklin Lakes, NJ), and APC labeled IFN-γ (Cat No. 554413, Becton Dickinson, Franklin Lakes, NJ). Alternatively, another antibody cocktail used is as follows: FITC labeled CD90.1 (Thy1.1, Cat No. 554897, Becton Dickinson, Franklin Lakes, NJ) or CD45.1 (Cat No. 553775, Becton Dickinson, Franklin Lakes, NJ), PE labeled CD8 (Cat No. 553032, Becton Dickinson, Franklin Lakes, NJ), PerCP labeled CD3 (Cat No. 553067, Becton Dickinson, Franklin Lakes, NJ), and APC labeled IFN-γ.

9. Add 50 µl of staining solution in each well, and incubate on ice for 30 min in the dark.
10. Wash cells 2x with 200 µl of 1x BD Perm/Wash buffer. Cells can be kept in Perm/Wash buffer for 24 hours. Otherwise, remove the supernatant after final wash and resuspend cells in staining buffer for flow cytometer read. Cells are to be analyzed using FACSCalibur flow cytometer (Becton Dickinson, Franklin Lakes, NJ) with CellQuest (Becton Dickinson, Franklin Lakes, NJ) and FlowJo Software (Treestar, Ashland, OR).

Subsection 2B. *In vivo* Mechanistic Studies Protocols

Splenocyte Isolation. See Chapter 4 Section 2.

Adoptive Transfer. See Chapter 4 Section 2.

Protein Vaccine Immunization. See Chapter 4 Section 2.

Vesicular Stomatitis Virus Vaccine Immunization. See Chapter 4 Section 2.

Bleeding and Blood Collection. After adoptive transfer of T cells and appropriate vaccination, mice were tail-bled on Days 3, 5, and 7 post adoptive transfer. Mice were placed under heated lamp and later onto tail bleeding chamber. The tip of their tail was

cut with a scissor. 5 drops of blood were collected into a 1.5mL eppendorf vial with 50µl of heparin solution (1000 USP units/mL).

Blood Staining.

1. Lyse blood with heparin solution with RBC lysis solution (Cat No. 158904, Qiagen, Valencia, CA). Add 1 mL of RBC lysis solution for 8 minutes.
2. Centrifuge blood for 5 minutes on Table Centrifuge (Eppendorf Centrifuge 5415D, Hauppauge, NY) at 13,200 rpm (16100 rcf) at room temperature. Discard supernatant.
3. Wash blood with 1mL of PBS by centrifuging blood with PBS for 5 minutes on Table Centrifuge (Eppendorf Centrifuge 5415D) at 13,200 rpm (16100 rcf) at room temperature and discard supernatant.
4. Prepare staining cocktail while washing. In general, dilute antibodies 1:50 in PBS (# of vials x 50 µl = total volume). Antibodies used are as follows: FITC labeled CD90.1 (Thy1.1 Cat No. 554897, Becton Dickinson, Franklin Lakes, NJ) , PerCP labeled CD8 (Cat No. 553036, Becton Dickinson, Franklin Lakes, NJ), and APC labeled CD44 (Cat No. 559250, Becton Dickinson, Franklin Lakes, NJ). Alternatively, antibodies were also used as follows: FITC labeled CD90.1, PE labeled CD8 (Cat No. 553032, Becton Dickinson, Franklin Lakes, NJ), PerCP labeled CD3 (Cat No. 553067, Becton Dickinson, Franklin Lakes, NJ), and APC labeled CD44.
5. Stain blood with 50 µl of staining cocktail and incubate on ice for 30 minutes.

6. Wash blood with PBS and later fix with 1% Paraformaldehyde/1% Bovine Serum Albumin Solution in PBS.
7. Analyze blood using FACSCalibur flow cytometer (Becton Dickinson, Franklin Lakes, NJ) with CellQuest (Becton Dickinson, Franklin Lakes, NJ) and FlowJo Software (Treestar, Ashland, OR).

Section 3. Experimental Setup

Subsection 3A. *In vitro* Mechanism Experiments

Crosspresentation of gp100 epitope by DC to pmel-1.

First, DC were loaded with:

1. mBD2-gp100T – Experimental group – Addition of mBD2 and antigen
2. gp100T – Control, No mBD2, antigen only
3. mBD2-OVA – Negative control, irrelevant antigen but mBD2 included
4. PBS – Negative control, no antigen or mBD2

Next, pmel-1 were conincubated with:

1. DC loaded with mBD2-gp100T – Experimental group – Addition of mBD2 and antigen
2. DC loaded with gp100T – Control, No mBD2, antigen only
3. DC loaded with mBD2-OVA – Negative control, irrelevant antigen but mBD2 included
4. DC alone – Negative control, no antigen or mBD2
5. $gp100_{25\text{-}33}$ KVPRNQDWL peptide – Positive Control
6. PBS – Negative control

Note: Experiment done in triplicates.

Percentages of IFN-γ+CD3+CD8+ and optionally CD90.1+ cells between groups (1-6) above were measured and compared.

Crosspresentation of OVA epitope by DC to OT-I.

First, DC were loaded with:

1. mBD2-OVA – Experimental group – Addition of mBD2 and antigen
2. OVA – Control, No mBD2, antigen only
3. mBD2-gp100T – Negative control, irrelevant antigen but mBD2 included
4. PBS – Negative control, no antigen or mBD2

Next, OT-I were conincubated with:

1. DC loaded with mBD2-OVA – Experimental group – Addition of mBD2 and antigen
2. DC loaded with OVA – Control, No mBD2, antigen only
3. DC loaded with mBD2-gp100T – Negative control, irrelevant antigen but mBD2 included
4. DC alone – Negative control, no antigen or mBD2
5. $OVA_{257-264}$ SIINFEKL peptide – Positive Control
6. PBS – Negative control

Note: Experiment done in triplicates.

Percentages of IFN-γ+CD3+CD8+ and optionally CD45.1+ cells between groups (1-6) above were measured and compared.

Crosspresentation of OVA epitope by DC to OT-I and Effect of CCR6 removal on Crosspresentation of mBD2 fused Antigen.

First, DC were loaded with:

1. mBD2-OVA – Experimental group – Addition of mBD2 and antigen
2. OVA – Control, No mBD2, antigen only
3. mBD2-gp100T – Negative control, irrelevant antigen but mBD2 included
4. PBS – Negative control, no antigen or mBD2

Concurrently, CCR6KO-DC were loaded with:

1. mBD2-OVA – Experimental group – Addition of mBD2 and antigen
2. OVA – Control, No mBD2, antigen only
3. mBD2-gp100T – Negative control, irrelevant antigen but mBD2 included
4. PBS – Negative control, no antigen or mBD2

Next, OT-I were conincubated with:

1. DC loaded with mBD2-OVA – Experimental group – Addition of mBD2 and antigen
2. DC loaded with OVA – Control, No mBD2, antigen only
3. DC loaded with mBD2-gp100T – Negative control, irrelevant antigen but mBD2 included
4. DC alone – Negative control, no antigen or mBD2
5. CCR6KO-DC loaded with mBD2-OVA – CCR6KO counterpart of Group 1
6. CCR6KO-DC loaded with OVA – CCR6KO counterpart of Group 2

7. CCR6KO-DC loaded with mBD2-gp100T – CCR6KO counterpart of Group 3

8. CCR6KO-DC alone – CCR6KO counter part of Group 4.

9. $OVA_{257-264}$ SIINFEKL peptide – Positive Control

10. PBS – Negative control

Note: Experiment done in triplicates.

Percentages of IFN-γ+CD3+CD8+ and optionally CD45.1+ cells between groups (1-4 and 9-10) above were measured and compared. To measure CCR6KO effect, Group 5 was compared against Group 1, Group 6 with Group 2, Group 7 with Group 3, and Group 8 with Group 4.

To see CCR6 and mBD2 link, we should have seen a difference in Group 1 versus Group 5 while concurrently hold no difference between Group 2 versus Group 6 and Group 3 versus Group 7 and Group 4 versus Group 8.

Figure 5-3A-1. *In vitro* Crosspresentation Experiments Schema

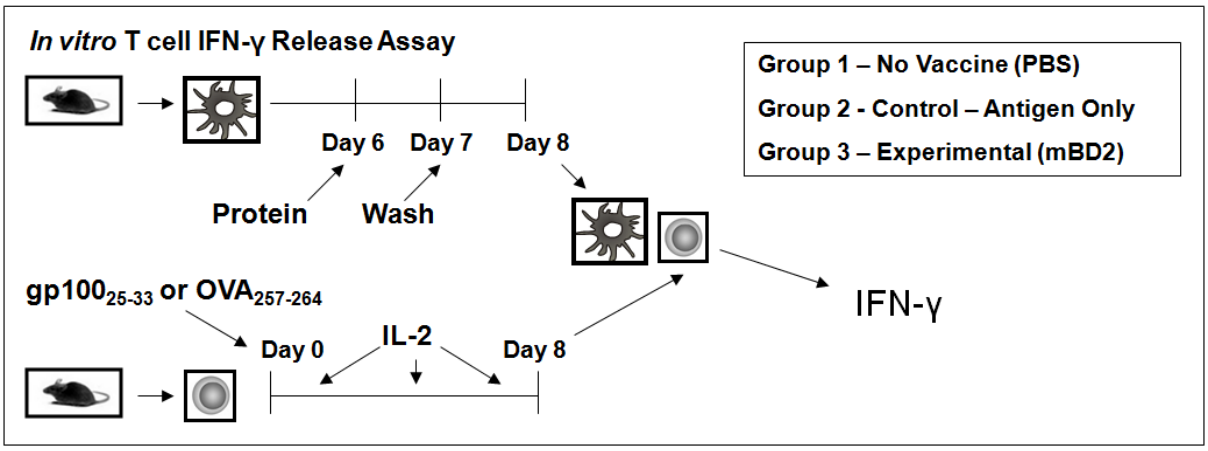

Figure 5-3A-1. The schema describes the experimental model for indirect measure of crosspresentation efficiency by IFN-γ expression measure by effector cells. The four parts to the experiment include: (1) APC development and loading with test vaccine protein, (2) antigen specific effector T cell activation and maintenance, (3) coincubation and crosspresentation of epitope (DC to effector T cells), (4) IFN-γ expression by T cells and measure. We wanted to see enhanced IFN-γ release by Group 3 (mBD2 group) versus Group 2 (Antigen Alone) and Group 1 (PBS).

Subsection 3B. *In vivo* Experiments

OT-I Expansion Measure after mBD2 Vaccine.

Wildtype mice received adoptive T cell therapy (OT-I) and vaccine as follows:

1. mBD2-OVA – mBD2 added experimental group

2. OVA – antigen alone control

3. PBS – Negative control, No vaccine

4. VSV-OVA – Positive control,

Note: Experiment was done with five mice per group

Percentages of OT-I+CD45.1+CD8+ cells between groups 1-4 were measured and compared.

OT-II Expansion Measure after mBD2 Vaccine.

Wildtype mice received adoptive T cell therapy (OT-II) and vaccine as follows:

1. mBD2-OVA – mBD2 added experimental group

2. OVA – antigen alone control

3. PBS – Negative control, No vaccine

4. VSV-OVA – Positive control,

Note: Experiment was done with five mice per group

Percentages of OT-II+CD45.1+CD4+ cells between groups 1-4 were compared.

OT-I Expansion Measure after mBD2 Vaccine with CCR6 Removal.

Wildtype mice received adoptive T cell therapy (OT-I) and vaccine as follows:

1. mBD2-OVA – mBD2 added experimental group

2. OVA – antigen alone control

3. PBS – Negative Control, No vaccine

4. VSV-OVA – Positive Control,

Concurrently, CCR6KO received adoptive T cell therapy (OT-I) and vaccine as follows:

5. mBD2-OVA – CCR6KO counterpart of Group 1.

Note: Experiment was done with five mice per group

Percentages of OT-I+CD45.1+CD8+ cells between groups 1-5 were measured and compared.

For effect on CCR6 removal we compared Group 1 versus Group 5 only. All other groups were controls.

OT-I Expansion Measure after mBD2 Vaccine with TLR4 Removal.

Wildtype mice received adoptive T cell therapy (OT-I) and vaccine as follows:

1. mBD2-OVA – mBD2 added experimental group

2. OVA – antigen alone control

3. PBS – Negative Control, No vaccine

4. VSV-OVA – Positive Control,

Concurrently, TLR4KO mice received adoptive T cell therapy (OT-I) and vaccine as follows:

5. mBD2-OVA – TLR4KO counterpart of Group 1.

Note: Experiment was done with five mice per group

Percentages of OT-I+CD45.1+CD8+ cells between groups 1-5 were measured and compared.

For effect on TLR4 removal we compared Group 1 versus Group 5 only. All other groups were controls.

OT-I Expansion Measure after mBD2 vaccine with TLR4 adjuvant.

Wildtype Mice received adoptive T cell therapy (OT-I) and vaccine and adjuvant as follows:

1. mBD2-OVA – mBD2 added experimental group

2. OVA – antigen alone control

3. PBS – Negative Control, No vaccine

4. VSV-OVA – Positive Control.

5. mBD2-OVA with TLR4 agonist– mBD2 enhanced and TLR4 agonist added experimental.

6. OVA with TLR4 agonist – antigen alone with TLR4 agonist.

Note: Experiment was done with five mice per group

Percentages of OT-I+CD45.1+CD8+ cells between groups 1-6 were measured and compared. To compare effect of TLR4 agonist addition to mBD2 vaccines, we compared Group 1 versus Group 5. To compare effect of TLR4 agonist addition to antigen alone vaccines, we compared Group 2 versus Group 6. Differences between

(Group 1 & Group 5) versus (Group 2 & Group 6) revealed TLR4 relationship with mBD2. Group 1 versus 6 relationship was also compared to see adjuvant comparison.

OT-I Expansion Measure after mBD2 vaccine with TLR9 adjuvant.

Wildtype Mice received adoptive T cell therapy (OT-I) and vaccine and adjuvant as follows:

1. mBD2-OVA – mBD2 added experimental group
2. OVA – antigen alone control
3. PBS – Negative Control, No vaccine
4. VSV-OVA – Positive Control.
5. mBD2-OVA with TLR9 agonist– mBD2 enhanced and TLR4 agonist added experimental.
6. OVA with TLR9 agonist – antigen alone with TLR4 agonist.

Note: Experiment was done with five mice per group

Percentages of OT-I+CD45.1+CD8+ cells between groups 1-6 was measured and compared. To compare effect of TLR9 agonist addition to mBD2 vaccines, we compared Group 1 versus Group 5. To compare effect of TLR9 agonist addition to antigen alone vaccines, we compared Group 2 versus Group 6. Differences between (Group 1 & Group 5) versus (Group 2 & Group 6) revealed TLR9 relationship with mBD2. Group 1 versus 6 was also compared to see adjuvant comparison.

Figure 5-3B-1. *In vivo* T cell expansion Experiments Schema

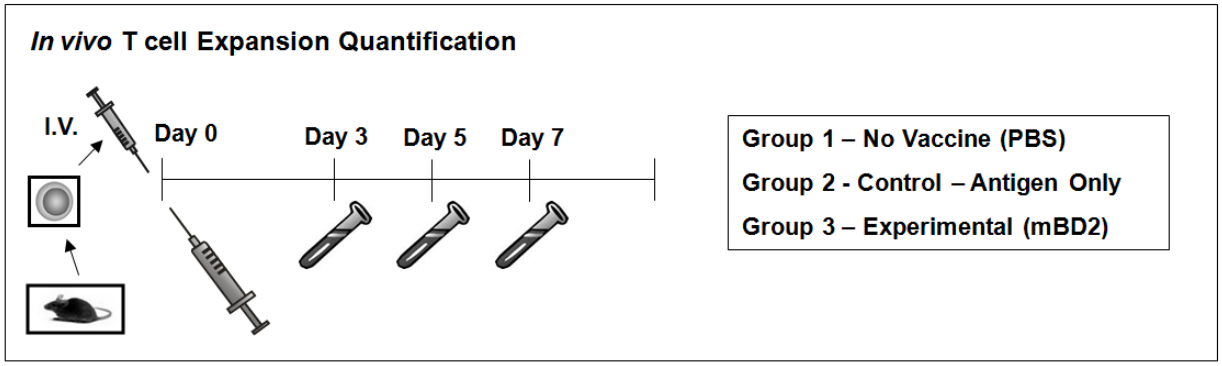

Figure 5-3B-1. T cell expansion/proliferation measure experiment schedule. First, wildtype mice were intravenously infused with effector T cells. Next, group determined vaccine was injected. Effector T cell percentage versus background wildtype mice T cell percentages were measured on Days 3, 5, and 7 to track a general pattern of effector T cell expansion rate. Patterns were compared by groups with Group 3 (mBD2) expected to generate the highest rate of expansion.

Section 4. Results

Subsection 4A. *In vitro* Mechanism Experiments

Subsection 4A(i). Crosspresentation of gp100 epitope by DC to pmel-1

Summary of Experiments. Three similar crosspresentation of gp100 by DC to pmel-1 experiments were performed with tweaks in variables tested (the proteins) and coincubation times. However, experiments were performed by following the same protocols and guidelines established on Section 2 Subsection 2A's BM-DC Generation and Protein Loading, Splenocyte Isolation, Simulation, and Maintenance, and DC/Splenocyte Coincubation and Intracellular Staining as well as Section 3 Subsection 3A's Crosspresentation of gp100 epiptope by DC to pmel-1.

Experiment #1 Date: October 22, 2008 - See Appendix for Chapter 5 (Table A5-4A(i)-1) for detail.

Experiment #2 Date: November 15, 2008 - See Appendix for Chapter 5 (Table A5-4A(i)-2) for detail.

Experiment #3 Date: November 26, 2008 - See Appendix for Chapter 5 (Table A5-4A(i)-3) for detail.

Figure 5-4A(i)-1. gp100 Crosspresentation Experiment #1 Results Graph

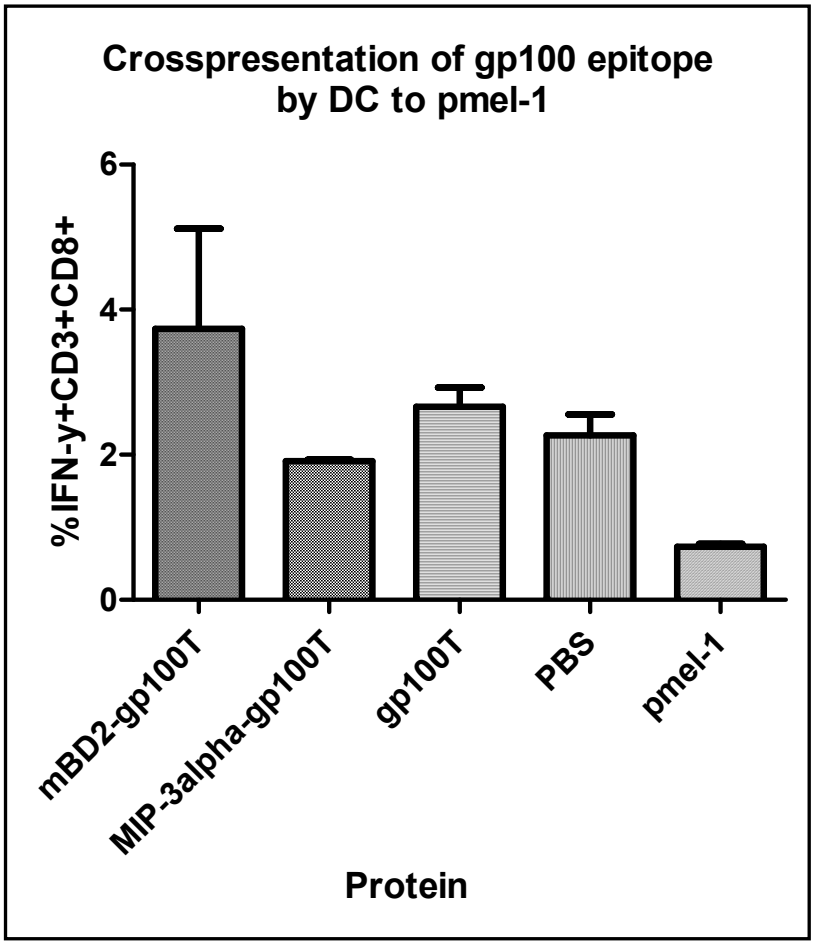

Figure 5-4A(i)-1. Graph representation of percentages of effector T cell's IFN-γ release differences determined by the protein loaded unto DC. Error bars represent standard deviation. Higher efficiency when loading mBD2 fused gp100T over non-fused. Positive controls (epitope peptide with pmel-1 and PHA with pmel-1 (Table A5-4A(i)-1)) and negative controls (PBS and pmel-1 alone) show proper functionality of effector T cells (pmel-1). Tweaked variables include a 9 hour DC and pmel-1 coincubation time and maturation factor added to DC after protein loading and prior to coincubation.

Figure 5-4A(i)-2. gp100 Crosspresentation Experiment #2 Results Graph

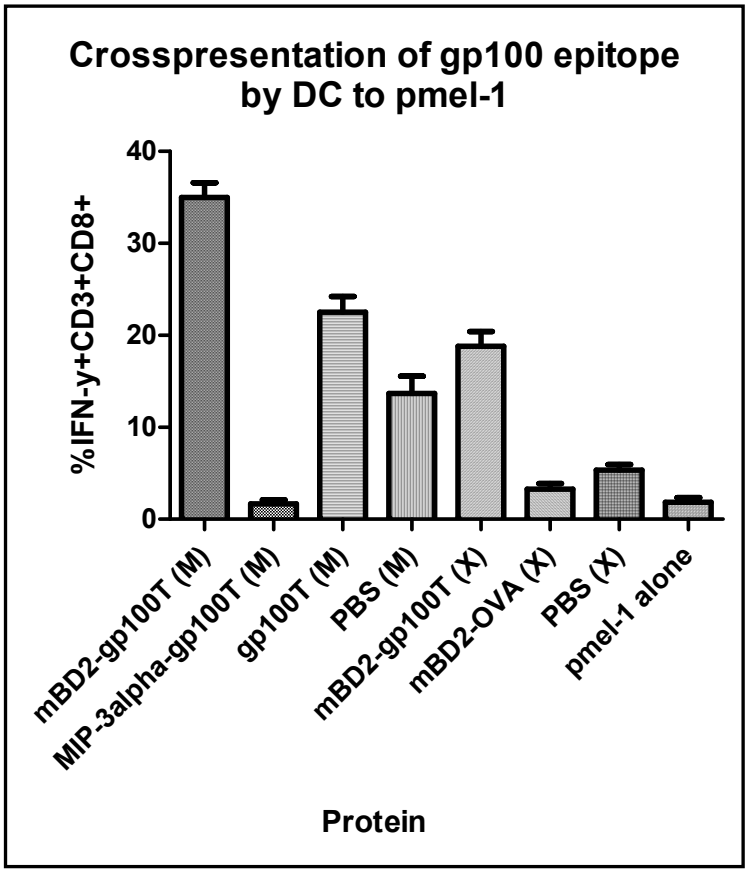

Figure 5-4A(i)-2. Graph representation of percentages of effector T cell's IFN-γ release differences determined by the protein loaded unto DC. Error bars represent standard deviation. Higher efficiency when loading mBD2 fused gp100T over non-fused. Positive controls (epitope peptide with pmel-1 and PHA with pmel-1(Table A5-4A(i)-2)) and negative controls (PBS and pmel-1 alone) show proper functionality of effector T cells (pmel-1). Tweaked variables include a 8 hour DC and pmel-1 coincubation time and maturation factor added to DC after protein loading and prior to coincubation for samples labeled (M) and not added if samples were labeled (X).

Figure 5-4A(i)-3. gp100 Crosspresentation Experiment #3 Results Graph

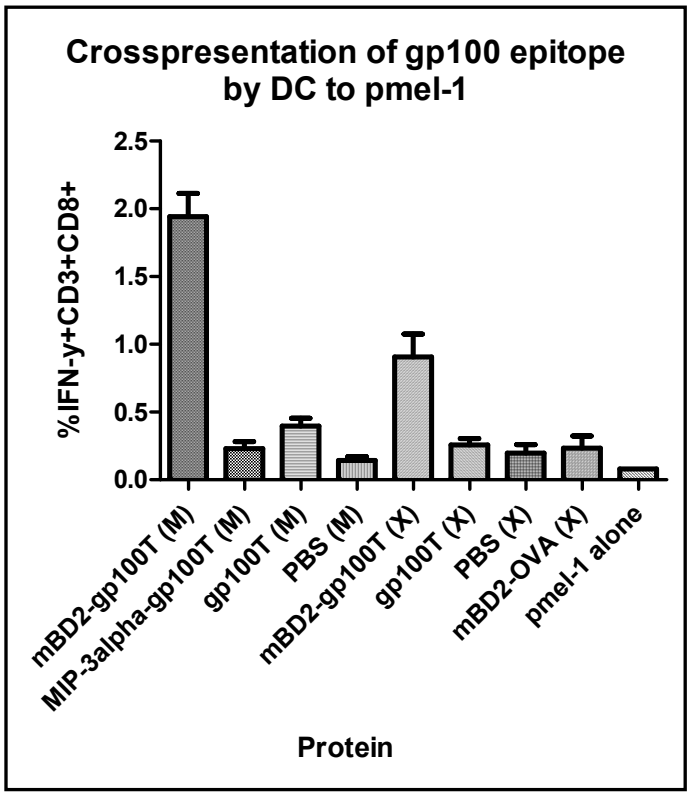

Figure 5-4A(i)-3. Graph representation of percentages of effector T cell's IFN-γ release differences determined by the protein loaded unto DC. Error bars represent standard deviation. Percentages of effector T cell's IFN-γ release differences show higher efficiency when loading mBD2 fused antigen over non-fused. Positive controls (epitope peptide with pmel-1(Table A5-4A(i)-3)) and negative controls (PBS and pmel-1 alone) show proper functionality of effector T cells (pmel-1). Tweaked variables include a 5.5 hour DC and pmel-1 coincubation time and maturation factor added to DC after protein loading and prior to coincubation for samples labeled (M) and not added if samples were labeled (X).

Interpretation of Experiments. Three similar crosspresentation of gp100 by DC to pmel-1 experiments were performed with tweaks in variables tested and coincubation times. However, antigen-specific CD8+ T cells (pmel-1) stimulated with BM-DC loaded with mBD2-gp100T consistently produced significantly higher levels of IFN-γ compared with BM-DC pulsed with unfused gp100T, mBD2-OVA (irrelevant antigen control) or PBS.

Subsection 4A(ii). Crosspresentation of OVA epitope by DC to OT-I

Summary of Experiments. Two similar crosspresentation of OVA by DC to OT-I experiments were performed with tweaks in variables (the proteins) tested. Experiments were performed by following the same protocols and guidelines established on Section 2 Subsection 2A's BM-DC Generation and Protein Loading, Splenocyte Isolation, Simulation, and Maintenance, and DC/Splenocyte Coincubation and Intracellular Staining as well as Section 3 Subsection 3A's Crosspresentation of OVA epiptope by DC to OT-I.

Experiment #1 Date: February 20, 2009 - See Appendix for Chapter 5 (Table A5-4A(ii)-1) for detail.

Experiment #2 Date: November 11, 2009 - See Appendix for Chapter 5 (Table A5-4A(ii)-2) for detail.

Figure 5-4A(ii)-1. OVA Crosspresentation Experiment #1 Results Graph

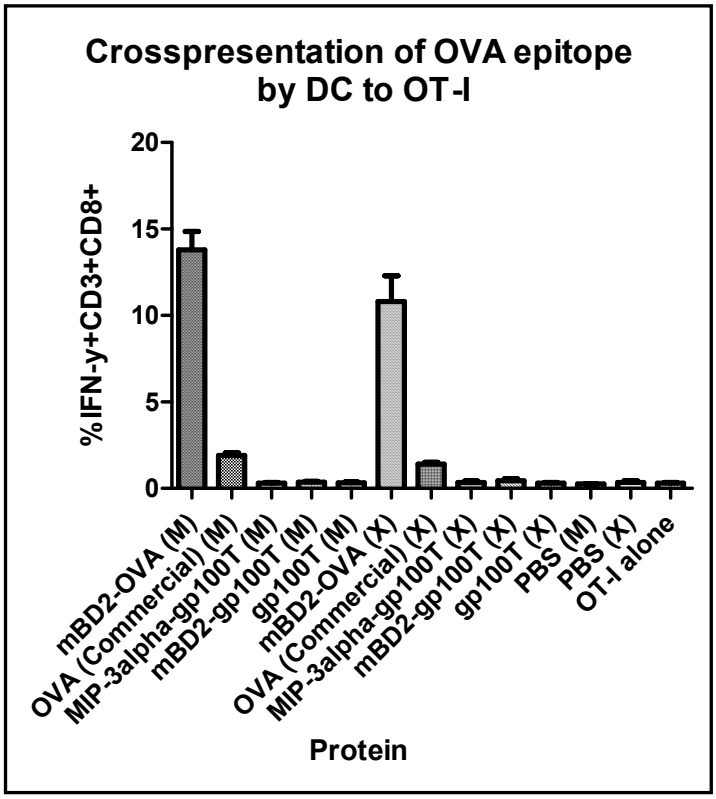

Figure 5-4A(ii)-1. Graph representation of percentages of effector T cell's IFN-γ release differences determined by the protein loaded unto DC. Error bars represent standard deviation. Percentages of effector T cell's IFN-γ release differences show higher efficiency when loading mBD2 fused OVA over non-fused. Positive controls (epitope peptide with OT-I (Table A5-4A(ii)-1)) and negative controls (PBS and OT-I alone) show proper functionality of effector T cells (OT-I). Other variables include a 5.5 hour DC and OT-I coincubation time and maturation factor added to DC after protein loading and prior to coincubation for samples labeled (M) and not added if samples were labeled (X).

Figure 5-4A(ii)-2. OVA Crosspresentation Experiment #2 Results Graph

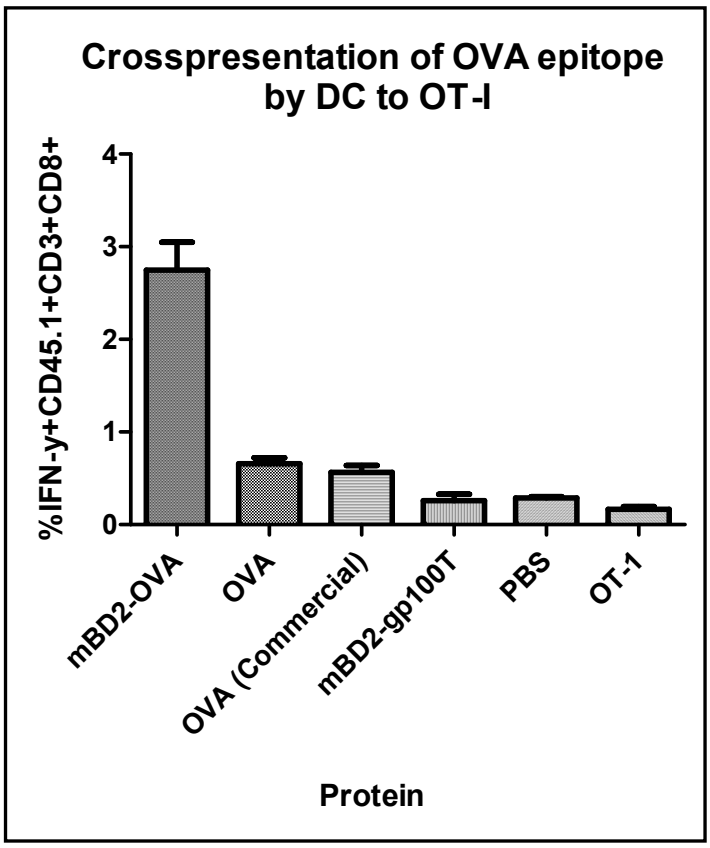

Figure 5-4A(ii)-2. Graph representation of percentages of effector T cell's IFN-γ release differences determined by the protein loaded unto DC. Error bars represent standard deviation. Percentages of effector T cell's IFN-γ release differences show higher efficiency when loading mBD2 fused OVA over non-fused. Positive controls (epitope peptide with OT-I (Table A5-4A(ii)-2) and negative controls (PBS and OT-I alone) show proper functionality of effector T cells (OT-I). A 5.5 hour DC and OT-I coincubation time was used and also no maturation was added.

Interpretation of Experiments. BM-DC pulsed with mBD2-OVA fusion proteins were superior in the stimulation of OVA-specific CD8+ T cells (OT-I) as assessed by IFN-γ production compared to OT-I cells stimulated by DC pulsed with PBS or mBD2 fused with an irrelevant antigen (mBD2-gp100T). This immunological effect on T cell activation was clearly dependent on fusing the antigen with mBD2, as unfused OVA proteins generated by the same approach only resulted in a marginal level of IFN-γ secretion by OT-I cells (Table A5-4A(ii)-1). With prolonged stimulation (8 hours), elevated levels of IFN-γ release were observed by both OVA and mBD2-OVA stimulated T cells, those stimulated by mBD2-OVA were still significantly higher (Data not shown).

Subsection 4A(iii). Crosspresentation of OVA epitope by DC to OT-I and effect of CCR6 removal on Crosspresentation of mBD2 fused antigen

Summary of Experiment. Crosspresentation of OVA by DC to OT-I experiments were performed concurrently to Crosspresentation of OVA by CCR6KO DC to same OT-I with same proteins and variables. Experiments were performed by following the same protocols and guidelines established on Section 2 Subsection 2A's BM-DC Generation and Protein Loading, Splenocyte Isolation, Simulation, and Maintenance, and DC/Splenocyte Coincubation and Intracellular Staining as well as Section 3 Subsection 3A's Crosspresentation of OVA epitope by DC to OT-I and Effect of CCR6 Removal on Crosspresentation of mBD2 fused Antigen.

Experiment Date: November 11, 2009 - See Appendix for Chapter 5 (Table A5-4A(iii)-1) for details.

Figure 5-4A(iii)-1. CCR6KO OVA Crosspresentation Experiments Results Graph

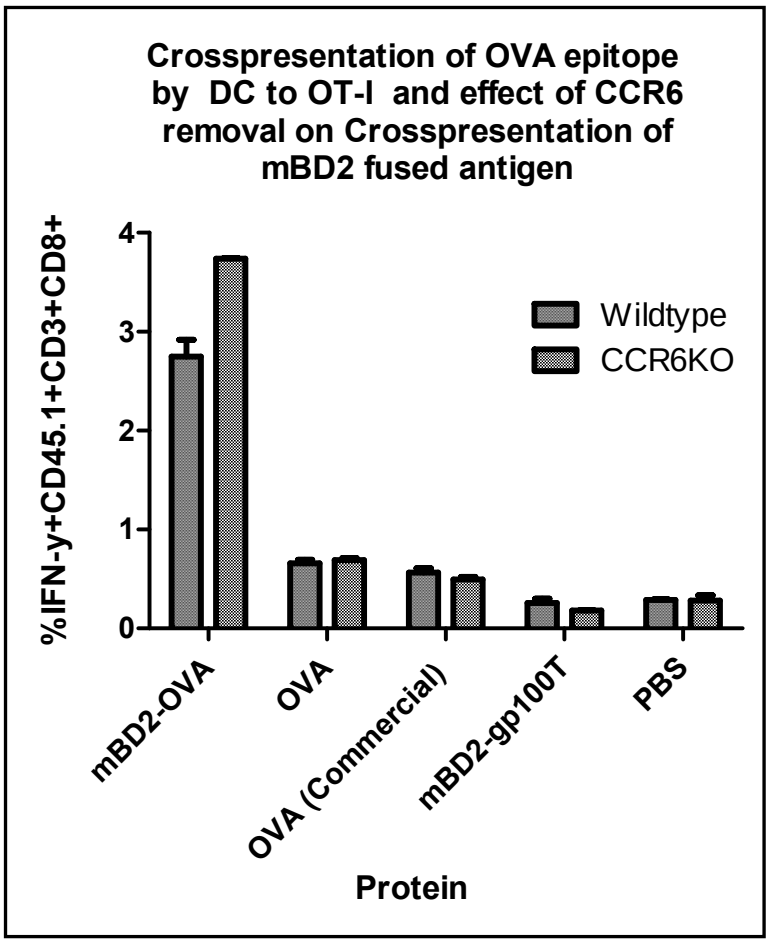

Figure 5-4A(iii)-1. Side by side (Wildtype versus CCR6KO) graph representation of percentages of effector T cell's IFN-γ release differences determined by the protein loaded unto DC. Error bars represent standard deviation. Graph shows minimal differences when comparing wildtype versus CCR6KO. The parallel experiments show no differences in percentages of effector T cell's IFN-γ release between CCR6KO groups versus wildtype groups for all variables. Positive controls (epitope peptide with OT-I) and negative controls (PBS and OT-I alone) show proper functionality of effector T cells. A 5.5 hour DC and OT-I coincubation time was used and also no maturation was added to DC.

Interpretation of Experiment. Given that mBD2 is a ligand for CCR6 (6), we hypothesized that the fusion protein-induced antigen cross-presentation would be CCR6 dependent. Thus, we performed the same experiment using BM-DC generated from CCR6 deficient mice. To our surprise, when we compared the levels of IFN-γ released by effector T cells stimulated with mBD2-OVA-pulsed CCR6 deficient or wild type BM-DC, there was no difference, suggesting that enhanced IFN-γ secretion induced by mBD2 is not dependent on CCR6.

Subsection 4B. *In vivo* Mechanism Experiments

Subsection 4B(i). OT-I Expansion Measure after mBD2 vaccine.

Summary of Experiments. Six equivalent experiments were performed to test enhanced OT-I expansion after mBD2 vaccine. The setup established on Section 3B's OT-I Expansion Measure after mBD2 Vaccine were followed. All mice in all six experiments received 1/30 of total donor OT-I+CD45.1+ spleen (~1-2x10^6 lymphocytes) via intravenous adoptive transfer on the tail followed by 150μg of recombinant protein (mBD2-OVA or OVA as determined by group) once subcutaneously on right flank of leg right. VSV-OVA immunized group was positive control group which received about 10^7 PFU of VSV per mouse. Mock immunized (PBS) group was negative control group.

Experiment #1 Date: August 11, 2009 - See Appendix for Chapter 5 (Table A5-4B(i)-1 and Figure A5-4B(i)-1) for details.

Experiment #2 Date: September 8, 2009 - See Table A5-4B(i)-2 and Figure A5-4B(i)-2.

Experiment #3 Date: October 31, 2009 - See Table A5-4B(i)-3 and Figure A5-4B(i)-3.

Experiment #4 Date: November 15, 2009 - See Table A5-4B(i)-4 and Figure A5-4B(i)-4.

Experiment #5 Date: December 11, 2009 - See Table A5-4B(i)-5 and Figure A5-4B(i)-5.

Experiment #6 Date: December 24, 2009 - See Table A5-4B(i)-6 and Figure A5-4B(i)-6.

Figure 5-4B(i)-1. OT-I Expansion Experiments Representative Graph

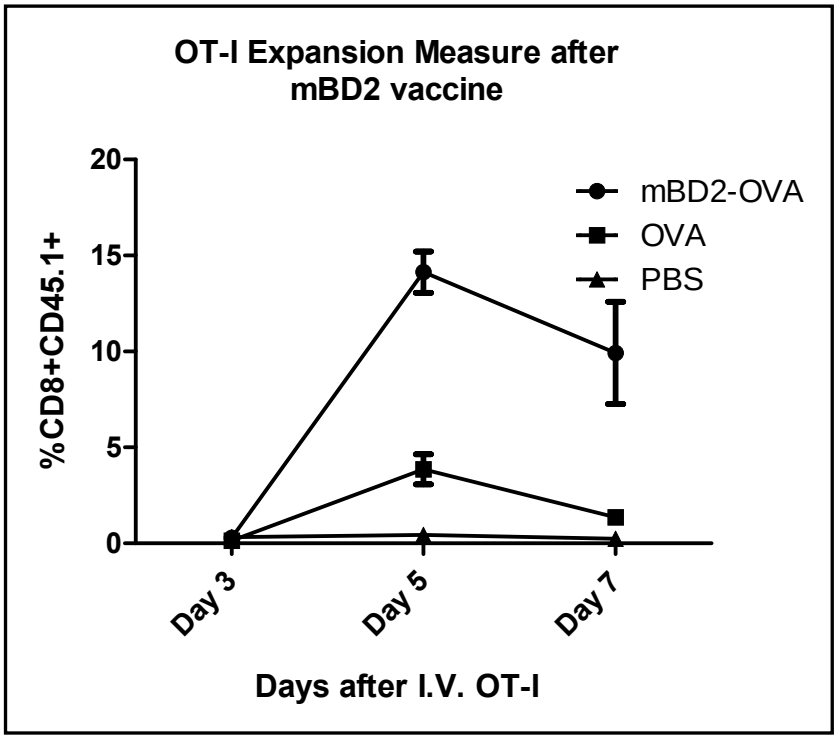

Figure 5-4B(i)-1. The actual measurements were on Day 3, 5, and 7. The lines serve as visual for the expansion pattern. Error bars are standard error of the mean. C57BL/6 mice received freshly isolated splenocytes (~1-2x10^6 cells) intravenously from OT-I+CD45.1+ transgenic mice followed by subcutaneous immunization with 150µg mBD2-OVA or OVA recombinant protein, or PBS. Mice were tail bled 3, 5, and 7 days post immunization. Blood was stained with appropriate flurochrome labeled CD8 or CD4 and CD45.1 antibodies and analyzed by flow cytometry. Differences between groups were statistically analyzed by 2 tailed student t-test. The data is shown as percentage CD45.1+ cells in the CD8+ population ± standard error of the mean. Representative experiment is Experiment #5 (Table A5-4B(i)-5).

Interpretation of Experiments. T cells derived from OT1+CD45.1+ transgenic mice were adoptively transferred into wild type C57BL/6 mice (CD45.2+ background), followed by vaccination the same day. The results revealed that single subcutaneous administration of 150 μg recombinant mBD2-OVA protein significantly stimulated the proliferation of adoptively transferred OT-I cells, determined by flow cytometry. The peak T-cell expansion appeared at about 5 days after vaccination. Although, vaccination with unfused OVA protein also was associated with OT-I cell expansion when compared to PBS controls; the level of expansion was significantly lower than that of mBD2-OVA.

Subsection 4B(ii). OT-II Expansion Measure after mBD2 vaccine.

Summary of Experiments. Two equivalent experiments were performed to test enhanced OT-II expansion after mBD2 vaccine. The setup established on Section 3B's OT-II Expansion Measure after mBD2 Vaccine were followed. All mice in all experiments received 1/30 of total donor OT-II+CD45.1+ spleen (~1-2x10^6 lymphocytes) via intravenous adoptive transfer on the tail followed by 150µg of recombinant protein (mBD2-OVA or OVA as determined by group) once subcutaneously on right flank of leg right. VSV-OVA immunized group was positive control group which received about 10^7 PFU of VSV per mouse. Mock immunized (PBS) group was negative control group.

Experiment #1 Date: October 13, 2009 - See Appendix for Chapter 5 (Table A5-4B(ii)-1 and Figure A5-4B(ii)-1) for details.

Experiment #2 Date: November 15, 2009 - See Appendix for Chapter 5 (Table A5-4B(ii)-2 and Figure A5-4B(ii)-2) for details.

Figure 5-4B(ii)-1. OT-II Expansion Experiments Representative Graph

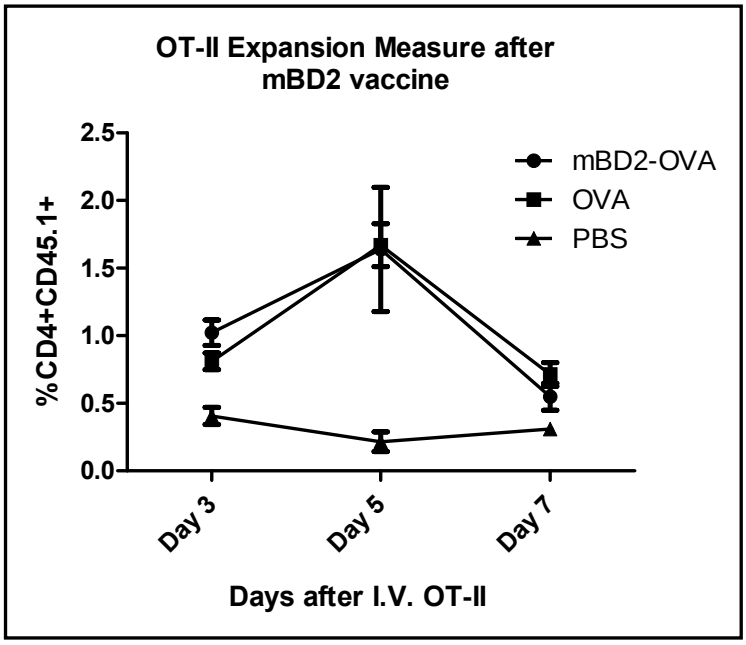

Figure 5-4B(ii)-1. The actual measurements were on Day 3, 5, and 7. The lines serve as visual for the expansion pattern. Error bars are standard error of the mean. Five C57BL/6 mice per group received freshly isolated splenocytes (~1-2x10^6 cells) intravenously from OT-II+CD45.1+ transgenic mice followed by subcutaneous immunization with 150µg mBD2-OVA or OVA recombinant protein, or PBS. Mice were tail bled 3, 5, and 7 days post immunization. Blood was stained with appropriate flurochrome labeled CD8 or CD4 and CD45.1 antibodies and analyzed by flow cytometry. Differences between groups were statistically analyzed by 2 tailed student t-test. The data is shown as percentage CD45.1+ cells in the CD8+ or CD4+ population ± standard error of the mean. Representative experiment is Experiment #1 (Table A5-4B(ii)-1).

Interpretation of Experiments. mBD2-OVA vaccination failed to enhance the proliferation of transferred OVA-specific CD4+ T cells derived from OT-II+CD45.1+ transgenic mice unlike OT-I+CD45.1+ T cells. mBD2-OVA may be more lenient towards generating a class I T cell response.

Subsection 4B(iii). OT-I Expansion Measure after mBD2 vaccine with CCR6 removal

Summary of Experiments. Two equivalent experiments were performed to test enhanced OT-I expansion after mBD2 vaccine in the setting where the recipient mouse does not have CCR6. The setup established on Section 3B's OT-I Expansion Measure after mBD2 Vaccine with CCR6 Removal was followed. All mice in all experiments received 1/30 of total donor OT-I+CD45.1+ spleen (~1-2x10^6 lymphocytes) via intravenous adoptive transfer on the tail followed by 150µg of recombinant mBD2-OVA once subcutaneously on right flank of leg right. The comparison was between wildtype recipient versus CCR6KO recipient having received same treatment.

Experiment #1 Date: October 31, 2009 - See Appendix for Chapter 5 (Table A5-4B(iii)-1 and Figure A5-4B(iii)-1) for details.

Experiment #2 Date: December 11, 2009 - See Appendix for Chapter 5 (Table A5-4B(iii)-2 and Figure A5-4B(iii)-2) for details.

Figure 5-4B(iii)-1. OT-I Expansion Experiments in CCR6KO Representative Graph

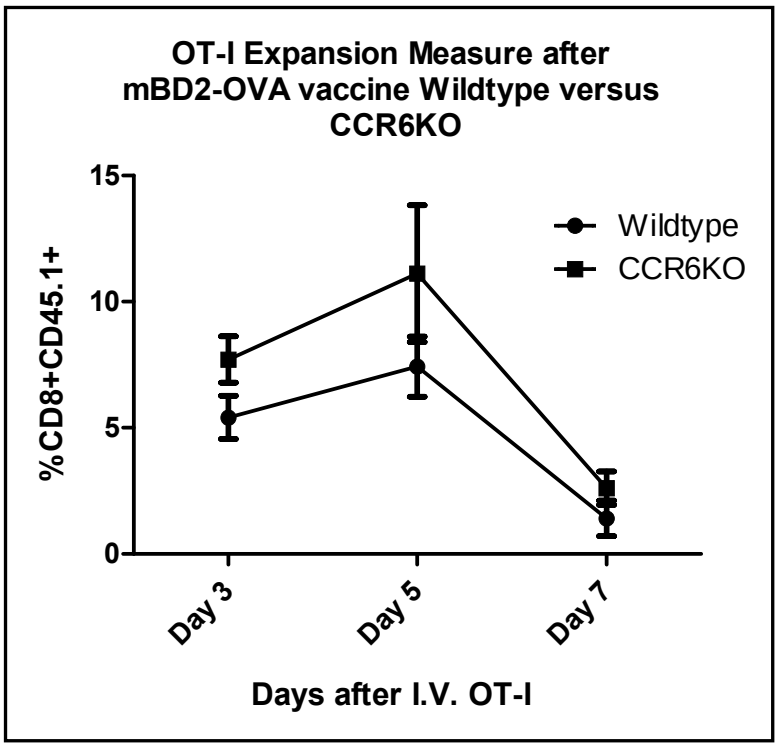

Figure 5-4B(iii)-1. Approximate expansion trajectory for all groups. The actual measurements were on Day 3, 5, and 7. The lines serve as visual for the expansion pattern. Error bars are standard error of the mean. C57BL/6 wildtype and CCR6 deficient (CCR6KO) mice per group received freshly isolated splenocytes intravenously (~1-2x10^6 cells) from OT-I+CD45.1+ transgenic mice. The adoptive T cell transfer was combined with subcutaneous immunization with 150µg mBD2-OVA recombinant protein, and the percentages of CD8+CD45.1+ cells in the blood were determined on days 3, 5, and 7. Representative experiment is Experiment #1 (Table A5-4B(iii)-1).

Interpretations of Experiments. Consistent with our *in vitro* data that suggested CCR6 independent cross-presentation of mBD2-OVA fusion protein (Figure 5-4A(iii)-1), expansion of OT-I T cells after adoptive transfer and vaccination was comparable in wildtype and CCR6 deficient hosts. The results suggest CCR6 independence for mBD2 vaccine's ability to expand CD8+ T cells .

Subsection 4B(iv). OT-I Expansion Measure after mBD2 vaccine with TLR4 removal

Summary of Experiments. Two equivalent experiments were performed to test enhanced OT-I expansion after mBD2 vaccine in the setting where the recipient mouse does not have TLR4. The setup established on Section 3B's OT-I Expansion Measure after mBD2 Vaccine with TLR4 Removal was followed. All mice in all experiments received 1/30 of total donor OT-I+CD45.1+ spleen (~1-2x10^6 lymphocytes) via intravenous adoptive transfer on the tail followed by 150µg of recombinant mBD2-OVA once subcutaneously on right flank of leg right. The comparison was between wildtype recipient versus TLR4KO recipient having received same treatment.

Experiment #1 Date: December 11, 2009 - See Appendix for Chapter 5 (Table A5-4B(iv)-1 and Figure A5-4B(iv)-1) for details.

Experiment #2 Date: December 24, 2009 - See Appendix for Chapter 5 (Table A5-4B(iv)-2 and Figure A5-4B(iv)-2) for details.

Figure 5-4B(iv)-1. OT-I Expansion Experiments in TLR4KO Representative Graph

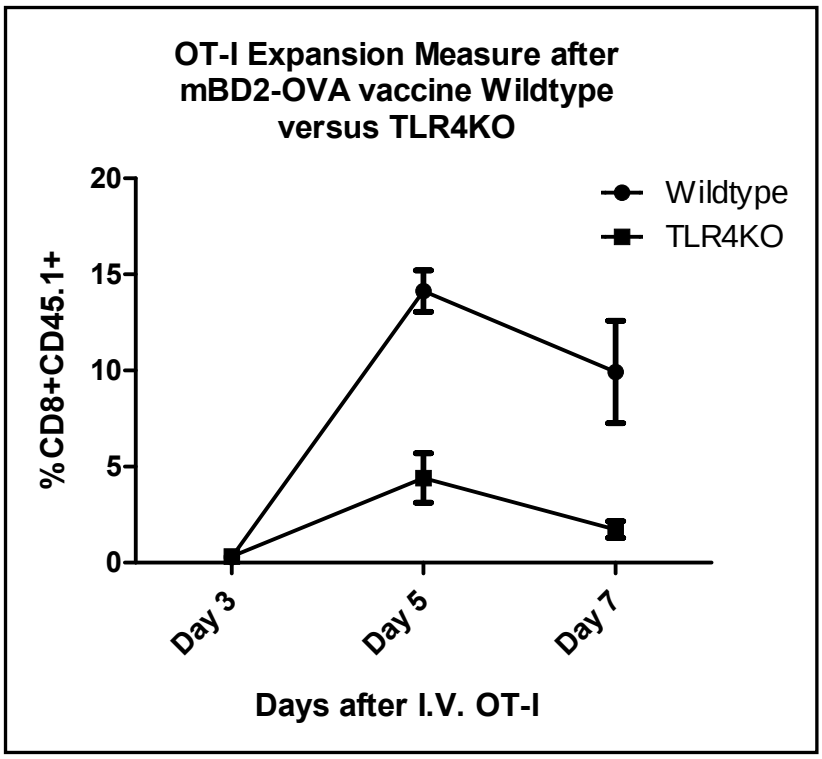

Figure 5-4B(iv)-1. Approximate expansion trajectory for all groups. The actual measurements were on Day 3, 5, and 7. The lines serve as visual for the expansion pattern. Error bars are standard error of the mean. C57BL/6 wildtype or TLR4 deficient (TLR4KO) mice per group received freshly isolated splenocytes intravenously (~1-2x10^6 cells) from OT-I+CD45.1+ transgenic mice. The adoptive T cell transfer was combined with subcutaneous immunization with 150μg mBD2-OVA recombinant protein, and the percentages of CD8+CD45.1+ cells in the blood were determined on days 3, 5, and 7. Representative experiment is Experiment #1 (Table A5-4B(iv)-1).

Interpretation of Experiments. Expansion of OT-I T cells after adoptive transfer and mBD2 vaccine vaccination was dramatically reduced in mice deficient of TLR4 under same experimental conditions versus wildtype, highlighting the dependence of TLR4 for mBD2 vaccine's ability to expand CD8+ T cells .

Subsection 4B(v). OT-I Expansion Measure after mBD2 vaccine with TLR4 adjuvant

Summary of Experiments. Two equivalent experiments were performed to test enhanced OT-I expansion after mBD2 vaccine and also in combination with TLR4 agonist adjuvant. The setup established on Section 3B's OT-I Expansion Measure after mBD2 Vaccine with TLR4 adjuvant was followed. All mice in all experiments received 1/30 of total donor OT-I+CD45.1+ spleen (~1-2x10^6 lymphocytes) via intravenous adoptive transfer on the tail followed by 150µg of recombinant (mBD2-OVA or OVA according to groups) once subcutaneously on right flank of leg right. Also, 50µg of TLR4 agonist (MPL) was mixed with vaccine in adjuvant added groups. Pairwise comparisons between all groups assessed synergy relationship between adjuvant and mBD2 vaccine.

Experiment #1 Date: October 31, 2009 - See Appendix for Chapter 5 (Table A5-4B(v)-1, Table A5-4B(v)-2, Figure A5-4B(v)-1, Figure A5-4B(v)-2, and Figure A5-4B(v)-3) for details.

Experiment #2 Date: November 15, 2009 - See Appendix for Chapter 5 (Table A5-4B(v)-3, Table A5-4B(v)-4, Figure A5-4B(v)-4, Figure A5-4B(v)-5, and Figure A5-4B(v)-6) for details.

Figure 5-4B(v)-1. OT-I Expansion with TLR4 Adjuvant Graph - mBD2-OVA versus mBD2-OVA MPL

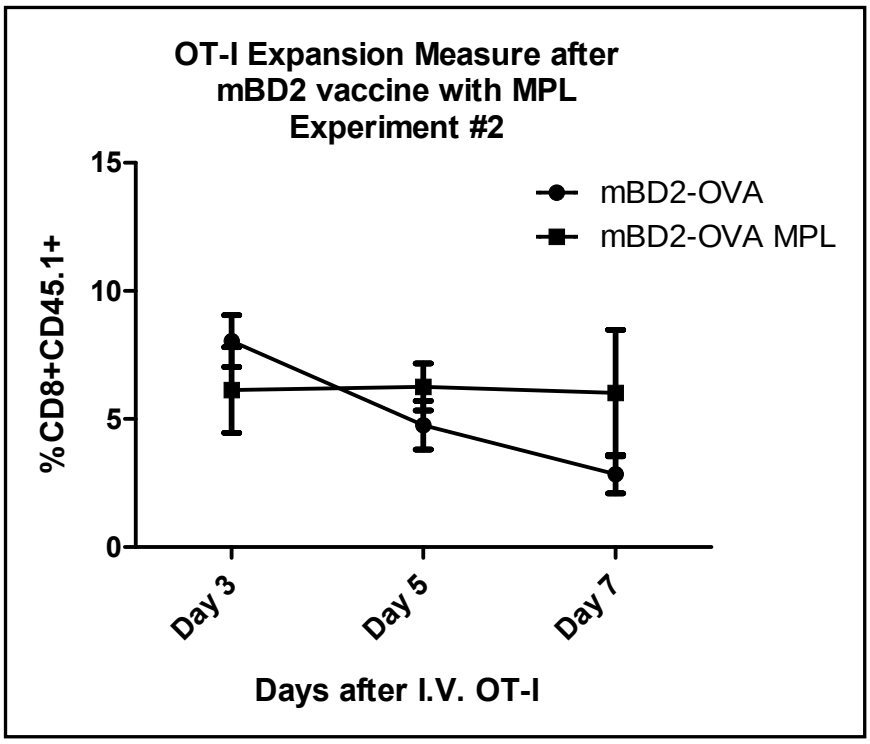

Figure 5-4B(v)-1. Approximate expansion trajectory for mBD2-OVA versus mBD2-OVA with MPL, TLR4 agonist adjuvant. The actual measurements were on Day 3, 5, and 7. The lines serve as visual for the expansion pattern. Error bars are standard error of the mean. C57BL/6 wildtype received freshly isolated splenocytes intravenously (~1-2x10^6 cells) from OT-I+CD45.1+ transgenic mice. The adoptive T cell transfer was combined with subcutaneous immunization with 150μg mBD2-OVA recombinant protein either with or without 50 μg MPL mixed with fusion protein, and the percentages of CD8+CD45.1+ cells in the blood were determined on days 3, 5, and 7. Representative experiment is Experiment #2 (Table A5-4B(v)-3).

Figure 5-4B(v)-2. OT-I Expansion with TLR4 Adjuvant Graph - OVA versus OVA MPL

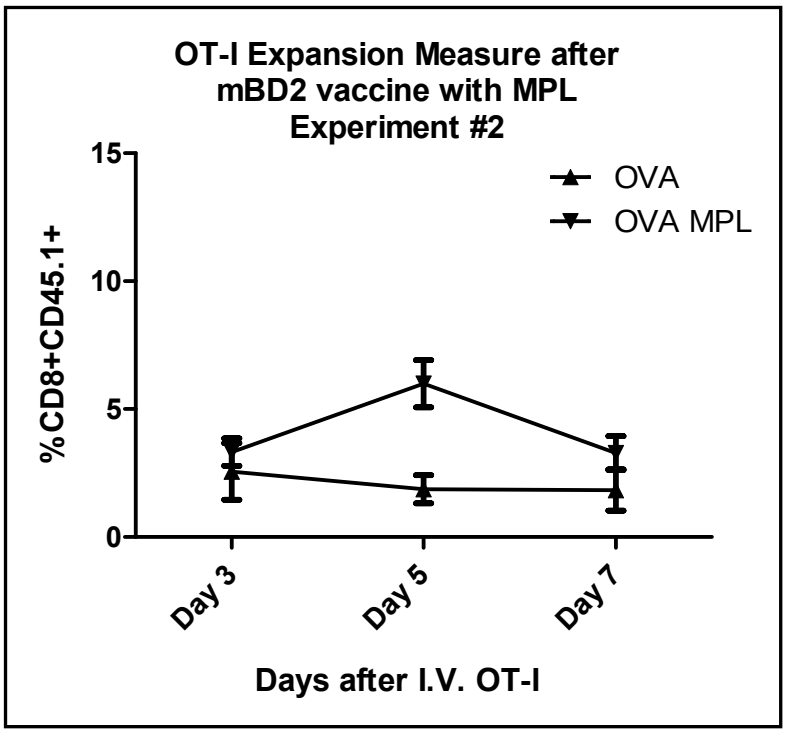

Figure 5-4B(v)-2. Approximate expansion trajectory for groups OVA and OVA with MPL, TLR4 agonist adjuvant. The actual measurements were on Day 3, 5, and 7. The lines serve as visual for the expansion pattern. Error bars are standard error of the mean. C57BL/6 wildtype received freshly isolated splenocytes intravenously (~1-2x10^6 cells) from OT-I+CD45.1+ transgenic mice. The adoptive T cell transfer was combined with subcutaneous immunization with 150µg OVA recombinant protein either with or without 50 µg MPL mixed with fusion protein, and the percentages of CD8+CD45.1+ cells in the blood were determined on days 3, 5, and 7. Representative experiment is Experiment #2 (Table A5-4B(v)-3).

Figure 5-4B(v)-3. OT-I Expansion with TLR4 Adjuvant Graph - mBD2-OVA versus OVA MPL

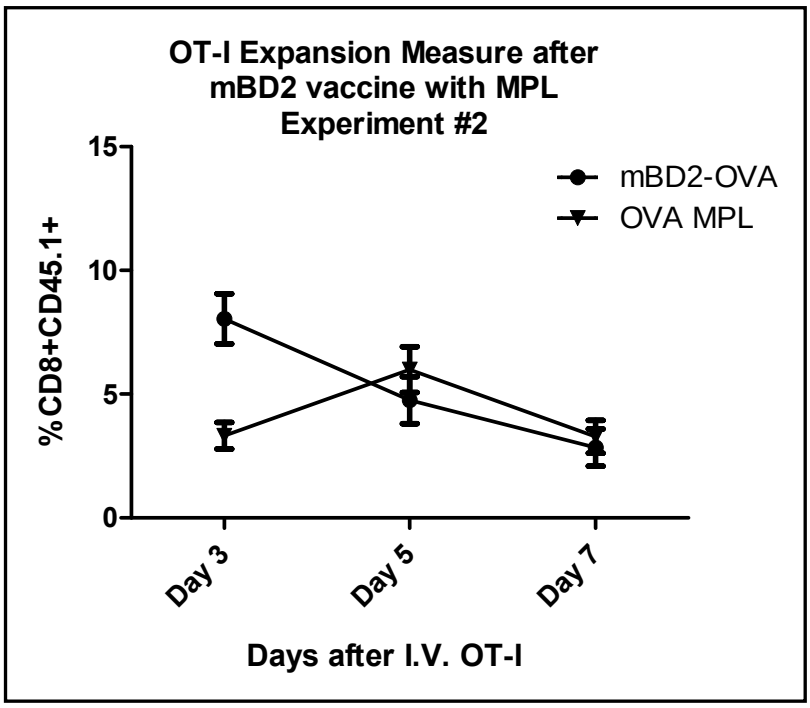

Figure 5-4B(v)-3. Approximate expansion trajectory for groups mBD2-OVA and OVA with MPL, TLR4 agonist adjuvant. The actual measurements were on Day 3, 5, and 7. The lines serve as visual for the expansion pattern. Error bars are standard error of the mean. C57BL/6 wildtype received freshly isolated splenocytes intravenously (~1-2x10^6 cells) from OT-I+CD45.1+ transgenic mice. The adoptive T cell transfer was combined with subcutaneous immunization with 150µg mBD2-OVA recombinant protein alone or OVA with 50 µg MPL mixed with fusion protein, and the percentages of CD8+CD45.1+ cells in the blood were determined on days 3, 5, and 7. Representative experiment is Experiment #2 (Table A5-4B(v)-3).

Interpretation of Experiments. The addition of MPL, TLR4 agonist, boosted T-cell expansion in mice vaccinated with unfused OVA but not with mBD2-OVA fusion proteins. Thus, combined with previous data with TLR4 deficient mice (Figure 5-4B(iv)-1) provides additional evidence for mBD2 playing a role with TLR4 as unfused OVA's ability to boost CD8+ T cell expansion increased with MPL while mBD2-OVA did not benefit.

Subsection 4B(vi). OT-I Expansion Measure after mBD2 vaccine with TLR9 adjuvant

Summary of Experiment. OT-I expansion after mBD2 vaccine and also in combination with TLR9 agonist adjuvant (CPG) was tested. The setup established on Section 3B's OT-I Expansion Measure after mBD2 Vaccine with TLR9 Adjuvant was followed. All mice in all experiments received 1/30 of total donor OT-I+CD45.1+ spleen (~1-2x10^6 lymphocytes) via intravenous adoptive transfer on the tail followed by 150µg of recombinant (mBD2-OVA or OVA according to groups) once subcutaneously on right flank of leg right. Also, 50µg of TLR9 agonist, CPG, was mixed with vaccine in adjuvant added groups. Pairwise comparisons between all groups assessed synergy relationship between adjuvant and mBD2 vaccine.

Experiment Date: August 11, 2009 - See Appendix for Chapter 5 (Table A5-4B(vi)-1) for details.

Table 5-4B(vi)-1. OT-I Expansion with TLR9 Adjuvant Experiment Results and Statistics Table

t-test (p-value)			
	Day 3	**Day 5**	**Day 7**
mBD2-OVA CPG versus mBD2-OVA	0.509734509	0.4643408	0.113991
mBD2-OVA CPG versus OVA CPG	0.349055814	0.33147143	0.375264
mBD2-OVA CPG versus OVA	0.084636112	0.10440237	0.093579
mBD2-OVA versus OVA CPG	0.091873118	0.56601647	0.511147
mBD2-OVA versus OVA	0.022237737	0.00308334	0.665394
OVA CPG versus OVA	0.053144583	0.35916448	0.417678

Table 5-4B(vi)-1. Pairwise 2 tailed unequal variance t-test for all groups. Statistical differences between all major groups. Five C57BL/6 mice per group received freshly isolated splenocytes (~1-2x10^6 cells) intravenously from OT-I+CD45.1+ transgenic mice followed by subcutaneous immunization with 150µg mBD2-OVA or OVA recombinant protein with or without 50µg of TLR9 agonist (CPG) or PBS. Mice were tail bled 3, 5, and 7 days post immunization. Blood was stained with appropriate flurochrome labeled CD8 or CD4 and CD45.1 antibodies and analyzed by flow cytometry.

Figure 5-4B(vi)-1. OT-I Expansion with TLR9 Adjuvant Experiment Graph - mBD2-OVA versus OVA CPG

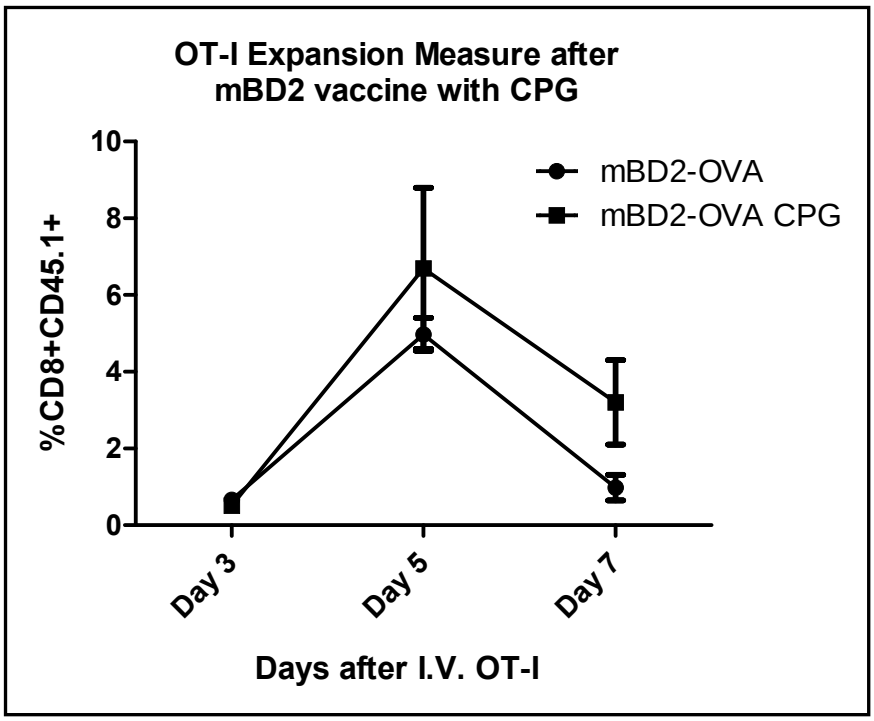

Figure 5-4B(vi)-1. Approximate expansion trajectory for mBD2-OVA versus mBD2-OVA with TLR9 agonist (CPG). The actual measurements were on Day 3, 5, and 7. The lines serve as visual for the expansion pattern. Error bars are standard error of the mean. Five C57BL/6 mice per group received freshly isolated splenocytes (~1-2x10^6 cells) intravenously from OT-I+CD45.1+ transgenic mice followed by subcutaneous immunization with 150µg mBD2-OVA recombinant protein with or without 50µg of CPG. Mice were tail bled 3, 5, and 7 days post immunization. Blood was stained with appropriate flurochrome labeled CD8 or CD4 and CD45.1 antibodies and analyzed by flow cytometry.

Figure 5-4B(vi)-2. OT-I Expansion with TLR9 Adjuvant Experiment Graph - OVA versus OVA CPG

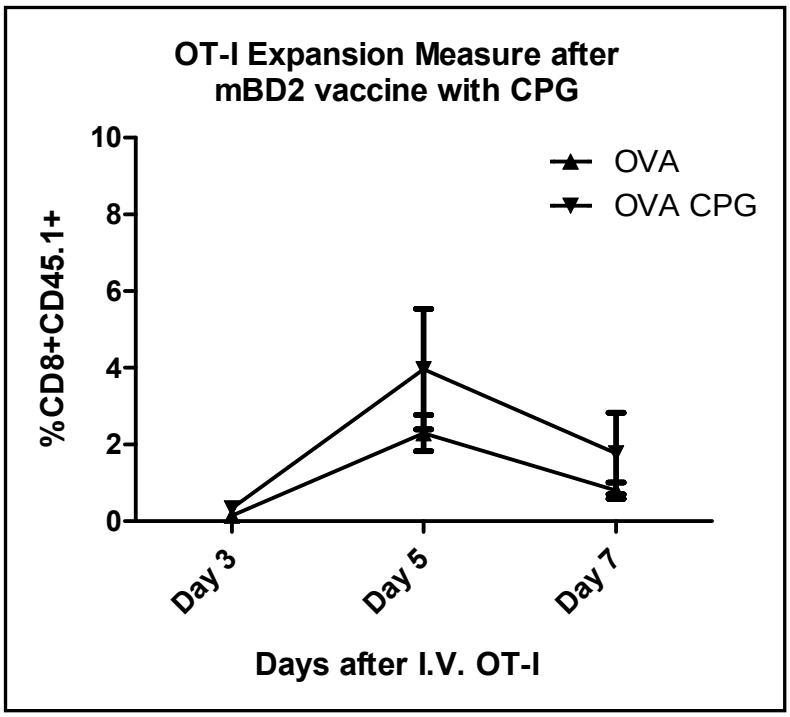

Figure 5-4B(vi)-2. Approximate expansion trajectory for OVA versus OVA with TLR9 agonist (CPG). The actual measurements were on Day 3, 5, and 7. The lines serve as visual for the expansion pattern. Error bars are standard error of the mean. Five C57BL/6 mice per group received freshly isolated splenocytes (~1-2x10^6 cells) intravenously from OT-I+CD45.1+ transgenic mice followed by subcutaneous immunization with 150µg OVA recombinant protein with or without 50µg of TLR9 agonist CPG. Mice were tail bled 3, 5, and 7 days post immunization. Blood was stained with appropriate flurochrome labeled CD8 or CD4 and CD45.1 antibodies and analyzed by flow cytometry.

Figure 5-4B(vi)-3. OT-I Expansion with TLR9 Adjuvant Experiment Graph - mBD2-OVA versus OVA CPG

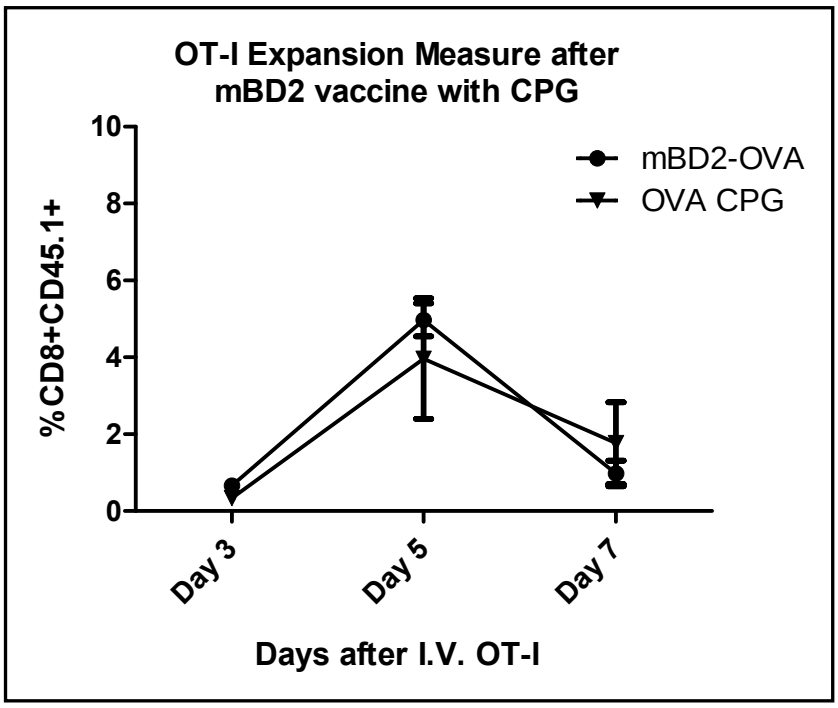

Figure 5-4B(vi)-3. Approximate expansion trajectory for mBD2-OVA versus OVA with TLR9 agonist (CPG). The actual measurements were on Day 3, 5, and 7. The lines serve as visual for the expansion pattern. Error bars are standard error of the mean. Five C57BL/6 mice per group received freshly isolated splenocytes (~1-2x10^6 cells) intravenously from OT-I+CD45.1+ transgenic mice followed by subcutaneous immunization with 150µg mBD2-OVA or OVA recombinant protein with 50µg of CPG. Mice were tail bled 3, 5, and 7 days post immunization. Blood was stained with appropriate flurochrome labeled CD8 or CD4 and CD45.1 antibodies and analyzed by flow cytometry.

Interpretation of Experiment. The addition of TLR9 agonist, CPG, did not enhance CD8+ T-cell expansion in mice vaccinated with unfused OVA or mBD2-OVA in a statistically significant manner. However, setting statistics aside, CPG does seem to enhance both unfused OVA or mBD2-OVA's ability to expand antigen specific CD8+ T cell population, albeit slightly.

Section 5. Discussion

Immunogenicity of Antigen Protein is Enhanced by fusion to mBD2. We wanted to test if adding mBD2 to the antigen would enhance antigen crosspresentation by DC. More specifically, we wanted to know if DC loaded with mBD2 fused antigen protein would induce higher IFN-γ release by antigen specific effector T cells through antigen presentation.

First, we generated bone marrow-derived DC (BM-DC) from naïve C57BL/6 mouse. Later, we generated mBD2-gp100T and gp100T protein. Using our *in vitro* cross presentation and intracellular IFN-γ release model with pmel-1 T cells, we noted differences in IFN-γ release between T cells coincubated with DC loaded with mBD2-gp100 versus gp100 (Figure 5-4A(i)-1, Figure 5-4A(i)-2, and Figure 5-4A(i)-3). Effector pmel-1 T cells stimulated with DC loaded with mBD2-gp100 generated significantly higher levels of IFN-γ compared to gp100 and mBD2-OVA (irrelevant antigen control) (Figure 5-4A(i)-2 and Figure 5-4A(i)-3). To make sure pmel-1 cells were functional, pmel-1 cells were incubated with positive control KVPRNQDWL peptide ($gp100_{25\text{-}33}$) which showed very high IFN-γ levels (Table A5-4A(i)-1, Table A5-4A(i)-2, and Table A5-4A(i)-3). On the other hand, negative control pmel-1 alone and pmel-1 with DC loaded with PBS showed minimal IFN-γ release. Thus, the release of IFN-γ was significantly enhanced if the correct antigen had mBD2 fused to it.

Next, we repeated the same *in vitro* cross presentation and intracellular IFN-γ release model used with pmel-1 T cells with OT-I T cells and mBD2-OVA/OVA protein instead. We noted OT-I T cells coincubated with DC loaded with mBD2-OVA generated

significantly higher levels of IFN-γ when compared to OT-I coincubated with DC with OVA or mBD2-gp100 (Figure 5-4A(ii)-1 and Figure 5-4A(ii)-2). Our negative control groups, OT-I alone and OT-I with DC loaded with PBS showed minimal IFN-γ release. Also, our positive control SIINFEKL ($OVA_{257-264}$) presented OT-I showed that OT-I were functional. Thus again, we showed T cell immunological effect being dependent on the presence of mBD2 with antigen.

In paraellel, knowing mBD2 to be a ligand for CCR6 (6), we hyptothesized that mBD2's crosspresentation enhancement would be CCR6 dependent. Thus, we performed the same *in vitro* cross presentation experiments except we also generated the DC from bone marrow derived from CCR6KO mouse. To our surprise, when we compared the amount of IFN-γ released by effector T cells incubated with CCR6-/- DC or CCR6+ DC, there was no difference (Figure 5-4A(iii)-1).

Enhanced CD8+ T cell Expansion with mBD2 fusion to Antigen. We were also aiming to test the mBD2 vaccine in an adoptive T cell immunotherapy strategy. Thus, we wanted to see the effect on antigen specific CD8+ T cell proliferation in the presence mBD2 fused antigen versus antigen alone. We also wanted an *in vivo* model rather than an *in vitro* one for the enhancement of antigen immunogenicity generated by mBD2. The availability of OT-I+CD45.1+ transgenic mouse allows us to track antigen specific CD45.1+ T cells introduced into wild type C57BL/6 mice (CD45.2+ background). Thus, after intravenous adoptive transfer of antigen specific T cells and subcutaneous vaccination of OVA protein, we noticed the antigen specific T cells to positively expand until reaching peak at about 5 days after treatment (Figures A5-4B(i)-1 to A5-4B(i)-6).

However, we noticed that the proliferation slope was much higher if the mice were vaccinated with mBD2-OVA instead (Figures A5-4B(i)-1 to A5-4B(i)-6). Statistical analysis also shows that this difference is statistically significant (Tables A5-4B(i)-1 to A5-4B(i)-6). Testing also revealed that subcutaneous injection of protein was better than an intraperitoneal injection (Data not shown). In addition, multiple subcutaneous vaccinations did not necessarily enhance the proliferation (Data not shown). Of course, poor proliferation was detected when PBS was injected (Figures A5-4B(i)-1 to A5-4B(i)-6).

No Enhancement of CD4+ T cell Proliferation with mBD2 fusion to Antigen. We had a working *in vivo* immune response model with CD8 T cells and we wanted one for CD4 T cells as well. Thus, knowing that OT-II+CD45.1+ transgenic mice were available, we decided to take the same measuring model used to trace CD8+ antigen specific T cell proliferation for CD4 T cells instead. CD4+ T cell dependency for the anti-tumor response by chemokine vaccines was previously demonstrated (10). Thus, we were expecting to see a similar proliferation pattern shown with OT-I cells, however, there was no difference in OT-II proliferation between OVA and mBD-2-OVA vaccinated mice (Figure A5-4B(ii)-1 and Figure A5-4B(ii)-2). Statistical analysis also revealed no significant difference in the proliferation of antigen specific CD4+ T cells (Table A5-4B(ii)-1 and Table A5-4B(ii)-2). Finally, poor proliferation was detected when PBS was injected.

Enhanced CD8+ T cell Proliferation by mBD2 fusion is CCR6 independent but TLR4 dependent. We were very surprised that CCR6-/- DC crosspresented mBD2 fused OVA to OT-I as effectively as CCR6+ DC (Figure 5-4A(iii)-1). The functionality of mBD2 was thought to be at least partly due to CCR6. The hypothesis of chemokine receptor mediated endocytosis presented previously (10, 11, 83)would have also implicated a crosspresentation efficiency reduction without CCR6. But of course, CCR6 is not the only chemokine receptor on DCs and other mechanisms could have compensated for the lack of CCR6. Yet, we needed to confirm our previous results, preferably *in vivo*. Thus, we intravenously infused OT-I+ T cells unto CCR6KO mice and wildtype mice, vaccinated them with mBD2-OVA protein, and compared their proliferation. The *in vitro* results using DC alone matched our proliferation results. There was no difference in the proliferation of antigen specific CD8+ T cells in CCR6+ versus CCR6KO mice (Figure A5-4B(iii)-1 and Figure A5-4B(iii)-2).

Knowing that mBD2 is a TLR4 ligand (8), we wanted to see the requirement of TLR4 for the enhanced proliferation. Using the same *in vivo* model used to test CCR6 dependency, we noted that the proliferation was significantly impaired in TLR4KO mouse which received mBD2-OVA protein in comparison to wild type mouse which also received mBD2-OVA protein vaccine (Figure A5-4B(iv)-1 and Figure A5-4B(iv)-2). In fact, the rate of proliferation was equal to wild type mouse which received OVA protein (Data not Shown). Thus, statistical analysis revealed significant statistical difference between wildtype mouse and TLR4KO where both groups received mBD2-OVA vaccine (Table A5-4B(iv)-1 and Table A5-4B(iv)-2). There was no statistical difference between TLR4KO mouse that received mBD2-OVA and wild type mouse

which received OVA (Data not shown).

Effects of TLR4 and TLR9 agonist Adjuvants on mBD2 Vaccine. Our goal is to significantly optimize our chemokine vaccine repertoire. The use of adjuvants to increase efficacy of vaccines is common (3, 20). We hypothesized that we would see an enhanced proliferation effect if the adjuvant helped the antigen increase immunogenicity. Knowing that mBD2 is a TLR4 ligand (8) and the availability of many studies using TLR agonists as adjuvants, pushed us to choose TLR agonists as adjuvants. We chose two of the most popular TLR receptors, TLR4 and TLR9, as our targets of choice.

We wanted to see synergy between mBD2 vaccine and adjuvant. When MPL was tested, the proliferation enhancement was statistically higher for OVA alone but not for mBD2-OVA (Table A5-4B(v)-2 and Table A5-4B(v)-4). Not seeing a proliferation enhancement when adding MPL to mBD2-OVA made sense as both mBD2 and MPL target the same TLR4 receptor. When CPG (TLR9 agonist) was tested, the proliferation enhancement was higher but not statistically significant over either OVA or mBD2-OVA (Table 5-4B(vi)-1).

Chapter 6. Conclusions and Recommendations

Section 1. Conclusions

Overall Summary. This study focuses on the investigation of the protein mBD2 vaccine. This vaccine can easily be produced on a large scale with an insect cell system (Chapter 3) but it was noted that the process of separating insect cell protein and desired vaccine protein (protein purification) can be difficult. This purification process is heavily dependent on the antigen.

It had previously been noted (6, 11, 12) and shown again that the DNA mBD2 vaccine can induce an anti-tumor response (Figure 4-4A-1). The decision to combine adoptive T cell therapy along with protein mBD2 vaccine came as a response to many attempts to enhance the efficacy of mBD2 vaccines. It was noted that the intravenous infusion of class I T cells specific to OVA antigen along with protein vaccine with component mBD2 fused to OVA antigen generated a strong protective immune response (Figure 4-4B-1). This protective response could overcome a lethal dose of tumor infusion with no treatment. On separate experiments with tumor antigen gp100, the adoptive transfer of class I gp100 specific T cells with mBD2-gp100T immunization also provided a significantly superior tumor protection response (Figure 4-4C-1).

The study also focused on finding the mechanism of the mBD2 vaccine's protective response. The study first shows that DC which have absorbed mBD2 fused antigen induces antigen specific effector T cells to release greater amounts of IFN-γ than T cells which have been activated by DC which absorbed antigen alone (Figure 5-4A(i)-

1 to Figure 5-4A(i)-3 and Figure 5-4A(ii)-1 to Figure 5-4A(ii)-2). Enhanced secretion of IFN-γ by T cells correlates to T cell activation, response modulation, and expansion. Hence, the study associates mBD2 to enhanced T cell response.

Next, the study shows that in an *in vivo* model, the immunization of mBD2 fused antigen protein vaccine causes an enhanced expansion of class I specific T cells but not class II specific T cells (Figure A5-4B(i)-1 to Figure A5-4B(i)-6 and Figure A5-4B(ii)-1 to Figure A5-4B(ii)-2). This response is further noted to be CCR6 independent but TLR4 dependent (Figure A5-4B(iii)-1 to Figure A5-4B(iii)-2 and Figure A5-4B(iv)-1 to Figure A5-4B(iv)-2) . And lastly, this enhanced class I T cell response by mBD2 vaccine is not significantly enhanced even if TLR4 or TLR9 agonist adjuvant is combined on top (Table A5-4B(v)-2, Table A5-4B(v)-4, and Table 5-4B(vi)-2).

Author's Opinions. A tremendous amount of effort has been placed in the elucidation of the mechanism behind the function of chemokine vaccines (5-7, 9-12) and due to mBD2's link with CCR6 (6, 84), mBD2 vaccine's functional mechanism has been assumed to be the same as that of other chemokine vaccines. Whether this holds true or not, the unproven speculation behind a chemokine vaccine's power lies in an unintentional absorption of antigen by chemokine receptors via chemokine receptor mediated endocytosis due to the chemokine's fusion with antigen. Showing that the immunization with chemokine fused antigen generated better T cell responses than antigen mix with free chemokine showed the possibility that maybe a chemokine receptor mediated endocytosis of chemokine fused antigen would take antigen in a separate vesicle or internalization pathway inside the cell that lead to a more direct or

effective antigen processing and crosspresentation conduit versus other antigen processing pathways. This is the general theoretical functional model of the chemokine vaccine.

However, when mBD2 vaccines worked even in the absence of CCR6, it was brought into light the possibility of mBD2 vaccines working without chemokine receptor mediated endocytosis and further question the chemokine receptor mediated crosspresentation pathway for mBD2 vaccines. mBD2 vaccines may instead depend on TLR4 mediated endocytosis or unidentified receptor absorption. Further, mBD2 vaccines could also or instead assist antigen to a crosspresentation pathway once the antigen has been internalized. Thus, the endocytosis of antigen could solely be antigen dependent.

Thus, it is feasible that mBD2-fused antigen proteins are able to target or be absorbed by the appropriate APC and enter the correct subcellular compartment to mediate TLR4 dependent crosspresentation to CD8+ T cells. This appropriate APC has the most potential to be DC but not limited to DCs. A good suspect for this subcellular compartment would be the early endocytic compartment (EEC) described previously (85). Previous studies have found that the MyD88 pathway controls the efficiency of crosspresentation (86) and further shown that a TLR4-MyD88 dependent recruitment of the essential MHC class I antigen processing and loading component, transporter associated with antigen processing (TAP), to the EEC occurs (85). Thus in the now suggested hypothetical model, it is possible that mBD2-fused antigen protein once endocytosed by DC enters the EEC and mBD2 recruits TAP via TLR4-MyD88 signaling to the EEC. Thus, in the absence of mBD2, TAP is not recruited to the EEC and

crosspresentation is less efficient. Accordingly the final processing of the mBD2 fused antigen and increased TAP presence to mediate MHC class I antigen peptide loading would enhance crosspresentation.

In this study, T-cell crosspriming was also associated with protective anti-tumor immunity. When combined with adoptive T cell therapy, mBD2 vaccine immunization generated stronger anti-tumor protection over antigen alone. Tumor resistance was apparent against lethal doses of B16-OVA and B16 melanoma, respectively, which typically are very aggressive tumors in syngeneic mice (76). However, immunization of mBD2 vaccine alone did not induce visible or statistically different tumor resistance metrics over antigen alone when adoptive T cell therapy was not combined (Data not shown). This may be the result of technical error as the protein vaccine may have not been tested sufficiently in a stand-alone basis or instead the tumor challenge may have been too strong or it is also possible that this vaccine only works if an established load of antigen specific T cells exists in order to generate a sufficiently potent immune response against target. Ultimately, clinical translation may require combining mBD2 vaccines with T cell therapy to eradicate established tumors (87).

Section 2. Recommendations

Future Directions. The future of the mBD2 vaccine comes in further improving its efficacy and developing the pathway to taking it to the clinic. Still many questions need to be answered before the mBD2 vaccine can be a success in the clinic. The pathway for the testing of the DNA chemokine vaccine in the clinic is already underway (as of

December 2009). Also, adoptive T cell therapy is also undergoing much breakthrough and available (88). The bulk of the effort in the future will involve answering efficacy based questions in how to combine mBD2 vaccines with adoptive T cell therapy to generate robust cancer immunotherapy strategies in patients. Finding the answer to these questions will eventually explain the mechanism of this vaccine and immunotherapy in general. Short term goals include the optimization of vaccine production as well as vaccine dosage for the most effective response. Lastly, short term goals for which endeavors were established in this study but ultimately not included due to technical problems include answering questions on finding the internalization pathway of mBD2 vaccine protein, the alternate internal crosspresentation pathway or new crosspresentation subcellular compartment used by mBD2 vaccine protein, the APC responsible for crosspresentation of mBD2 vaccine protein, and the role of antigen for mBD2 vaccine protein.

One short term goal worth pursuing is moving forwards on proving or disproving the alternative mBD2-fused antigen protein internalization and crosspresentation hypothetical model presented previously (Chapter 6, Section 1, Author's Opinions). The proposed model involves mBD2-fused antigen protein entering DC via endocytosis to EEC and mBD2 recruiting TAP via TLR4-MyD88 signaling to the EEC, and accordingly the final processing of the mBD2 fused antigen and increased TAP presence promotes MHC class I antigen peptide loading and thus crosspresentation enhancement.

The first step would involve labeling both OVA and mBD2-OVA protein with a fluorochrome, preferably Invitrogen's Qdot® crystal. In addition, the labeling of antibodies for different the different intracellular comparments/endosomes namely anti-

EEA1 (early endosomal Marker), anti-Rab7 (late endosomal marker), anti-LAMP-1 (Lysosome marker), and other intracellular endosomal markers with different Qdot® crystals at different fluorescence wavelengths would be a start. Additionally, the labeling of 25-D1.16 (H2 Kb and $OVA_{257-264}$ (SIINFEKL) recognizing antidoby - Dr. Jonathan Yewdell (National Institutes of Health)), mannose receptor recognizing antibody, MHC class I recognizing antibody, and MHC class II recognizing antibody would also be necessary.

After the labeling of mBD2-OVA and OVA protein and intracellular pathway segment antibodies, it would be necessary to find the pathway which the protein takes within the DC by pulsing the labeled proteins separately and later having the DC fixed at different time points after protein pulsing and incubation of DC in media with protein at 37°C. After endosomal segment antibody labeling and confocal microscopy the pathway within the DC at different time points for both mBD2-OVA protein and OVA could be determined. EEC should also be elucidated.

Next after the elucidation of the pathway and identity of EEC, taking DC derived from TAP, TLR4, and MyD88 deficient mice, pulsing with mBD2-OVA or OVA protein, and screening for the amount of 25-D1.16 binding within elucidated endosomal compartment (possibly the EEC aforementioned) would demonstrate mBD2 TAP recruitment, mBD2 and TLR4-MyD88 signaling dependence, and increased presence of MHC class I antigen peptide (epitope) dependent on mBD2, TAP, and TLR4. Of course, the hypothetical model could also be totally disproved.

Author's Curiosity. When mice were infused with splenocytes from OT-I+CD45.1+ transgenic mice via adoptive transfer and later immunized with mBD2-OVA instead of OVA, a greater expansion of CD8+CD45.1+ T cells was seen. However, this occurrence was not duplicated in the pmel-1+CD90.1+ system model with mBD2-gp100T versus gp100T (Data not shown). The most likely suspect for the inability to duplicate is technical. Technical problems exist most likely due to the difficulty in extracting properly folded gp100 protein. The more unlikely but possible reason is due to the immunogenicity of gp100. Yet, another reason why the mBD2 vaccine worked in the OVA model and not in the gp100 might be because OVA targets the mannose receptor (85). It might be possible that a link between the mannose receptor and TLR4 is the key for enhancing crosspresentation. If this is true, testing and comparing OVA fused to gp100T and mBD2 fused to both OVA and gp100T in the pmel-1+CD90.1+ system model might be an experiment worth pursuing to answer if the OVA and mannose receptor link can play an important role in generating antigen specific immunity.

Chapter 7. Bibliography

1. Finn, O. J. 2003. Cancer vaccines: between the idea and the reality. Nat Rev Immunol 3:630-641.
2. Overwijk, W. W. 2005. Breaking tolerance in cancer immunotherapy: time to ACT. Curr Opin Immunol 17:187-194.
3. McKee, A. S., M. W. Munks, and P. Marrack. 2007. How do adjuvants work? Important considerations for new generation adjuvants. Immunity 27:687-690.
4. Stevenson, F. K., J. Rice, C. H. Ottensmeier, S. M. Thirdborough, and D. Zhu. 2004. DNA fusion gene vaccines against cancer: from the laboratory to the clinic. Immunol Rev 199:156-180.
5. Biragyn, A., K. Tani, M. C. Grimm, S. Weeks, and L. W. Kwak. 1999. Genetic fusion of chemokines to a self tumor antigen induces protective, T-cell dependent antitumor immunity. Nat Biotechnol 17:253-258.
6. Biragyn, A., M. Surenhu, D. Yang, P. A. Ruffini, B. A. Haines, E. Klyushnenkova, J. J. Oppenheim, and L. W. Kwak. 2001. Mediators of innate immunity that target immature, but not mature, dendritic cells induce antitumor immunity when genetically fused with nonimmunogenic tumor antigens. J Immunol 167:6644-6653.
7. Biragyn, A., I. M. Belyakov, Y. H. Chow, D. S. Dimitrov, J. A. Berzofsky, and L. W. Kwak. 2002. DNA vaccines encoding human immunodeficiency virus-1 glycoprotein 120 fusions with proinflammatory chemoattractants induce systemic and mucosal immune responses. Blood 100:1153-1159.

8. Biragyn, A., P. A. Ruffini, C. A. Leifer, E. Klyushnenkova, A. Shakhov, O. Chertov, A. K. Shirakawa, J. M. Farber, D. M. Segal, J. J. Oppenheim, and L. W. Kwak. 2002. Toll-like receptor 4-dependent activation of dendritic cells by beta-defensin 2. Science 298:1025-1029.

9. Ruffini, P. A., A. Biragyn, M. Coscia, L. K. Harvey, S. C. Cha, B. Bogen, and L. W. Kwak. 2004. Genetic fusions with viral chemokines target delivery of nonimmunogenic antigen to trigger antitumor immunity independent of chemotaxis. J Leukoc Biol 76:77-85.

10. Biragyn, A., P. A. Ruffini, M. Coscia, L. K. Harvey, S. S. Neelapu, S. Baskar, J. M. Wang, and L. W. Kwak. 2004. Chemokine receptor-mediated delivery directs self-tumor antigen efficiently into the class II processing pathway in vitro and induces protective immunity in vivo. Blood 104:1961-1969.

11. Schiavo, R., D. Baatar, P. Olkhanud, F. E. Indig, N. Restifo, D. Taub, and A. Biragyn. 2006. Chemokine receptor targeting efficiently directs antigens to MHC class I pathways and elicits antigen-specific CD8+ T-cell responses. Blood 107:4597-4605.

12. Biragyn, A., R. Schiavo, P. Olkhanud, K. Sumitomo, A. King, M. McCain, F. E. Indig, G. Almanzar, and D. Baatar. 2007. Tumor-associated embryonic antigen-expressing vaccines that target CCR6 elicit potent CD8+ T cell-mediated protective and therapeutic antitumor immunity. J Immunol 179:1381-1388.

13. Gurunathan, S., D. M. Klinman, and R. A. Seder. 2000. DNA vaccines: immunology, application, and optimization*. Annu Rev Immunol 18:927-974.

14. Park, H. J., and S. S. Neelapu. 2008. Developing idiotype vaccines for lymphoma: from preclinical studies to phase III clinical trials. Br J Haematol 142:179-191.

15. Ribas, A., L. H. Butterfield, J. A. Glaspy, and J. S. Economou. 2003. Current developments in cancer vaccines and cellular immunotherapy. J Clin Oncol 21:2415-2432.

16. Rosenberg, S. A., J. C. Yang, and N. P. Restifo. 2004. Cancer immunotherapy: moving beyond current vaccines. Nat Med 10:909-915.

17. Yu, Z., and N. P. Restifo. 2002. Cancer vaccines: progress reveals new complexities. J Clin Invest 110:289-294.

18. Rosenberg, S. A. 2004. Shedding light on immunotherapy for cancer. N Engl J Med 350:1461-1463.

19. Neelapu, S. S., B. L. Gause, L. Harvey, S. T. Lee, A. R. Frye, J. Horton, R. J. Robb, M. C. Popescu, and L. W. Kwak. 2007. A novel proteoliposomal vaccine induces antitumor immunity against follicular lymphoma. Blood 109:5160-5163.

20. Guy, B. 2007. The perfect mix: recent progress in adjuvant research. Nat Rev Microbiol 5:505-517.

21. Gilboa, E. 2007. DC-based cancer vaccines. J Clin Invest 117:1195-1203.

22. Zhang, L., Y. Tang, H. Akbulut, D. Zelterman, P. J. Linton, and A. B. Deisseroth. 2003. An adenoviral vector cancer vaccine that delivers a tumor-associated antigen/CD40-ligand fusion protein to dendritic cells. Proc Natl Acad Sci U S A 100:15101-15106.

23. Tao, M. H., and R. Levy. 1993. Idiotype/granulocyte-macrophage colony-stimulating factor fusion protein as a vaccine for B-cell lymphoma. Nature 362:755-758.

24. Schmidt, S. M., K. Schag, M. R. Muller, M. M. Weck, S. Appel, L. Kanz, F. Grunebach, and P. Brossart. 2003. Survivin is a shared tumor-associated antigen expressed in a broad variety of malignancies and recognized by specific cytotoxic T cells. Blood 102:571-576.

25. Knutson, K. L., K. Schiffman, and M. L. Disis. 2001. Immunization with a HER-2/neu helper peptide vaccine generates HER-2/neu CD8 T-cell immunity in cancer patients. J Clin Invest 107:477-484.

26. Thomas, A. M., L. M. Santarsiero, E. R. Lutz, T. D. Armstrong, Y. C. Chen, L. Q. Huang, D. A. Laheru, M. Goggins, R. H. Hruban, and E. M. Jaffee. 2004. Mesothelin-specific CD8(+) T cell responses provide evidence of in vivo cross-priming by antigen-presenting cells in vaccinated pancreatic cancer patients. J Exp Med 200:297-306.

27. Coulie, P. G., V. Karanikas, C. Lurquin, D. Colau, T. Connerotte, T. Hanagiri, A. Van Pel, S. Lucas, D. Godelaine, C. Lonchay, M. Marchand, N. Van Baren, and T. Boon. 2002. Cytolytic T-cell responses of cancer patients vaccinated with a MAGE antigen. Immunol Rev 188:33-42.

28. Joyce, J. A. 2005. Therapeutic targeting of the tumor microenvironment. Cancer Cell 7:513-520.

29. Medzhitov, R., and C. Janeway, Jr. 2000. Innate immunity. N Engl J Med 343:338-344.

30. Medzhitov, R., and C. A. Janeway, Jr. 1997. Innate immunity: impact on the adaptive immune response. Curr Opin Immunol 9:4-9.

31. Aguilar, J. C., and E. G. Rodriguez. 2007. Vaccine adjuvants revisited. Vaccine 25:3752-3762.

32. Craft, N., K. W. Bruhn, B. D. Nguyen, R. Prins, J. W. Lin, L. M. Liau, and J. F. Miller. 2005. The TLR7 agonist imiquimod enhances the anti-melanoma effects of a recombinant Listeria monocytogenes vaccine. J Immunol 175:1983-1990.

33. Morefield, G. L., L. D. Hawkins, S. T. Ishizaka, T. L. Kissner, and R. G. Ulrich. 2007. Synthetic Toll-like receptor 4 agonist enhances vaccine efficacy in an experimental model of toxic shock syndrome. Clin Vaccine Immunol 14:1499-1504.

34. Peng, G., Z. Guo, Y. Kiniwa, K. S. Voo, W. Peng, T. Fu, D. Y. Wang, Y. Li, H. Y. Wang, and R. F. Wang. 2005. Toll-like receptor 8-mediated reversal of CD4+ regulatory T cell function. Science 309:1380-1384.

35. Guyre, P. M., R. F. Graziano, J. Goldstein, P. K. Wallace, P. M. Morganelli, K. Wardwell, and A. L. Howell. 1997. Increased potency of Fc-receptor-targeted antigens. Cancer Immunol Immunother 45:146-148.

36. Engering, A. J., M. Cella, D. M. Fluitsma, E. C. Hoefsmit, A. Lanzavecchia, and J. Pieters. 1997. Mannose receptor mediated antigen uptake and presentation in human dendritic cells. Adv Exp Med Biol 417:183-187.

37. Schmid, D., and C. Munz. 2007. Innate and adaptive immunity through autophagy. Immunity 27:11-21.

38. Curiel, T. J. 2007. Tregs and rethinking cancer immunotherapy. J Clin Invest 117:1167-1174.

39. Pardoll, D. 2003. Does the immune system see tumors as foreign or self? Annu Rev Immunol 21:807-839.

40. Sakaguchi, S., and F. Powrie. 2007. Emerging challenges in regulatory T cell function and biology. Science 317:627-629.

41. Yang, Z. Z., A. J. Novak, M. J. Stenson, T. E. Witzig, and S. M. Ansell. 2006. Intratumoral CD4+CD25+ regulatory T-cell-mediated suppression of infiltrating CD4+ T cells in B-cell non-Hodgkin lymphoma. Blood 107:3639-3646.

42. Litzinger, M. T., R. Fernando, T. J. Curiel, D. W. Grosenbach, J. Schlom, and C. Palena. 2007. IL-2 immunotoxin denileukin diftitox reduces regulatory T cells and enhances vaccine-mediated T-cell immunity. Blood 110:3192-3201.

43. Dannull, J., Z. Su, D. Rizzieri, B. K. Yang, D. Coleman, D. Yancey, A. Zhang, P. Dahm, N. Chao, E. Gilboa, and J. Vieweg. 2005. Enhancement of vaccine-mediated antitumor immunity in cancer patients after depletion of regulatory T cells. J Clin Invest 115:3623-3633.

44. Mahnke, K., K. Schonfeld, S. Fondel, S. Ring, S. Karakhanova, K. Wiedemeyer, T. Bedke, T. S. Johnson, V. Storn, S. Schallenberg, and A. H. Enk. 2007. Depletion of CD4+CD25+ human regulatory T cells in vivo: kinetics of Treg depletion and alterations in immune functions in vivo and in vitro. Int J Cancer 120:2723-2733.

45. Barnett, B., I. Kryczek, P. Cheng, W. Zou, and T. J. Curiel. 2005. Regulatory T cells in ovarian cancer: biology and therapeutic potential. Am J Reprod Immunol 54:369-377.

46. Jarnicki, A. G., J. Lysaght, S. Todryk, and K. H. Mills. 2006. Suppression of antitumor immunity by IL-10 and TGF-beta-producing T cells infiltrating the growing tumor: influence of tumor environment on the induction of CD4+ and CD8+ regulatory T cells. J Immunol 177:896-904.

47. Wei, S., I. Kryczek, L. Zou, B. Daniel, P. Cheng, P. Mottram, T. Curiel, A. Lange, and W. Zou. 2005. Plasmacytoid dendritic cells induce CD8+ regulatory T cells in human ovarian carcinoma. Cancer Res 65:5020-5026.

48. Taniguchi, M., M. Harada, S. Kojo, T. Nakayama, and H. Wakao. 2003. The regulatory role of Valpha14 NKT cells in innate and acquired immune response. Annu Rev Immunol 21:483-513.

49. Almand, B., J. I. Clark, E. Nikitina, J. van Beynen, N. R. English, S. C. Knight, D. P. Carbone, and D. I. Gabrilovich. 2001. Increased production of immature myeloid cells in cancer patients: a mechanism of immunosuppression in cancer. J Immunol 166:678-689.

50. Kryczek, I., L. Zou, P. Rodriguez, G. Zhu, S. Wei, P. Mottram, M. Brumlik, P. Cheng, T. Curiel, L. Myers, A. Lackner, X. Alvarez, A. Ochoa, L. Chen, and W. Zou. 2006. B7-H4 expression identifies a novel suppressive macrophage population in human ovarian carcinoma. J Exp Med 203:871-881.

51. Peng, G., H. Y. Wang, W. Peng, Y. Kiniwa, K. H. Seo, and R. F. Wang. 2007. Tumor-infiltrating gammadelta T cells suppress T and dendritic cell function via

mechanisms controlled by a unique toll-like receptor signaling pathway. Immunity 27:334-348.

52. Salazar-Onfray, F. 1999. Interleukin-10: a cytokine used by tumors to escape immunosurveillance. Med Oncol 16:86-94.

53. Liu, V. C., L. Y. Wong, T. Jang, A. H. Shah, I. Park, X. Yang, Q. Zhang, S. Lonning, B. A. Teicher, and C. Lee. 2007. Tumor evasion of the immune system by converting CD4+CD25- T cells into CD4+CD25+ T regulatory cells: role of tumor-derived TGF-beta. J Immunol 178:2883-2892.

54. Gabrilovich, D. I., H. L. Chen, K. R. Girgis, H. T. Cunningham, G. M. Meny, S. Nadaf, D. Kavanaugh, and D. P. Carbone. 1996. Production of vascular endothelial growth factor by human tumors inhibits the functional maturation of dendritic cells. Nat Med 2:1096-1103.

55. Zamanakou, M., A. E. Germenis, and V. Karanikas. 2007. Tumor immune escape mediated by indoleamine 2,3-dioxygenase. Immunol Lett 111:69-75.

56. Marincola, F. M., E. M. Jaffee, D. J. Hicklin, and S. Ferrone. 2000. Escape of human solid tumors from T-cell recognition: molecular mechanisms and functional significance. Adv Immunol 74:181-273.

57. Drake, C. G., E. Jaffee, and D. M. Pardoll. 2006. Mechanisms of immune evasion by tumors. Adv Immunol 90:51-81.

58. Droin, N., J. B. Hendra, P. Ducoroy, and E. Solary. 2009. Human defensins as cancer biomarkers and antitumour molecules. J Proteomics 72:918-927.

59. Wu, M., S. A. McClellan, R. P. Barrett, and L. D. Hazlett. 2009. Beta-defensin-2 promotes resistance against infection with P. aeruginosa. J Immunol 182:1609-1616.

60. Bals, R., X. Wang, R. L. Meegalla, S. Wattler, D. J. Weiner, M. C. Nehls, and J. M. Wilson. 1999. Mouse beta-defensin 3 is an inducible antimicrobial peptide expressed in the epithelia of multiple organs. Infect Immun 67:3542-3547.

61. Morrison, G. M., D. J. Davidson, and J. R. Dorin. 1999. A novel mouse beta defensin, Defb2, which is upregulated in the airways by lipopolysaccharide. FEBS Lett 442:112-116.

62. Palazzo, M., A. Balsari, A. Rossini, S. Selleri, C. Calcaterra, S. Gariboldi, L. Zanobbio, F. Arnaboldi, Y. F. Shirai, G. Serrao, and C. Rumio. 2007. Activation of enteroendocrine cells via TLRs induces hormone, chemokine, and defensin secretion. J Immunol 178:4296-4303.

63. Selleri, S., F. Arnaboldi, M. Palazzo, S. Gariboldi, L. Zanobbio, E. Opizzi, Y. F. Shirai, A. Balsari, and C. Rumio. 2007. Toll-like receptor agonists regulate beta-defensin 2 release in hair follicle. Br J Dermatol 156:1172-1177.

64. Gariboldi, S., M. Palazzo, L. Zanobbio, S. Selleri, M. Sommariva, L. Sfondrini, S. Cavicchini, A. Balsari, and C. Rumio. 2008. Low molecular weight hyaluronic acid increases the self-defense of skin epithelium by induction of beta-defensin 2 via TLR2 and TLR4. J Immunol 181:2103-2110.

65. Hussain, T., N. Nasreen, Y. Lai, B. F. Bellew, V. B. Antony, and K. A. Mohammed. 2008. Innate immune responses in murine pleural mesothelial cells:

Toll-like receptor-2 dependent induction of beta-defensin-2 by staphylococcal peptidoglycan. Am J Physiol Lung Cell Mol Physiol 295:L461-470.

66. Biragyn, A., M. Coscia, K. Nagashima, M. Sanford, H. A. Young, and P. Olkhanud. 2008. Murine beta-defensin 2 promotes TLR-4/MyD88-mediated and NF-kappaB-dependent atypical death of APCs via activation of TNFR2. J Leukoc Biol 83:998-1008.

67. Wu, M., S. A. McClellan, R. P. Barrett, Y. Zhang, and L. D. Hazlett. 2009. Beta-defensins 2 and 3 together promote resistance to Pseudomonas aeruginosa keratitis. J Immunol 183:8054-8060.

68. Ma, X. T., B. Xu, L. L. An, C. Y. Dong, Y. M. Lin, Y. Shi, and K. F. Wu. 2006. Vaccine with beta-defensin 2-transduced leukemic cells activates innate and adaptive immunity to elicit potent antileukemia responses. Cancer Res 66:1169-1176.

69. Xu, B., C. Y. Dong, F. Zhang, Y. M. Lin, K. F. Wu, and X. T. Ma. 2007. Synergistic antileukemia effect of combinational gene therapy using murine beta-defensin 2 and IL-18 in L1210 murine leukemia model. Gene Ther 14:1181-1187.

70. Wang, Y. S., G. Q. Wang, Y. J. Wen, L. Wang, X. C. Chen, P. Chen, B. Kan, J. Li, C. Huang, Y. Lu, Q. Zhou, N. Xu, D. Li, L. Y. Fan, T. Yi, H. B. Wu, and Y. Q. Wei. 2007. Immunity against tumor angiogenesis induced by a fusion vaccine with murine beta-defensin 2 and mFlk-1. Clin Cancer Res 13:6779-6787.

71. Zhu, K., H. Qin, S. C. Cha, S. S. Neelapu, W. Overwijk, G. A. Lizee, J. L. Abbruzzese, P. Hwu, L. Radvanyi, L. W. Kwak, and D. Z. Chang. 2007. Survivin

DNA vaccine generated specific antitumor effects in pancreatic carcinoma and lymphoma mouse models. Vaccine 25:7955-7961.

72. Leitner, W. W., H. Ying, and N. P. Restifo. 1999. DNA and RNA-based vaccines: principles, progress and prospects. Vaccine 18:765-777.

73. Liu, C., Y. Lou, G. Lizee, H. Qin, S. Liu, B. Rabinovich, G. J. Kim, Y. H. Wang, Y. Ye, A. G. Sikora, W. W. Overwijk, Y. J. Liu, G. Wang, and P. Hwu. 2008. Plasmacytoid dendritic cells induce NK cell-dependent, tumor antigen-specific T cell cross-priming and tumor regression in mice. J Clin Invest 118:1165-1175.

74. Kim, S. K., K. S. Schluns, and L. Lefrancois. 1999. Induction and visualization of mucosal memory CD8 T cells following systemic virus infection. J Immunol 163:4125-4132.

75. Overwijk, W. W., M. R. Theoret, S. E. Finkelstein, D. R. Surman, L. A. de Jong, F. A. Vyth-Dreese, T. A. Dellemijn, P. A. Antony, P. J. Spiess, D. C. Palmer, D. M. Heimann, C. A. Klebanoff, Z. Yu, L. N. Hwang, L. Feigenbaum, A. M. Kruisbeek, S. A. Rosenberg, and N. P. Restifo. 2003. Tumor regression and autoimmunity after reversal of a functionally tolerant state of self-reactive CD8+ T cells. J Exp Med 198:569-580.

76. Overwijk, W. W., and N. P. Restifo. 2001. B16 as a mouse model for human melanoma. Curr Protoc Immunol Chapter 20:Unit 20 21.

77. Cravens, P. D., and P. E. Lipsky. 2002. Dendritic cells, chemokine receptors and autoimmune inflammatory diseases. Immunol Cell Biol 80:497-505.

78. McColl, S. R. 2002. Chemokines and dendritic cells: a crucial alliance. Immunol Cell Biol 80:489-496.

79. Dieu-Nosjean, M. C., A. Vicari, S. Lebecque, and C. Caux. 1999. Regulation of dendritic cell trafficking: a process that involves the participation of selective chemokines. J Leukoc Biol 66:252-262.

80. Pardoll, D. M. 2002. Spinning molecular immunology into successful immunotherapy. Nat Rev Immunol 2:227-238.

81. Overwijk, W. W., K. E. de Visser, F. H. Tirion, L. A. de Jong, T. W. Pols, Y. U. van der Velden, J. G. van den Boorn, A. M. Keller, W. A. Buurman, M. R. Theoret, B. Blom, N. P. Restifo, A. M. Kruisbeek, R. A. Kastelein, and J. B. Haanen. 2006. Immunological and antitumor effects of IL-23 as a cancer vaccine adjuvant. J Immunol 176:5213-5222.

82. Martin-Orozco, N., Y. H. Wang, H. Yagita, and C. Dong. 2006. Cutting Edge: Programmed death (PD) ligand-1/PD-1 interaction is required for CD8+ T cell tolerance to tissue antigens. J Immunol 177:8291-8295.

83. Qin, H., S. C. Cha, S. S. Neelapu, Y. Lou, J. Wei, Y. J. Liu, and L. W. Kwak. 2009. Vaccine site inflammation potentiates idiotype DNA vaccine-induced therapeutic T cell-, and not B cell-, dependent antilymphoma immunity. Blood 114:4142-4149.

84. Yang, D., O. Chertov, S. N. Bykovskaia, Q. Chen, M. J. Buffo, J. Shogan, M. Anderson, J. M. Schroder, J. M. Wang, O. M. Howard, and J. J. Oppenheim. 1999. Beta-defensins: linking innate and adaptive immunity through dendritic and T cell CCR6. Science 286:525-528.

85. Burgdorf, S., C. Scholz, A. Kautz, R. Tampe, and C. Kurts. 2008. Spatial and mechanistic separation of cross-presentation and endogenous antigen presentation. Nat Immunol 9:558-566.

86. Chen, M., C. Barnfield, T. I. Naslund, M. N. Fleeton, and P. Liljestrom. 2005. MyD88 expression is required for efficient cross-presentation of viral antigens from infected cells. J Virol 79:2964-2972.

87. Dudley, M. E., J. R. Wunderlich, P. F. Robbins, J. C. Yang, P. Hwu, D. J. Schwartzentruber, S. L. Topalian, R. Sherry, N. P. Restifo, A. M. Hubicki, M. R. Robinson, M. Raffeld, P. Duray, C. A. Seipp, L. Rogers-Freezer, K. E. Morton, S. A. Mavroukakis, D. E. White, and S. A. Rosenberg. 2002. Cancer regression and autoimmunity in patients after clonal repopulation with antitumor lymphocytes. Science 298:850-854.

88. Dudley, M. E., J. R. Wunderlich, J. C. Yang, P. Hwu, D. J. Schwartzentruber, S. L. Topalian, R. M. Sherry, F. M. Marincola, S. F. Leitman, C. A. Seipp, L. Rogers-Freezer, K. E. Morton, A. Nahvi, S. A. Mavroukakis, D. E. White, and S. A. Rosenberg. 2002. A phase I study of nonmyeloablative chemotherapy and adoptive transfer of autologous tumor antigen-specific T lymphocytes in patients with metastatic melanoma. J Immunother 25:243-251.

Appendix.

Chapter 4. Detailed Experiments Data.

Table A4-4A-1. MIP-3α DNA Vaccine Group Survival

MouseID	Status	Time of Event (Days Post Challenge)
101	Dead	23
102	Dead	25
103	Dead	30
104	Dead	32
105	Dead	32
106	Dead	32
107	Dead	32
108	Dead	32
109	Dead	32
110	Dead	32
111	Dead	32
112	Dead	37
113	Alive	37
114	Alive	37

Table A4-4A-1. Survival tally of all mice (n=14) who received MIP-3α-gp100F. The event tallied is death of mice, determined by actual death or mice euthanized due to high tumor burden of over 400mm^2. Experiment stopped at Day 37.

Table A4-4A-2. mBD2 DNA Vaccine Group Survival

MouseID	Status	Time of Event (Days Post Challenge)
201	Dead	23
202	Dead	25
203	Dead	28
204	Dead	32
205	Dead	32
206	Dead	32
207	Dead	32
208	Dead	32
209	Dead	32
210	Dead	32
211	Dead	32
212	Dead	32
213	Dead	37
214	Dead	37

Table A4-4A-2. Survival tally of all mice (n=14) who received mBD2-gp100F. The event tallied is death of mice, determined by actual death or mice euthanized due to high tumor burden of over 400mm^2.

Table A4-4A-3. MCP-3 DNA Vaccine Group Survival

MouseID	Status	Time of Event (Days Post Challenge)
301	Dead	21
302	Dead	21
303	Dead	23
304	Dead	25
305	Dead	25
306	Dead	28
307	Dead	28
308	Dead	30
309	Dead	32
310	Dead	32
311	Dead	32
312	Dead	32
313	Dead	32
314	Alive	37

Table A4-4A-3. Survival tally of all mice (n=14) who received MCP-3-gp100F. The event tallied is death of mice, determined by actual death or mice euthanized due to high tumor burden of over 400mm^2. Experiment stopped at Day 37.

Table A4-4A-4. RANTES DNA Vaccine Group Survival

MouseID	Status	Time of Event (Days Post Challenge)
401	Dead	16
402	Dead	21
403	Dead	23
404	Dead	25
405	Dead	25
406	Dead	25
407	Dead	30
408	Dead	30
409	Dead	32
410	Dead	32
411	Dead	32
412	Dead	32
413	Dead	32
414	Dead	32

Table A4-4A-4. Survival tally of all mice (n=14) who received RANTES-gp100F. The event tallied is death of mice, determined by actual death or mice euthanized due to high tumor burden of over 400mm^2.

Table A4-4A-5. No Vaccine (PBS) DNA Vaccine Group Survival

MouseID	Status	Time of Event (Days Post Challenge)
501	Dead	21
502	Dead	25
503	Dead	25
504	Dead	25
505	Dead	25
506	Dead	25
507	Dead	25
508	Dead	28
509	Dead	30
510	Dead	32
511	Dead	32
512	Dead	32
513	Dead	32
514	Dead	32

Table A4-4A-5. Survival tally of all mice (n=14) who received mock vaccine (PBS). The event tallied is death of mice, determined by actual death or mice euthanized due to high tumor burden of over 400mm^2.

Table A4-4B-1. mBD2-OVA Protein Vaccine Group Results

MouseID	Status	Experiment #	Time (Days Post Challenge)
101	Alive	1	60
102	Alive	1	60
103	Alive	1	60
104	Alive	1	60
105	Alive	1	60
106	Alive	2	60
107	Alive	2	60
108	Alive	2	60
109	Alive	2	60
110	Alive	2	60
111	Alive	3	60
112	Alive	3	60
113	Alive	3	60
114	Alive	3	60
115	Alive	3	60
116	Alive	4	60
117	Alive	4	60
118	Alive	4	60
119	Alive	4	60
120	Alive	4	60

Table A4-4B-1. Survival tally of all mice (n=20) who received experimental vaccine mBD2-OVA. The event tallied is death of mice, determined by actual death or mice euthanized due to high tumor burden of over 400mm^2. Experiment stopped on Day 60.

Table A4-4B-2. OVA Protein Vaccine Group Results

MouseID	Status	Experiment #	Time (Days Post Challenge)
201	Dead	1	17
202	Dead	1	21
203	Dead	3	27
204	Dead	1	33
205	Dead	1	33
206	Dead	3	33
207	Dead	2	35
208	Dead	3	37
209	Dead	3	57
210	Dead	4	60
211	Alive	1	60
212	Alive	2	60
213	Alive	2	60
214	Alive	2	60
215	Alive	2	60
216	Alive	3	60
217	Alive	4	60
218	Alive	4	60
219	Alive	4	60
220	Alive	4	60

Table A4-4B-2. Survival tally of all mice (n=20) who received control vaccine (antigen alone) OVA. The event tallied is death of mice, determined by actual death or mice euthanized due to high tumor burden of over 400mm^2. Experiment stopped on Day 60.

Table A4-4B-3. No Protein Vaccine (PBS) Group Results

MouseID	Status	Experiment #	Time (Days Post Challenge)
301	Dead	1	19
302	Dead	1	19
303	Dead	3	21
304	Dead	1	21
305	Dead	1	21
306	Dead	3	23
307	Dead	2	25
308	Dead	3	25
309	Dead	3	25
310	Dead	4	25
311	Dead	1	28
312	Dead	2	28
313	Dead	2	28
314	Dead	2	28
315	Dead	2	32
316	Dead	3	32
317	Dead	4	39
318	Dead	4	39
319	Dead	4	52
320	Alive	4	60

Table A4-4B-3. Survival tally of all mice (n=20) who received mock vaccine (PBS). The event tallied is death of mice, determined by actual death or mice euthanized due to high tumor burden of over 400mm^2. Experiment stopped on Day 60.

Table A4-4C-1. mBD2-gp100T Group Survival Results

MouseID	Status	Experiment #	Time (Days Post Challenge)
101	Dead	2	20
102	Dead	2	22
103	Dead	2	22
104	Dead	2	22
105	Dead	2	22
106	Dead	1	22
107	Dead	1	22
108	Dead	1	22
109	Dead	2	25
110	Dead	1	26
111	Dead	2	27
112	Dead	2	27
113	Dead	2	27
114	Dead	1	29
115	Dead	2	34

Table A4-4C-1. Survival tally of all mice (n=15) who received experimental vaccine mBD2-gp100T. The event tallied is death of mice, determined by actual death or mice euthanized due to high tumor burden of over 400mm^2.

Table A4-4C-2. gp100T Group Survival Results

MouseID	Status	Experiment #	Time (Days Post Challenge)
201	Dead	1	17
202	Dead	1	17
203	Dead	2	18
204	Dead	1	19
205	Dead	2	20
206	Dead	2	20
207	Dead	2	20
208	Dead	1	22
209	Dead	1	22
210	Dead	2	25

Table A4-4C-2. Survival tally of all mice (n=10) who received control vaccine (antigen alone) gp100T. The event tallied is death of mice, determined by actual death or mice euthanized due to high tumor burden of over 400mm^2.

Table A4-4C-3. No Protein Vaccine (PBS) Group Survival Results

MouseID	Status	Experiment #	Time (Days Post Challenge)
301	Dead	1	17
302	Dead	1	17
303	Dead	2	18
304	Dead	2	18
305	Dead	2	18
306	Dead	2	18
307	Dead	2	18
308	Dead	2	18
309	Dead	2	18
310	Dead	2	18
311	Dead	2	18
312	Dead	1	19
313	Dead	2	20
314	Dead	1	22
315	Dead	1	22

Table A4-4C-3. Survival tally of all mice (n=15) who received mock vaccine (PBS). The event tallied is death of mice, determined by actual death or mice euthanized due to high tumor burden of over 400mm^2.

Chapter 5. Detailed Experiments Data.

Table A5-4A(i)-1. gp100 Crosspresentation Experiment #1 Results Table

%IFN-γ+CD3+CD8+			
	1	**2**	**3**
mBD2-gp100T	4.07	4.92	2.22
MIP-3α -gp100T	1.93	1.89	1.92
gp100T	2.43	2.95	2.6
PBS	2.53	2.32	1.96
pmel-1 alone	0.76	0.7	x
Positive Control (epitope)	88.81	86.23	x
Positive Control (PHA)	87.64	x	x

Table A5-4A(i)-1. Percentages of effector T cell's IFN-γ release differences show higher efficiency when loading mBD2 fused antigen over non-fused. Positive controls (epitope peptide with pmel-1 and PHA with pmel-1) and negative controls (PBS and pmel-1 alone) show proper functionality of effector T cells. Tweaked variables include a 9 hour DC and pmel-1 coincubation time and maturation factor added to DC after protein loading and prior to coincubation.

Table A5-4A(i)-2. gp100 Crosspresentation Experiment #2 Results Table

%IFN-γ+CD3+CD8+			
	1	**2**	**3**
mBD2-gp100T (M)	36.83	34.26	33.84
MIP-3α-gp100T (M)	1.21	1.98	1.9
gp100T (M)	20.55	23.41	23.56
PBS (M)	14.79	14.72	11.5
mBD2-gp100T (X)	19.39	20.07	17.02
mBD2-OVA (X)	3.9	3.27	2.67
PBS (X)	5.93	5.37	4.73
pmel-1 alone	1.37	1.83	2.37
Positive Contro (gp100 epitope)	78.74	80.07	79.43
Positive Control (PHA)	83.64	85.57	84.31

Table A5-4A(i)-2. Percentages of effector T cell's IFN-γ release differences show higher efficiency when loading mBD2 fused antigen over non-fused. Positive controls (epitope peptide with pmel-1 and PHA with pmel-1) and negative controls (PBS and pmel-1 alone) show proper functionality of effector T cells. Tweaked variables include a 8 hour DC and pmel-1 coincubation time and maturation factor added to DC after protein loading and prior to coincubation for samples labeled (M) and not added if samples were labeled (X).

Table A5-4A(i)-3. gp100 Crosspresentation Experiment #3 Results Table

%IFN-γ+CD3+CD8+			
	1	**2**	**3**
mBD2-gp100T (M)	2.13	1.9	1.8
MIP-3α-gp100T (M)	0.29	0.2	0.2
gp100T (M)	0.43	0.43	0.33
PBS (M)	0.16	0.16	0.11
mBD2-gp100T (X)	1.05	0.95	0.72
gp100T (X)	0.29	0.2	0.28
PBS (X)	0.16	0.16	0.27
mBD2-OVA (X)	0.24	0.14	0.32
pmel-1 alone	0.08	X	x
Positive Control (gp100 epitope)	83.46	X	x

Table A5-4A(i)-3. Percentages of effector T cell's IFN-γ release differences show higher efficiency when loading mBD2 fused antigen over non-fused. Positive controls (epitope peptide with pmel-1) and negative controls (PBS and pmel-1 alone) show proper functionality of effector T cells. Tweaked variables include a 5.5 hour DC and pmel-1 coincubation time and maturation factor added to DC after protein loading and prior to coincubation for samples labeled (M) and not added if samples were labeled (X).

Table A5-4A(ii)-1. OVA Crosspresentation Experiment #1 Results Table

%IFN-γ+CD3+CD8+			
	1	**2**	**3**
mBD2-OVA (M)	14.83	13.85	12.69
OVA (Commercial) (M)	2.04	1.93	1.76
MIP-3α-gp100T (M)	0.28	0.34	0.3
mBD2-gp100T (M)	0.42	0.34	0.33
gp100T (M)	0.3	0.31	0.38
mBD2-OVA (X)	11.82	11.5	9.12
OVA (Commercial) (X)	1.31	1.44	1.49
MIP-3α -gp100T (X)	0.4	0.38	0.23
mBD2-gp100T (X)	0.36	0.58	0.36
gp100T (X)	0.34	0.3	0.27
PBS (M)	0.26	0.26	0.24
PBS (X)	0.45	0.34	0.26
OT-I alone	0.33	0.33	0.25
Positive Control (OVA epitope)	64.43	62.92	60.98

Table A5-4A(ii)-1. Percentages of effector T cell's IFN-γ release differences show higher efficiency when loading mBD2 fused antigen over non-fused. Positive controls (epitope peptide with OT-I) and negative controls (PBS and OT-I alone) show proper functionality of effector T cells. Other variables include a 5.5 hour DC and OT-I coincubation time and maturation factor added to DC after protein loading and prior to coincubation for samples labeled (M) and not added if samples were labeled (X).

Table A5-4A(ii)-2. OVA Crosspresentation Experiment #2 Results Table

%IFN-γ+CD45.1+CD3+CD8+			
	1	**2**	**3**
mBD2-OVA	3.05	2.45	2.74
OVA	0.62	0.73	0.62
OVA (Commercial)	0.65	0.53	0.52
mBD2-gp100T	0.33	0.19	0.26
PBS	0.29	0.28	0.3
OT-1 Alone	0.2	0.14	0.15
Positive Control (OVA epitope)	69.06	69.37	68.04

Table A5-4A(ii)-2. Percentages of effector T cell's IFN-γ release differences show higher efficiency when loading mBD2 fused antigen over non-fused. Positive controls (epitope peptide with OT-I) and negative controls (PBS and OT-I alone) show proper functionality of effector T cells. A 5.5 hour DC and OT-I coincubation time was used and also no maturation was added.

Table A5-4A(iii)-1. CCR6KO OVA Crosspresentation Experiment Results Table

Wildtype			
%IFN-γ+CD45.1+CD3+CD8+			
	1	**2**	**3**
mBD2-OVA	3.05	2.45	2.74
OVA	0.62	0.73	0.62
OVA (Commercial)	0.65	0.53	0.52
mBD2-gp100T	0.33	0.19	0.26
PBS	0.29	0.28	0.3

CCR6KO			
%IFN-γ+CD45.1+CD3+CD8+			
	1	**2**	**3**
mBD2-OVA	3.73	3.75	3.73
OVA	0.73	0.66	0.68
OVA (Commercial)	0.53	0.51	0.44
mBD2-gp100T	0.18	0.19	0.17
PBS	0.24	0.21	0.39

Controls			
%IFN-γ+CD45.1+CD3+CD8+			
	1	**2**	**3**
OT-1 Alone	0.2	0.14	0.15
Positive Control (OVA epitope)	69.06	69.37	68.04

Table A5-4A(iii)-1. The parallel experiments show no differences in percentages of effector T cell's IFN-γ release between CCR6KO groups versus wildtype groups for all variables. Positive controls (epitope peptide with OT-I) and negative controls (PBS and OT-I alone) show proper functionality of effector T cells. A 5.5 hour DC and OT-I coincubation time was used and also no maturation was added to DC.

Table A5-4B(i)-1. OT-I Expansion Experiment #1 Results and Statistics Table

%CD8+CD45.1+				
		Day 3	**Day 5**	**Day 7**
mBD2-OVA	**1**	0.52	5.34	0.32
	2	0.75	4.16	1.45
	3	0.17	4.11	0.56
	4	0.88	4.82	0.5
	5	1	6.44	2.07
	Average	0.664	4.974	0.98
OVA	**1**	0	3.06	0.48
	2	0.21	1.29	0.4
	3	0.26	2.04	0.85
	4	0.14	1.4	0.67
	5	0.14	3.7	1.6
	Average	0.15	2.298	0.8
PBS	**1**	0.1	0.33	0.09
	2	0.24	0.21	0.08
	3	0.08	0.19	0.16
	4	0.12	0.19	0.09
	5	0.11	0.22	0.17
	Average	0.13	0.228	0.118
VSV-OVA	**1**	1.86	72.36	56.39
	2	0.24	42.2	23.34
	3	0.12	33.85	20.01
	4	0.02	0.17	16.44
	Average	0.56	37.145	29.045
t-test (p-value)				
		Day 3	**Day 5**	**Day 7**
mBD2-OVA vs OVA		0.022237737	0.00308334	0.665394

Table A5-4B(i)-1. Effector T cell over total T cell percentage measures on Day 3, 5, 7 along with statistical difference analysis.

Figure A5-4B(i)-1. OT-I Expansion Experiment #1 Graph

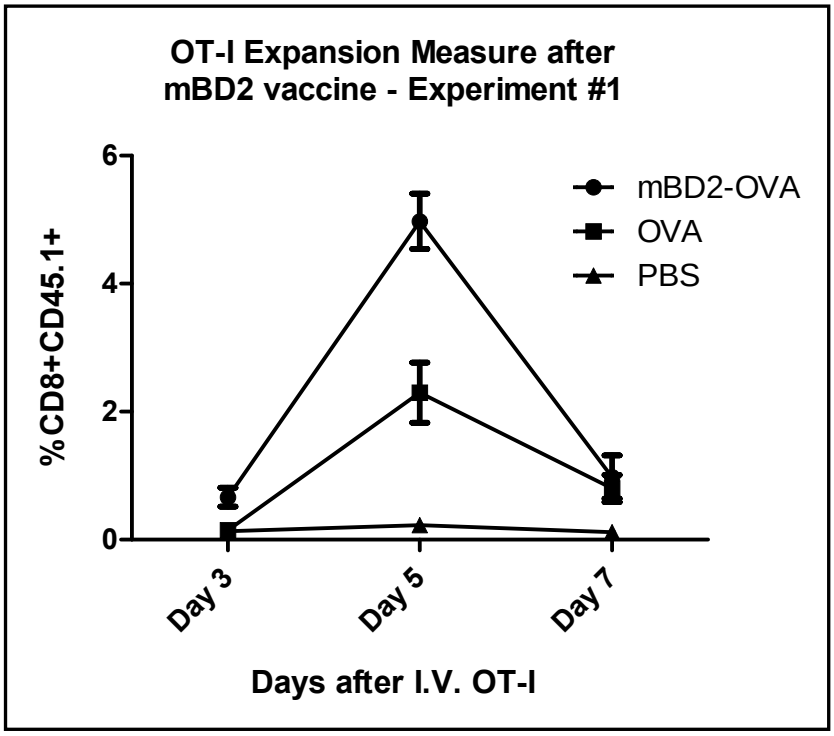

Figure A5-4B(i)-1. Approximate expansion trajectory for all groups. The actual measurements were on Day 3, 5, and 7. The lines serve as visual for the expansion pattern. Error bars are standard error of the mean.

Table A5-4B(i)-2. OT-I Expansion Experiment #2 Results and Statistics Table

%CD8+CD45.1+				
		Day 3	**Day 5**	**Day 7**
mBD2-OVA	**1**	2.97	23.79	7.08
	2	4.19	29.11	27.08
	3	5.12	63.52	45.06
	4	4.74	81.06	64.26
	5	0.63	33.95	30.48
	Average	3.53	46.286	34.792
OVA	**1**	3.51	2.05	0.4
	2	1.22	2.12	0.5
	3	1.12	5.24	0.64
	4	2.82	5.55	1.03
	5	0.28	3.22	1.2
	Average	1.79	3.636	0.754
PBS	**1**	0.05	0.06	0.1
	2	0.27	0.26	0.16
	3	0.09	0.12	0.05
	4	0.25	0.2	0.08
	5	0.05	0.19	0.03
	Average	0.142	0.166	0.084
VSV-OVA	**1**	1.64	62.94	29.46
	2	4.47	73.33	29.04
	3	1.57	74.85	34.26
	4	5.83	68.2	27.25
	5	1	72.03	23.94
	Average	2.902	70.27	28.79
t-test (p-value)				
		Day 3	**Day 5**	**Day 7**
mBD2-OVA vs OVA		0.125221984	0.018193	0.0234

Table A5-4B(i)-2. Effector T cell over total T cell percentage measures on Day 3, 5, 7 along with statistical difference analysis.

Figure A5-4B(i)-2. OT-I Expansion Experiment #2 Graph

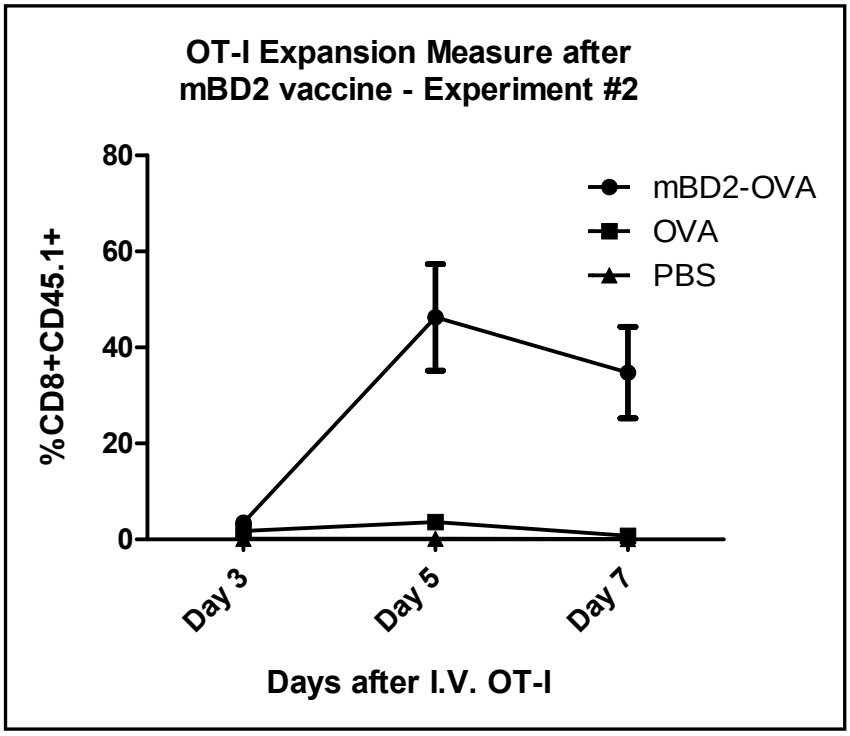

Figure A5-4B(i)-2. Approximate expansion trajectory for all groups. The actual measurements were on Day 3, 5, and 7. The lines serve as visual for the expansion pattern. Error bars are standard error of the mean.

Table A5-4B(i)-3. OT-I Expansion Experiment #3 Results and Statistics Table

%CD8+CD45.1+				
		Day 3	**Day 5**	**Day 7**
mBD2-OVA	**1**	8.14	11.56	4.18
	2	6.07	8.2	1.12
	3	5.09	6.66	0.78
	4	4.87	6.28	0.67
	5	2.89	4.43	0.29
	Average	5.412	7.426	1.408
OVA	**1**	5.79	2.85	0.58
	2	3.8	2.62	0.39
	3	3.59	1.98	0.34
	4	3.34	1.8	0.29
	5	3.11	1.19	0.23
	Average	3.926	2.088	0.366
PBS	**1**	0.32	0.56	0.22
	2	0.24	0.51	0.19
	3	0.22	0.4	0.19
	4	0.21	0.35	0.17
	5	0.18	0.31	0.14
	Average	0.234	0.426	0.182
VSV-OVA	**1**	6.18	59.95	15.53
	2	4.66	53.77	10.84
	3	2.47	53.64	10.45
	4	1.95	50.8	7.34
	5	1.07	39.37	7.03
	Average	3.266	51.506	10.238
t-test (p-value)				
		Day 3	**Day 5**	**Day 7**
mBD2-OVA vs OVA		0.178308	0.009511	0.214122

Table A5-4B(i)-3. Effector T cell over total T cell percentage measures on Day 3, 5, 7 along with statistical difference analysis.

Figure A5-4B(i)-3. OT-I Expansion Experiment #3 Graph

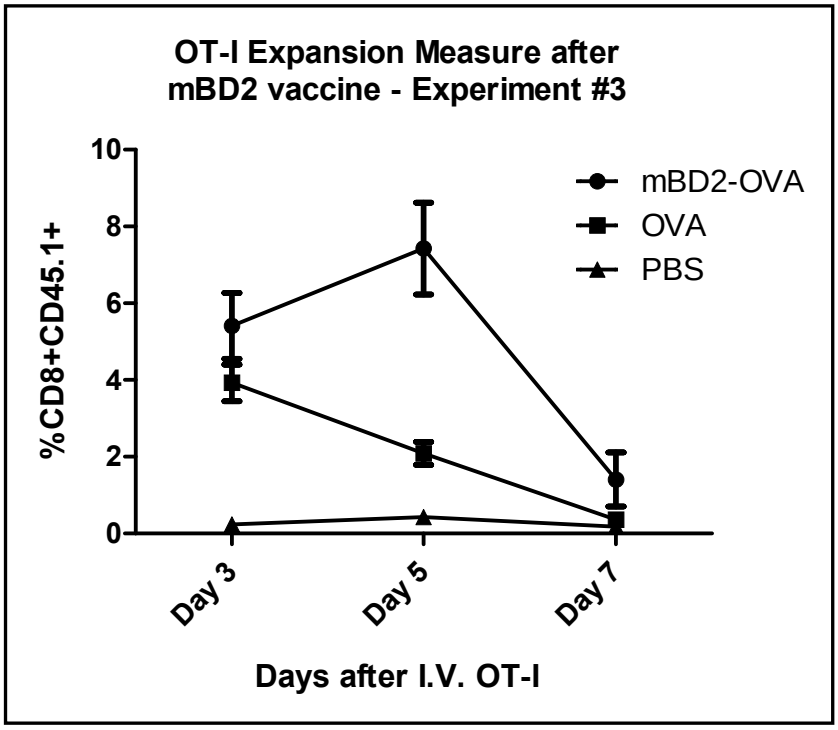

Figure A5-4B(i)-3. Approximate expansion trajectory for all groups. The actual measurements were on Day 3, 5, and 7. The lines serve as visual for the expansion pattern. Error bars are standard error of the mean.

Table A5-4B(i)-4. OT-I Expansion Experiment #4 Results and Statistics Table

%CD8+CD45.1+				
		Day 3	**Day 5**	**Day 7**
mBD2-OVA	**1**	11.13	4.49	3.09
	2	9.07	3.53	2.52
	3	8.11	5.42	5.12
	4	6.77	2.38	0.44
	5	5.15	7.97	3.06
	Average	8.046	4.758	2.846
OVA	**1**	6.66	1.82	2.46
	2	2.44	1.31	0.56
	3	1.95	1.11	4.74
	4	1.74	3.99	0.67
	5	0	1.11	0.75
	Average	2.558	1.868	1.836
PBS	**1**	0.73	0.4	0.17
	2	0.59	0.1	0.38
	3	0.47	0.07	0.08
	4	0.17	0.46	0.08
	5	0	0.49	0.64
	Average	0.392	0.304	0.27
VSV-OVA	**1**	4.92	36.7	36.15
	2	4.67	7.09	30.57
	3	4.02	51.15	27.84
	4	3.67	54.82	29.18
	5	0.11	37.91	28.59
	Average	3.478	37.534	30.466
t-test (p-value)				
		Day 3	**Day 5**	**Day 7**
mBD2-OVA vs OVA		0.006495	0.0363	0.385154

Table A5-4B(i)-4. Effector T cell over total T cell percentage measures on Day 3, 5, 7 along with statistical difference analysis.

Figure A5-4B(i)-4. OT-I Expansion Experiment #4 Graph

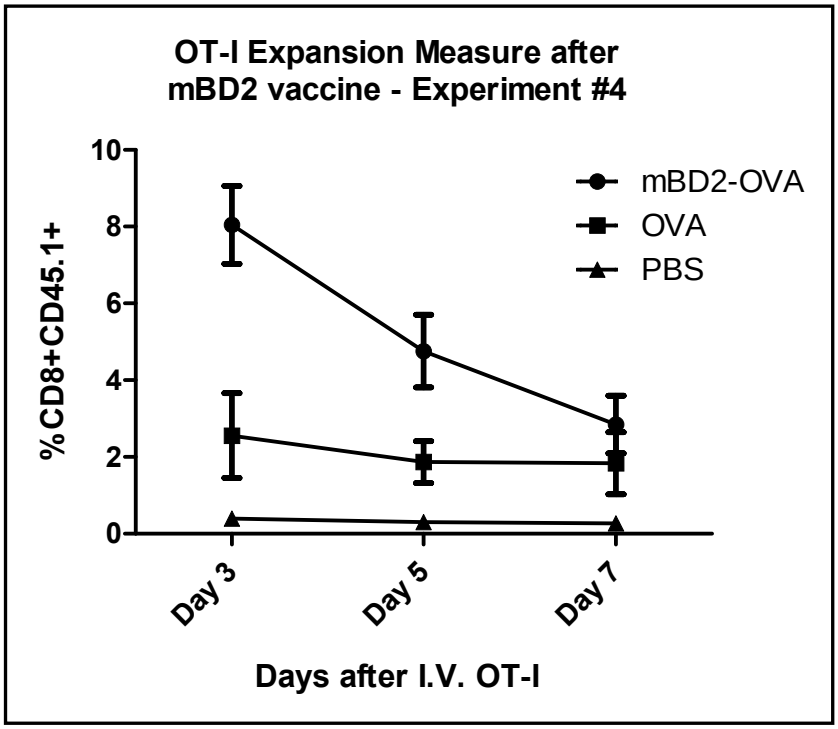

Figure A5-4B(i)-4. Approximate expansion trajectory for all groups. The actual measurements were on Day 3, 5, and 7. The lines serve as visual for the expansion pattern. Error bars are standard error of the mean.

Table A5-4B(i)-5. OT-I Expansion Experiment #5 Results and Statistics Table

%CD8+CD45.1+				
		Day 3	**Day 5**	**Day 7**
mBD2-OVA	**1**	0.55	12.51	1.62
	2	0.15	17.36	9.85
	3	0.1	11.24	7.23
	4	0.33	15.51	17.11
	5	0.3	14.05	13.81
	Average	0.286	14.134	9.924
OVA	**1**	0	3	2.81
	2	0.29	5.12	0.73
	3	0.27	4.63	1.12
	4	0.05	1.18	1.25
	5	0.1	5.38	0.89
	Average	0.142	3.862	1.36
PBS	**1**	0.37	0.78	0.06
	2	0.11	0.27	0.42
	3	0.31	0.34	0.35
	4	0.56	0.47	0.24
	5	0.25	0.32	0.17
	Average	0.32	0.436	0.248
VSV-OVA	**1**	0.07	50.86	7.98
	2	0.19	34	17.68
	3	0.31	35.77	10.87
	4	0.45	35.7	18.62
	5	0.38	31.89	11.28
	Average	0.28	37.644	13.286
t-test (p-value)				
		Day 3	**Day 5**	**Day 7**
mBD2-OVA versus OVA		0.184564	9.3485E-05	0.03202

Table A5-4B(i)-5. Effector T cell over total T cell percentage measures on Day 3, 5, 7 along with statistical difference analysis.

Figure A5-4B(i)-5. OT-I Expansion Experiment #5 Graph

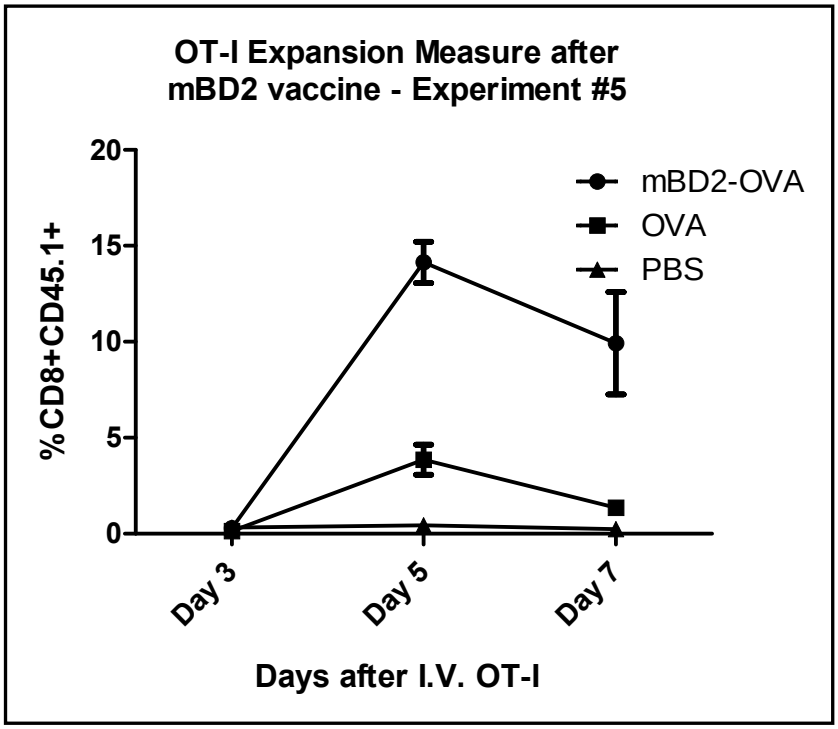

Figure A5-4B(i)-5. Approximate expansion trajectory for all groups. The actual measurements were on Day 3, 5, and 7. The lines serve as visual for the expansion pattern. Error bars are standard error of the mean.

Table A5-4B(i)-6. OT-I Expansion Experiment #6 Results and Statistics Table

%CD8+CD45.1+				
		Day 3	**Day 5**	**Day 7**
mBD2-OVA	**1**	1.33	20.25	20.74
	2	1.62	24.58	12.39
	3	1.49	24.04	9.76
	4	1.75	23.14	10.07
	5	1.97	21.27	10.55
	Average	1.632	22.656	12.702
OVA	**1**	0.91	2.79	0.49
	2	0.04	2.04	9.84
	3	0.99	11.28	3.79
	4	0.88	0.74	1.29
	5	0	17.1	1.38
	Average	0.564	6.79	3.358
PBS	**1**	0.17	0.19	0.57
	2	0.46	0.4	0.15
	3	0.28	0.48	0.26
	4	0.43	0.3	0.36
	5	0.29	0.21	0.39
	Average	0.326	0.316	0.346
VSV-OVA	**1**	0.01	67.61	32.28
	2	0.07	60.42	21.21
	3	0.05	26.29	21.47
	4	0.31	59.95	22.24
	Average	0.11	53.5675	24.3
t-test (p-value)				
		Day 3	**Day 5**	**Day 7**
mBD2-OVA vs OVA		0.00545	0.00610532	0.008661

Table A5-4B(i)-6. Effector T cell over total T cell percentage measures on Day 3, 5, 7 along with statistical difference analysis.

Figure A5-4B(i)-6. OT-I Expansion Experiment #6 Graph

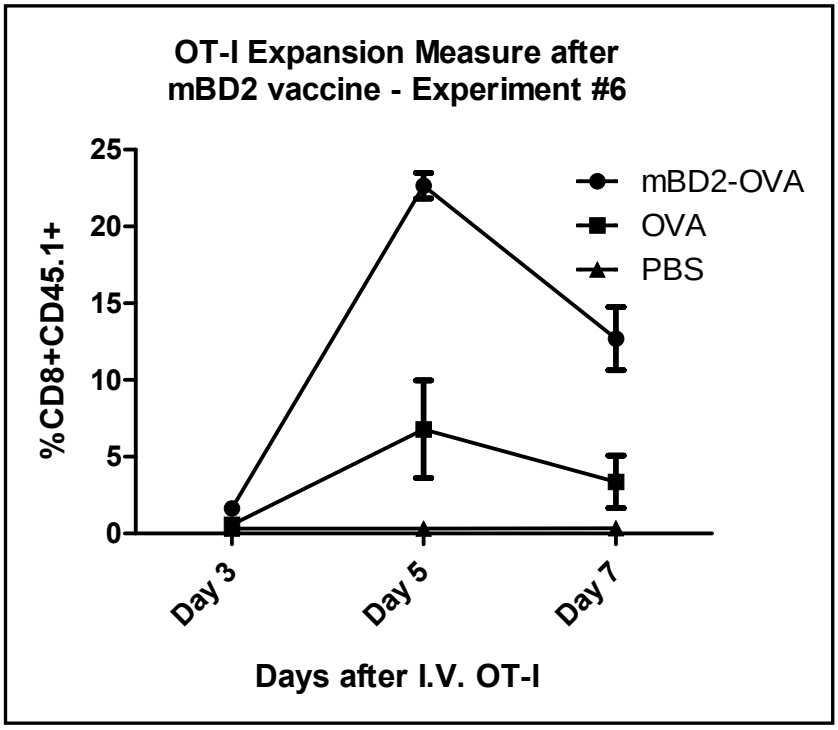

Figure A5-4B(i)-6. Approximate expansion trajectory for all groups. The actual measurements were on Day 3, 5, and 7. The lines serve as visual for the expansion pattern. Error bars are standard error of the mean.

Table A5-4B(ii)-1. OT-II Expansion Experiment #1 Results and Statistics Table

%CD4+CD45.1+				
		Day 3	**Day 5**	**Day 7**
mBD2-OVA	**1**	1.23	1.9	0.37
	2	1.09	3.31	0.47
	3	1.14	0.72	0.83
	4	0.96	1.07	0.34
	5	0.69	1.19	0.73
	Average	1.022	1.638	0.548
OVA	**1**	0.83	1.57	0.47
	2	0.98	1.65	0.98
	3	0.89	1.46	0.81
	4	0.64	1.39	0.6
	5	0.71	2.28	0.71
	Average	0.81	1.67	0.714
PBS	**1**	0.51	0.27	0.23
	2	0.25	0.14	0.39
	3	0.49	0	0.28
	4	0.53	0.44	0.38
	5	0.25	0.23	0.27
	Average	0.406	0.216	0.31
VSV-OVA	**1**	1.9	0.32	0.27
	2	1.84	0.78	0.19
	3	1.11	1.13	0.2
	4	0.62	0.56	0.03
	5	0.52	1.92	0.19
	Average	1.198	0.942	0.176
t-test (p-value)				
		Day 3	**Day 5**	**Day 7**
mBD2-OVA vs OVA		0.100788	0.950143	0.24308

Table A5-4B(ii)-1. Donor CD4+ T cell over total T cell percentage in recipient on Day 3, 5, 7 along with statistical difference analysis.

Figure A5-4B(ii)-1. OT-II Expansion Experiment #1 Graph

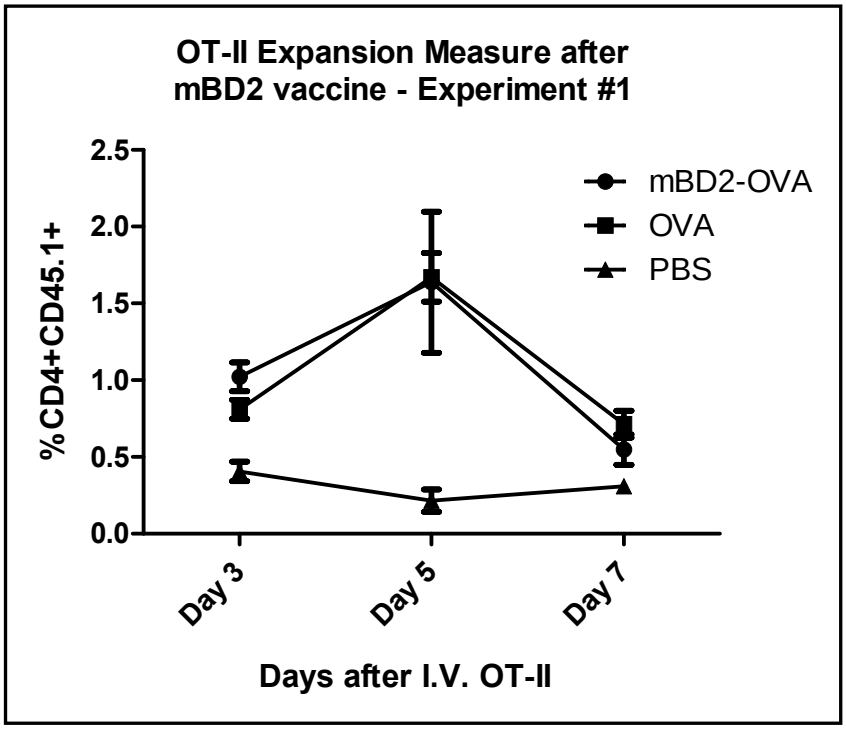

Figure A5-4B(ii)-1. Approximate expansion trajectory for all groups. The actual measurements were on Day 3, 5, and 7. The lines serve as visual for the expansion pattern. Error bars are standard error of the mean.

Table A5-4B(ii)-2. OT-II Expansion Experiment #2 Results and Statistics Table

%CD4+CD45.1+				
		Day 3	**Day 5**	**Day 7**
mBD2-OVA	**1**	1.35	0.25	0.24
	2	1.34	0.02	0.58
	3	0.61	0.54	0.1
	4	0.3	0.44	0.11
	5	0.02	0.04	0.11
	Average	0.724	0.258	0.228
OVA	**1**	0.85	0.51	0.21
	2	0.56	0.66	0.09
	3	0.39	0.11	0.15
	4	0.19	0.06	0.28
	5	0.03	0.43	0.38
	Average	0.404	0.354	0.222
PBS	**1**	0.34	0.03	0.62
	2	0.25	0.33	0.14
	3	0.03	0.08	0.07
	4	0.01	0.02	0.19
	5	0	0.09	0
	Average	0.126	0.11	0.204
VSV-OVA	**1**	0.22	4.93	3.86
	2	0.21	10	2.58
	3	0.16	3.8	4.95
	4	0.14	3.48	1.27
	5	0.12	16.38	9.48
	Average	0.17	7.718	4.428
t-test (p-value)				
		Day 3	**Day 5**	**Day 7**
mBD2-OVA versus OVA		0.335003	0.555547	0.956109

Table A5-4B(ii)-2. Donor CD4+ T cell over total T cell percentage in recipient on Day 3, 5, 7 along with statistical difference analysis.

Figure A5-4B(ii)-2. OT-II Expansion Experiment #2 Graph

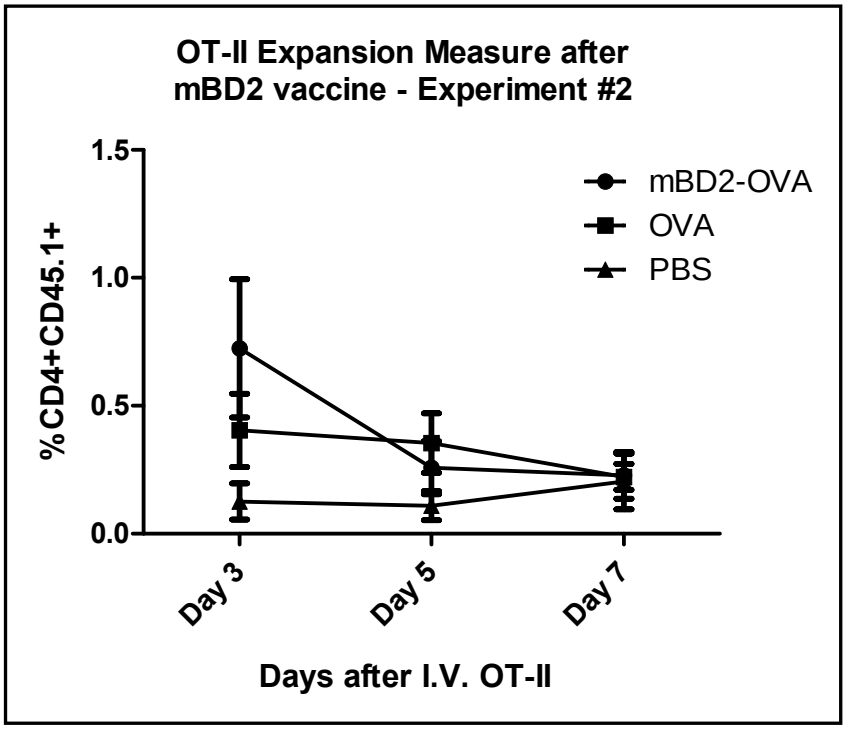

Figure A5-4B(ii)-2. Approximate expansion trajectory for all groups. The actual measurements were on Day 3, 5, and 7. The lines serve as visual for the expansion pattern. Error bars are standard error of the mean.

Table A5-4B(iii)-1. OT-I Expansion in CCR6KO Experiment #1 Results and Statistics Table

%CD8+CD45.1+				
		Day 3	**Day 5**	**Day 7**
mBD2-OVA	**1**	8.14	11.56	4.18
	2	6.07	8.2	1.12
	3	5.09	6.66	0.78
	4	4.87	6.28	0.67
	5	2.89	4.43	0.29
	Average	5.412	7.426	1.408
CCR6KO mBD2-OVA	**1**	9.74	20.8	5.08
	2	9.59	12.62	2.52
	3	8.02	9.09	2.47
	4	6.04	8.15	1.64
	5	5.17	4.94	1.32
	Average	7.712	11.12	2.606
t-test (p-value)				
		Day 3	**Day 5**	**Day 7**
Wildtype versus CCR6KO		0.104994	0.263071	0.250504

Table A5-4B(iii)-1. Effector T cell over total T cell percentage measures on Day 3, 5, 7 along with statistical difference analysis for wildtype versus CCR6KO.

Figure A5-4B(iii)-1. OT-I Expansion in CCR6KO Experiment #1 Graph

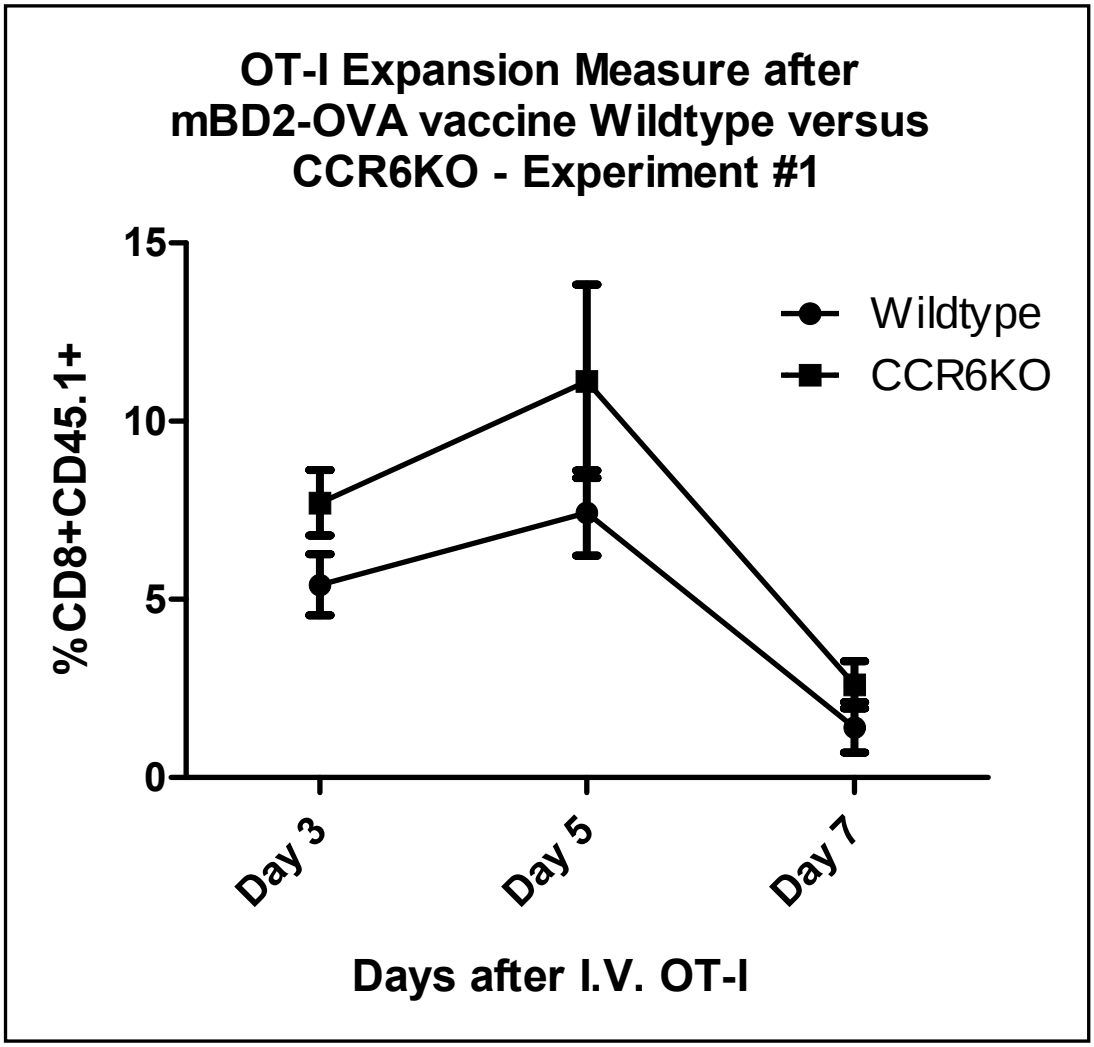

Figure A5-4B(iii)-1. Approximate expansion trajectory for all groups. The actual measurements were on Day 3, 5, and 7. The lines serve as visual for the expansion pattern. Error bars are standard error of the mean.

Table A5-4B(iii)-2. OT-I Expansion in CCR6KO Experiment #2 Results and Statistics Table

%CD8+CD45.1+				
		Day 3	**Day 5**	**Day 7**
mBD2-OVA	**1**	0.55	12.51	1.62
	2	0.15	17.36	9.85
	3	0.1	11.24	7.23
	4	0.33	15.51	17.11
	5	0.3	14.05	13.81
	Average	0.286	14.134	9.924
CCR6KO mBD2-OVA	**1**	0.47	16.6	9.04
	2	0.32	17.23	25.23
	3	0.53	16.58	12.6
	4	0.18	46.77	28.44
	5	0.56	31.79	10.96
	Average	0.412	25.794	17.254
t-test (p-value)				
		Day 3	**Day 5**	**Day 7**
Wiltype versus CCR6KO		0.27065	0.12376901	0.170466

Table A5-4B(iii)-2. Effector T cell over total T cell percentage measures on Day 3, 5, 7 along with statistical difference analysis for wildtype versus CCR6KO.

Figure A5-4B(iii)-2. OT-I Expansion in CCR6KO Experiment #2 Graph

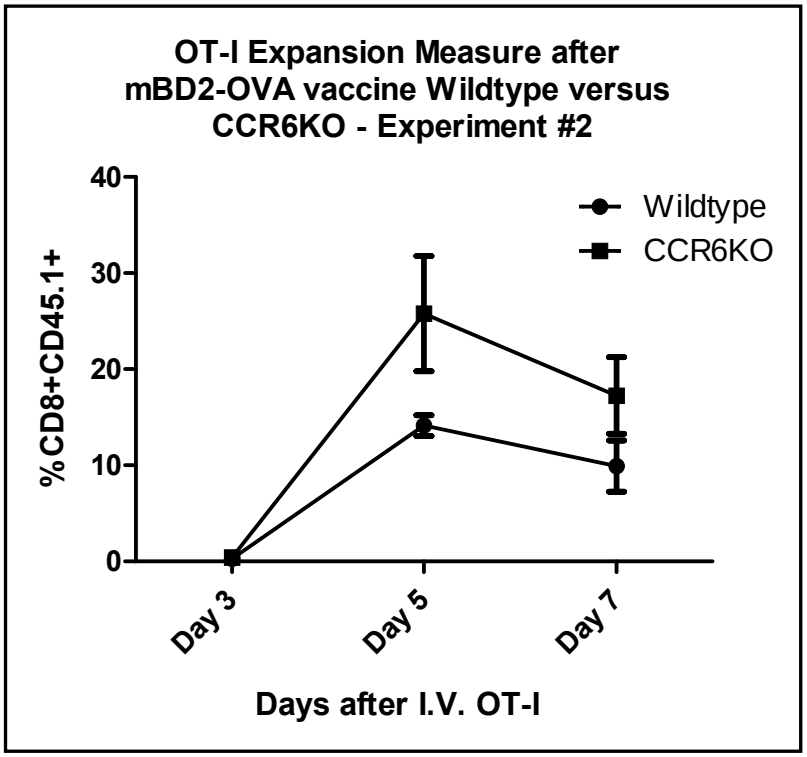

Figure A5-4B(iii)-2. Approximate expansion trajectory for all groups. The actual measurements were on Day 3, 5, and 7. The lines serve as visual for the expansion pattern. Error bars are standard error of the mean.

Table A5-4B(iv)-1. OT-I Expansion in TLR4KO Experiment #1 Results and Statistics Table

%CD8+CD45.1+				
		Day 3	**Day 5**	**Day 7**
mBD2-OVA	**1**	0.55	12.51	1.62
	2	0.15	17.36	9.85
	3	0.1	11.24	7.23
	4	0.33	15.51	17.11
	5	0.3	14.05	13.81
	Average	0.286	14.134	9.924
TLR4KO mBD2-OVA	**1**	0	1.92	0.78
	2	0.4	2.34	2.78
	3	0.37	2.81	2.76
	4	0.53	8.17	1.03
	5	0.3	6.81	1.3
	Average	0.32	4.41	1.73
t-test (p-value)				
		Day 3	**Day 5**	**Day 7**
Wildtype versus TLR4KO		0.781504	0.00045241	0.036467

Table A5-4B(iv)-1. Effector T cell over total T cell percentage measures on Day 3, 5, 7 along with statistical difference analysis for wildtype versus TLR4KO.

Figure A5-4B(iv)-1. OT-I Expansion in TLR4KO Experiment #1 Graph

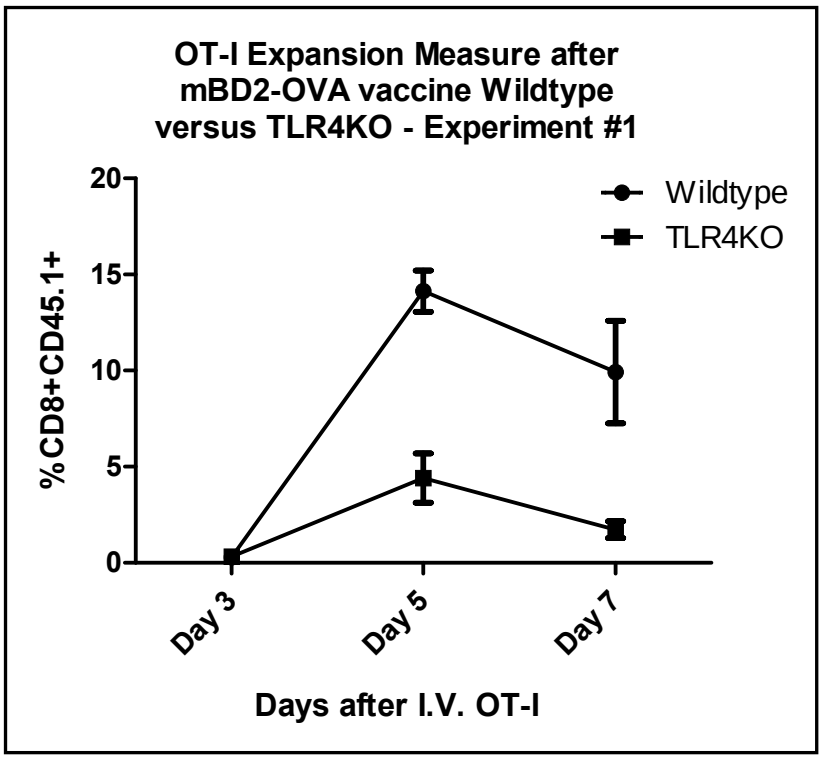

Figure A5-4B(iv)-1. Approximate expansion trajectory for all groups. The actual measurements were on Day 3, 5, and 7. The lines serve as visual for the expansion pattern. Error bars are standard error of the mean.

Table A5-4B(iv)-2. OT-I Expansion in TLR4KO Experiment #2 Results and Statistics Table

%CD8+CD45.1+				
		Day 3	**Day 5**	**Day 7**
mBD2-OVA	**1**	1.33	20.25	20.74
	2	1.62	24.58	12.39
	3	1.49	24.04	9.76
	4	1.75	23.14	10.07
	5	1.97	21.27	10.55
	Average	1.632	22.656	12.702
TLR4KO mBD2-OVA	**1**	4.23	8.66	1.71
	2	0.04	3.06	11.95
	3	3.2	7.3	4.17
	4	4.23	10.54	2.21
	5	3.13	19.39	6.33
	Average	2.966	9.79	5.274
t-test (p-value)				
		Day 3	**Day 5**	**Day 7**
mBD2-OVA versus OVA		0.158399	0.00688735	0.028296

Table A5-4B(iv)-2. Effector T cell over total T cell percentage measures on Day 3, 5, 7 along with statistical difference analysis for wildtype versus TLR4KO.

Figure A5-4B(iv)-2. OT-I Expansion in TLR4KO Experiment #2 Graph

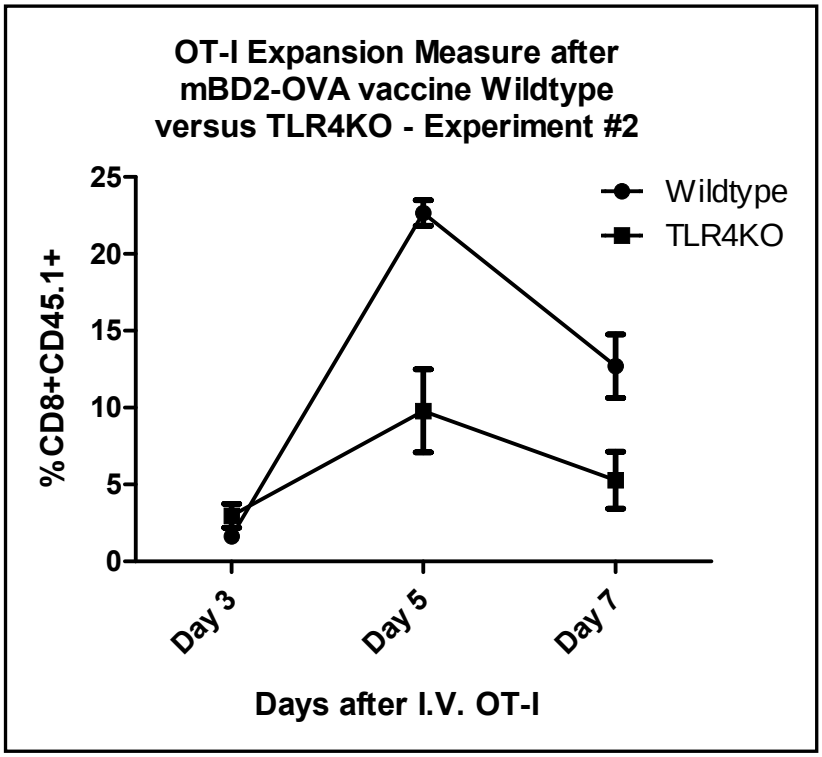

Figure A5-4B(iv)-2. Approximate expansion trajectory for all groups. The actual measurements were on Day 3, 5, and 7. The lines serve as visual for the expansion pattern. Error bars are standard error of the mean.

Table A5-4B(v)-1. OT-I Expansion with TLR4 Adjuvant Experiment #1 Results

%CD8+CD45.1+				
		Day 3	Day 5	Day 7
mBD2-OVA	1	8.14	11.56	4.18
	2	6.07	8.2	1.12
	3	5.09	6.66	0.78
	4	4.87	6.28	0.67
	5	2.89	4.43	0.29
	Average	5.412	7.426	1.408
mBD2-OVA MPL	1	12.6	10.82	1.21
	2	12.26	10.71	1.15
	3	9.37	8.07	1.03
	4	5.82	5.7	0.98
	5	5.63	4.85	0.63
	Average	9.136	8.03	1
OVA	1	5.79	2.85	0.58
	2	3.8	2.62	0.39
	3	3.59	1.98	0.34
	4	3.34	1.8	0.29
	5	3.11	1.19	0.23
	Average	3.926	2.088	0.366
OVA MPL	1	4.46	6.55	0.63
	2	4.44	3.81	0.56
	3	4.4	2.29	0.4
	4	3.47	1.68	0.21
	5	1.06	1.58	0.16
	Average	3.566	3.182	0.392
PBS	1	0.32	0.56	0.22
	2	0.24	0.51	0.19
	3	0.22	0.4	0.19
	4	0.21	0.35	0.17
	5	0.18	0.31	0.14
	Average	0.234	0.426	0.182
VSV-OVA	1	6.18	59.95	15.53
	2	4.66	53.77	10.84
	3	2.47	53.64	10.45
	4	1.95	50.8	7.34
	5	1.07	39.37	7.03
	Average	3.266	51.506	10.238

Table A5-4B(v)-1. Effector T cell over total T cell percentage on Day 3, 5, 7 for groups.

Table A5-4B(v)-2. OT-I Expansion with TLR4 Adjuvant Experiment #1 Statistics Table

t-test (p-value)			
	Day 3	**Day 5**	**Day 7**
mBD2-OVA MPL versus mBD2-OVA	0.072113	0.734344	0.596529
mBD2-OVA MPL versus OVA MPL	0.016747	0.015281	0.002237
mBD2-OVA MPL versus OVA	0.022639	0.007247	0.001301
mBD2-OVA versus OVA MPL	0.127344	0.024538	0.224268
mBD2-OVA versus OVA	0.178308	0.009511	0.214122
OVA MPL versus OVA	0.669974	0.315985	0.820515

Table A5-4B(v)-2. Pairwise 2 tailed unequal variance t-test for all groups. Statistical differences between all major groups.

Figure A5-4B(v)-1. OT-I Expansion with TLR4 Adjuvant Experiment #1 Graph mBD2-OVA versus mBD2-OVA MPL

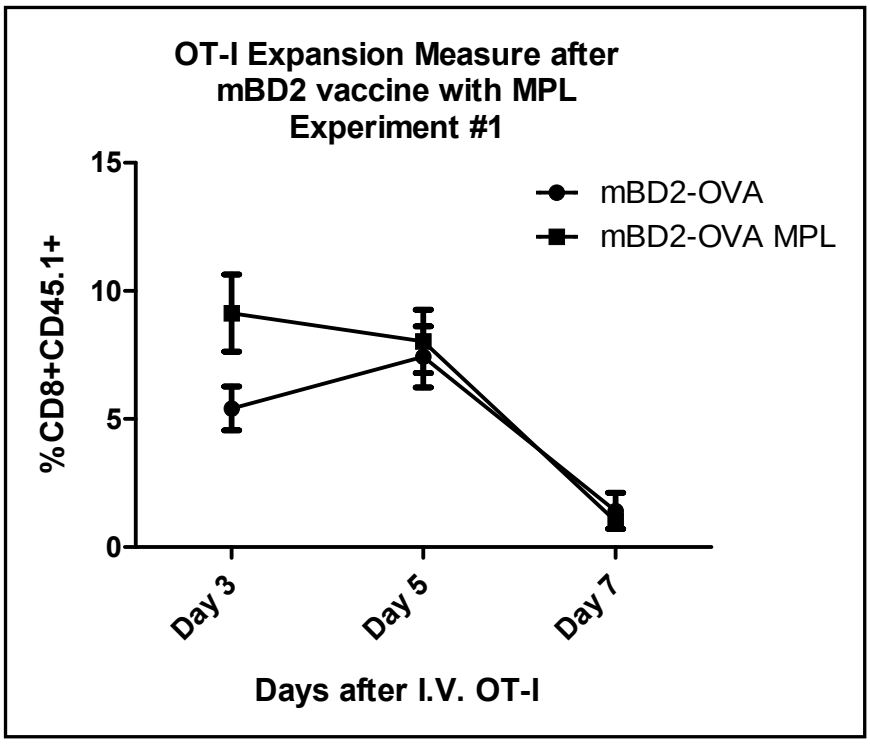

Figure A5-4B(v)-1. Approximate expansion trajectory for all groups. The actual measurements were on Day 3, 5, and 7. The lines serve as visual for the expansion pattern. Error bars are standard error of the mean.

Figure A5-4B(v)-2. OT-I Expansion with TLR4 Adjuvant Experiment #1 Graph OVA versus OVA MPL

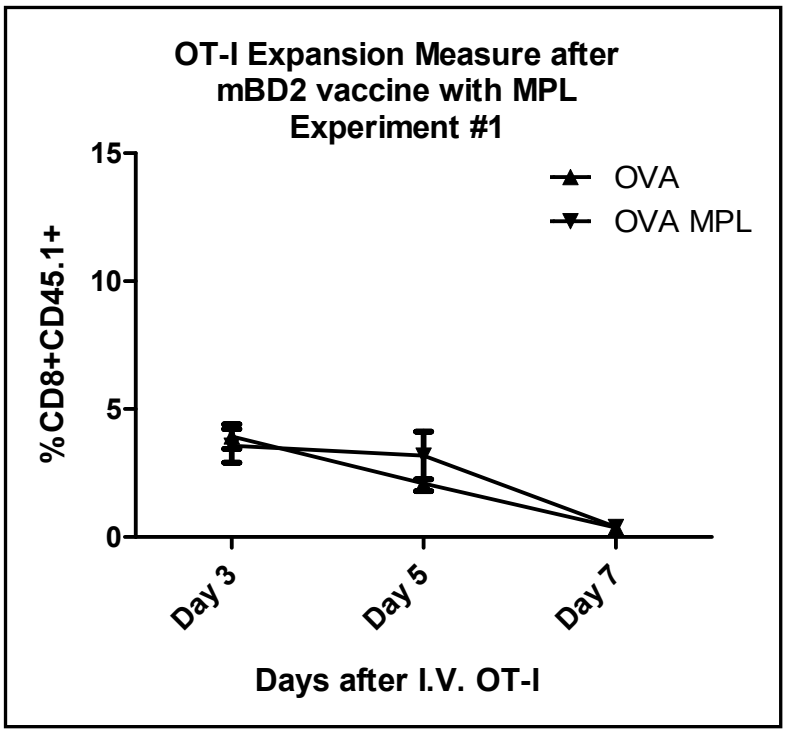

Figure A5-4B(v)-2. Approximate expansion trajectory for all groups. The actual measurements were on Day 3, 5, and 7. The lines serve as visual for the expansion pattern. Error bars are standard error of the mean.

Figure A5-4B(v)-3. OT-I Expansion with TLR4 Adjuvant Experiment #1 Graph mBD-OVA versus OVA MPL

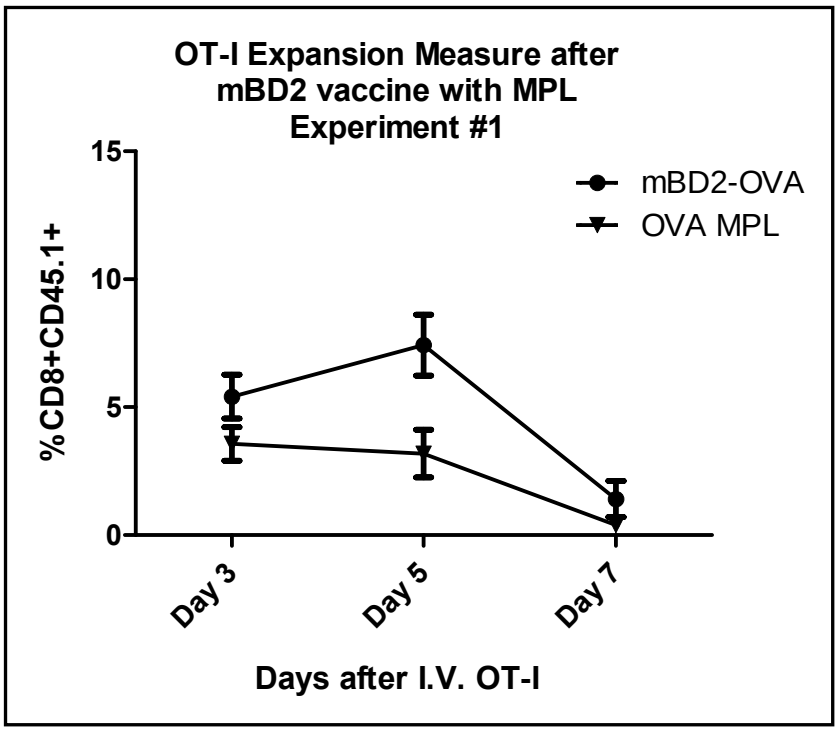

Figure A5-4B(v)-3. Approximate expansion trajectory for all groups. The actual measurements were on Day 3, 5, and 7. The lines serve as visual for the expansion pattern. Error bars are standard error of the mean.

Table A5-4B(v)-3. OT-I Expansion with TLR4 Adjuvant Experiment #2 Results

%CD8+CD45.1+				
		Day 3	Day 5	Day 7
mBD2-OVA	1	11.13	4.49	3.09
	2	9.07	3.53	2.52
	3	8.11	5.42	5.12
	4	6.77	2.38	0.44
	5	5.15	7.97	3.06
	Average	8.046	4.758	2.846
mBD2-OVA MPL	1	10.44	4.73	15.48
	2	8.33	5.16	6.34
	3	6.77	5.23	2.77
	4	4.45	9.75	3.23
	5	0.67	6.4	2.26
	Average	6.132	6.254	6.016
OVA	1	6.66	1.82	2.46
	2	2.44	1.31	0.56
	3	1.95	1.11	4.74
	4	1.74	3.99	0.67
	5	0	1.11	0.75
	Average	2.558	1.868	1.836
OVA MPL	1	4.49	7.78	3.23
	2	4.35	5.04	1.54
	3	3.62	3.4	3.21
	4	2.15	8.43	5.63
	5	1.97	5.31	2.8
	Average	3.316	5.992	3.282
PBS	1	0.73	0.4	0.17
	2	0.59	0.1	0.38
	3	0.47	0.07	0.08
	4	0.17	0.46	0.08
	5	0	0.49	0.64
	Average	0.392	0.304	0.27
VSV-OVA	1	0.22	4.93	3.86
	2	0.21	10	2.58
	3	0.16	3.8	4.95
	4	0.14	3.48	1.27
	5	0.12	16.38	9.48
	Average	0.17	7.718	4.428

Table A5-4B(v)-3. Effector T cell over total T cell percentage on Day 3, 5, 7 for groups.

Table A5-4B(v)-4. OT-I Expansion with TLR4 Adjuvant Experiment #2 Statistics Table

t-test (p-value)			
	Day 3	**Day 5**	**Day 7**
mBD2-OVA MPL versus mBD2-OVA	0.36396	0.289629	0.277028
mBD2-OVA MPL versus OVA MPL	0.17352	0.845851	0.338297
mBD2-OVA MPL versus OVA	0.119299	0.005258	0.170544
mBD2-OVA versus OVA MPL	0.006044	0.379644	0.674215
mBD2-OVA versus OVA	0.006495	0.0363	0.385154
OVA MPL versus OVA	0.560433	0.007499	0.204578

Table A5-4B(v)-4. Pairwise 2 tailed unequal variance t-test for all groups. Statistical differences between all major groups.

Figure A5-4B(v)-4. OT-I Expansion with TLR4 Adjuvant Experiment #2 Graph mBD-OVA versus mBD2-OVA MPL

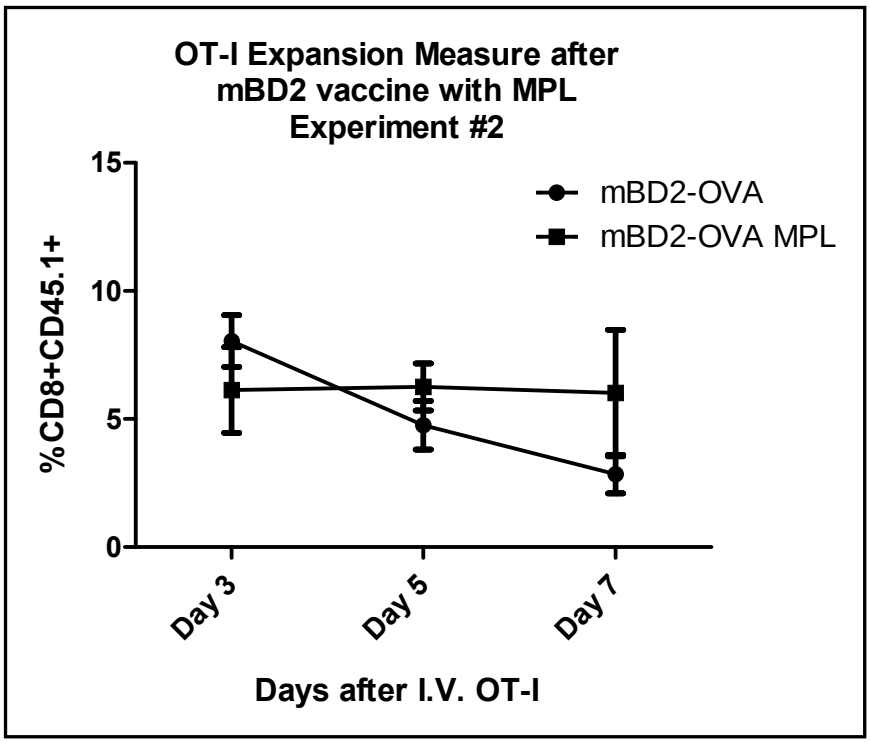

Figure A5-4B(v)-4. Approximate expansion trajectory for all groups. The actual measurements were on Day 3, 5, and 7. The lines serve as visual for the expansion pattern. Error bars are standard error of the mean.

Figure A5-4B(v)-5. OT-I Expansion with TLR4 Adjuvant Experiment #2 Graph OVA versus OVA MPL

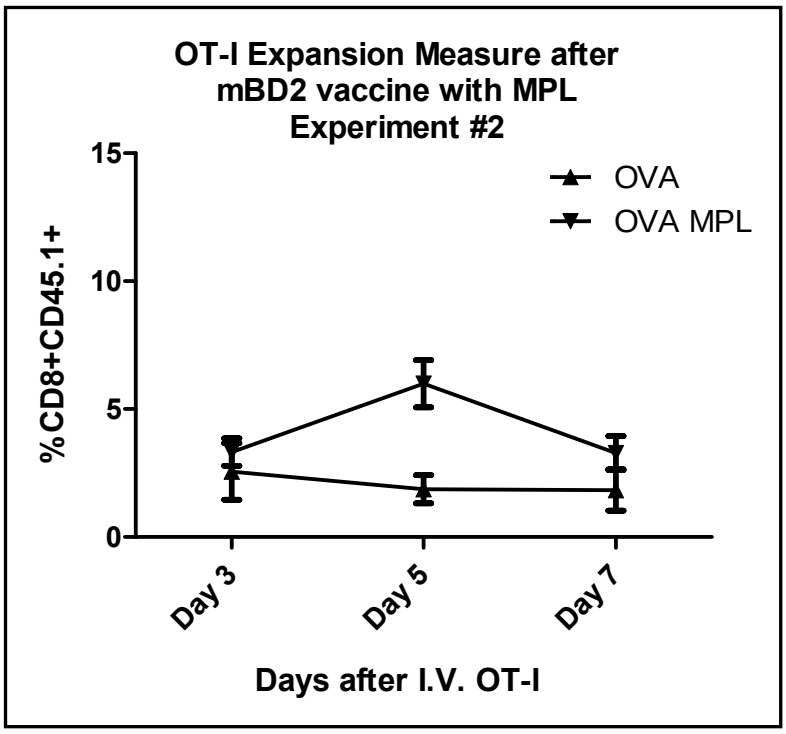

Figure A5-4B(v)-5. Approximate expansion trajectory for all groups. The actual measurements were on Day 3, 5, and 7. The lines serve as visual for the expansion pattern. Error bars are standard error of the mean.

Figure A5-4B(v)-6. OT-I Expansion with TLR4 Adjuvant Experiment #2 Graph mBD2-OVA versus OVA MPL

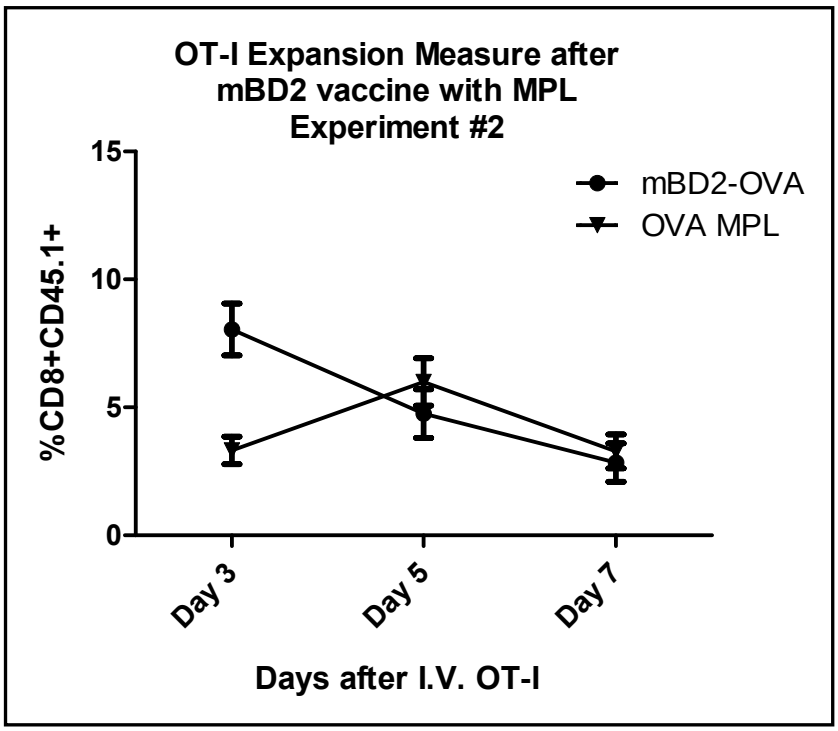

Figure A5-4B(v)-6. Approximate expansion trajectory for all groups. The actual measurements were on Day 3, 5, and 7. The lines serve as visual for the expansion pattern. Error bars are standard error of the mean.

Table A5-4B(vi)-1. OT-I Expansion with TLR9 Adjuvant Experiment Results

%CD8+CD45.1+				
		Day 3	**Day 5**	**Day 7**
mBD2-OVA	**1**	0.52	5.34	0.32
	2	0.75	4.16	1.45
	3	0.17	4.11	0.56
	4	0.88	4.82	0.5
	5	1	6.44	2.07
	Average	0.664	4.974	0.98
mBD2-OVA CPG	**1**	0.51	7.96	5.09
	2	1.03	3.95	0.99
	3	0.02	0.54	0.17
	4	0.47	12.98	4.23
	5	0.54	8.04	5.55
	Average	0.514	6.694	3.206
OVA	**1**	0	3.06	0.48
	2	0.21	1.29	0.4
	3	0.26	2.04	0.85
	4	0.14	1.4	0.67
	5	0.14	3.7	1.6
	Average	0.15	2.298	0.8
OVA CPG	**1**	0.42	9.73	5.91
	2	0.27	4.33	1.06
	3	0.49	1.24	0.23
	4	0.39	3.48	1.44
	5	0.11	1.05	0.21
	Average	0.336	3.966	1.77
PBS	**1**	0.1	0.33	0.09
	2	0.24	0.21	0.08
	3	0.08	0.19	0.16
	4	0.12	0.19	0.09
	5	0.11	0.22	0.17
	Average	0.13	0.228	0.118
VSV-OVA	**1**	1.86	72.36	56.39
	2	0.24	42.2	23.34
	3	0.12	33.85	20.01
	4	0.02	0.17	16.44
	Average	0.56	37.145	29.045

Table A5-4B(vi)-1. Effector T cell over total T cell percentage measures on Day 3, 5, 7 for all groups.

Vita

Hyun Jun (Robert) Park was born in Seoul, South Korea on December 2, 1982, the son of Young Ju Nam and Gun Chul Park. After completing his secondary level studies at the Alliance Academy, Quito, Ecuador in 2001, he entered Baylor University, Waco, Texas. He received the degree of Bachelor of Science in Informatics with a major in bioinformatics from Baylor in August, 2004. Soon after he started his Masters in Computer Science at Baylor University but never completed it. In May of 2005 he entered The University of Texas Health Science Center at Houston/The University of Texas M. D. Anderson Cancer Center Graduate School of Biomedical Sciences. Prior to completing his thesis he married Yaya Song.

Permanent address:

6703 Black Forest Dr.

Corona, CA 92880